Review

Propellants, Explosives, Pyrotechnics

DOI: 10.1002/prep.201700311

Review of Gasless Pyrotechnic Time Delays

Walter W. Focke,*[a] Shepherd M. Tichapondwa,[a] Yolandi C. Montgomery,[a] Johannes M. Grobler,[a] and Michel L. Kalombo[b]

Dedicated to the memory of Mike Taylor and Corrie Conradie.

Abstract: Gasless pyrotechnic delay compositions for time-sequencing energetic events are reviewed. They are mixtures of powdered fuels and oxidants capable of a highly exothermic oxidation-reduction reaction. Trends favor 'green' compositions targeted to replace compositions containing perchlorates, chromates, lead and barium. Thermite-based reactions dominate but intermetallics (especially multi-layered versions) and hybrids appear promising considering progress in self-propagating high temperature synthesis technology. Improving computer modelling will require better description of condensed phase reactions. Progress was made with the development of "hot spot" models and expressing reactivity in terms of the number of contact points (or contact surface area) between particles. Promising processing advances include mechanochemical synthesis of reactive particle composites by arrested milling or comminution of cold-rolled multilayer intermetallics. Dry mixing of reactive powders has made way for slurry mixing followed by spray drying.

Keywords: Pyrotechnic · time delay · thermite · intermetallic · burning rate

1 Introduction

The timing of energetic events is important in both mining and in military applications. For example, hand-held signals use a delay element to properly sequence the expulsion of illuminating rounds at the rockets' apex [1]. Similarly, effective mining blasts must follow a precisely controlled timing sequencing of the explosive charges according to an assigned firing order [2]. Only in this way can the required rock fragmentation and desired rock mass movement direction be achieved while at the same time minimizing undesirable vibration levels. In both cases pyrotechnic compositions can provide the necessary timing delays.

1.1 Safety Fuse and Gassy Delays

Pyrotechnic delay compositions can be considered gassy or gasless during their combustion. For confined environments 'gasless' compositions are preferred. In other applications, such as the unconfined fuse in a firework, gaseous combustion products are of little concern. In fact, there are applications where gassy 'chemical timers' offer advantages, e.g. in inexpensive munitions such as hand grenades and signaling devices [3]. Until World War II, black powder was the basis of virtually all delay elements and it is still used for this purpose among others. Modern gassy pyrotechnic time delay compositions include compositions based on combinations of boron carbide, sodium periodate, and PTFE [4], $Si/Bi_2O_3/Sb_2O_3$ and Ti/C-3Ni/Al [5].

Another promising avenue for gassy time delays is offered by red phosphorus/nano-metal oxide systems [6]. The combustion rates strongly depend on the nature of the metal oxide ($NiO < Fe_2O_3 \ll CuO$). The temperatures reached are high enough to cause the gasification of phosphoric anhydride produced by the combustion. For this reason, red phosphorus-nanothermites should be considered gas-generating systems. The CuO/red phosphorus system possesses an impressive reactivity. The combustion rate increases linearly with the fuel content and reaches 175 $mm\,s^{-1}$ at 50 wt-% red phosphorus.

Pyrotechnic fuses or safety fuses can be constructed from a variety of materials. They usually consist of a reactive core covered by a protective sleeve in order to prevent environmental damage to the core [7]. Black powder fuses constructed in this manner typically have a core composition consisting of 55–75 wt-% potassium nitrate 5–20 wt-% charcoal with the rest comprising of sulfur [7]. Upon ignition the black powder core will burn at a steady rate, transferring the flame front to the detonator. Alternatively, it has been suggested that fluoropolymer-based systems could be

[a] *W. W. Focke, S. M. Tichapondwa, Y. C. Montgomery, J. M. Grobler*
IAM, Department of Chemical Engineering
University of Pretoria
Private Bag X20, Hatfield 0028, Pretoria, South Africa
**e-mail: walter.focke@up.ac.za*
[b] *M. L. Kalombo*
Centre of Polymers and Composites
Materials Science and Manufacturing, CSIR
PO Box 395, Pretoria 0001, South Africa

used in a similar fashion [8]. The production of the fuse can be simplified by extruding a fluoropolymer filled with a suitable fuel, e.g. aluminum, since it will only consist of a single part. In this case the polymer acts as both the protective cover material as well as an active ingredient of the composition.

The drawback associated with the use of black powder is the significant volume of permanent gas formed during combustion (about 300 mL g^{-1} of mixture) [9]. Modern weapons require higher performance levels with respect to reliability and reproducibility under a wide range of environmental conditions (pressure, temperature, moisture). This led to the replacement of the gassy delay systems with gasless delays. Actually, the latter are not exactly gasless as they do produce a small amount of permanent gas during combustion [10]. However, they do provide an advantage with respect to greater combustion stability as the burn rate is less affected by pressurization of the burning front. Therefore, gasless delay elements provide constant time intervals that are largely unaffected by external conditions, i.e. the time delay is the same whether the system operates at great depth underwater or in the vacuum of space. Moreover, hermetically sealed delay elements incorporating gasless delays can be stored for long periods without deterioration [11].

There is a promising new field developing around multilayer-structured delay compositions. However, this review is limited to 'gasless' delay compositions based on compacted powder mixes.

1.2 Gasless Delay Elements

In modern mining and quarrying practice, shock tubing is used to transport the initiating signals to the explosive charges [12]. The delay element system is an assembly comprising an ignition source, a small-diameter tube containing a compressed composition and an ignition transfer system [11]. The delay elements in the shock tube detonators provide the required delay between the time of ignition (received from the spit of the shock tubes) and the initiation of the explosive base charges. The combustion process of the pyrotechnic composition provides the required delay time interval between successive explosive events. Typically this ranges from a fraction of a millisecond to several seconds.

The pyrotechnic time delay element itself typically consist of a metal tube (aluminum, brass, lead, etc.) that holds the compressed-powder time delay composition. Usually a small section of the time delay composition is replaced by a starter composition to ensure reliable ignition. Figure 1 shows a typical pyrotechnic time delay element along with its position as commonly used in non-electric detonators [13]. The operation of this type of detonator was explained by Tsang [13]. At the one end the shock tube is connected into the detonator delay element. The tube is isolated from the chemical reactants of the delay element by a plastic cup which is there to prevent any accidental electrostatic discharge from the tubing which might initiate the delay element. The plastic cup is easily broken by the shock wave as it enters the detonator. The spit of hot particles and gas from the shock tube enter the chamber, and ignite the starter composition. This composition is designed to pick up the initiation signal, facilitate the ignition of the time delay composition and to seal the rest of the pyrotechnic column. This prevents any gas produced by the chemical reaction within the delay column to escape. The combustion wave then travels down the delay element. When it reaches the end, it is converted back into a detonation wave by sequentially first initiating a primary explosive composition (e.g. lead azide) that then sets of a base charge, e.g. PETN.

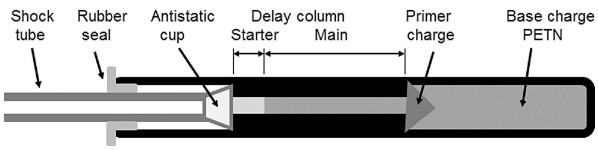

Figure 1. Typical pyrotechnic time delay composition along with its position as commonly used in non-electric detonators [13].

1.3 Delay Compositions

The required firing time delays in the detonator trains is provided by a suitable pyrotechnic composition. Typically it takes the form of an intimate mixture of solid, powdered fuels and oxidants capable of a highly exothermic propagat-

Professor Walter W Focke obtained a PhD in Polymer Science and Engineering from MIT. He is a full professor in the Department of Chemical Engineering and Director of the Institute of Applied Materials at the University of Pretoria. His research interests span carbon materials, pyrotechnics, polymer additive technology, and malaria vector control.

Shepherd M. Tichapondwa was born in Zimbabwe in 1984. He obtained his PhD in Chemical Engineering from the University of Pretoria. He is currently employed at the same institution as Senior Lecturer. His research interests include pyrotechnics and energetic materials with a particular interest in time delay compositions and mine detonators. He also conducts research in advanced water treatment technologies.

ing oxidation-reduction reaction [14]. The composition should be readily ignitable but should be safe from both the explosive and health points-of-view [14]. The delay combustion reaction must be exothermic, self-sustained and self-contained and proceed at a constant predetermined rate [15] unaffected by changes in the ambient temperature [14]. Since the detonator is a sealed unit, the combustion reaction should be relatively 'gasless' to minimize the effects of pressure on the burn rate [14]. Following ignition, a combustion wave travels down along the tube at a constant speed that ensures the transmission of initiation impulse to the detonator in a precisely adjustable time interval. Delay times will be constant and linearly related to the length of the element if all these requirement are met.

Any combustible composition will take a finite time to burn over a given length. However, the requirements of safety, time reproducibility and ignition transfer reliability, particularly in modern military applications, have resulted in the development of specific formulations known as pyrotechnic delays. Compositions of this type, when consolidated into a tube, burn at reproducible linear rates. Silicon fuel-based pyrotechnic compositions, e.g. Si/Pb_3O_4 [16] and $Si/BaSO_4$ [17] are widely used commercially in mining applications. Lead-based compounds are considered toxic and the mixtures are sensitive to ignition during dry mixing, whilst $BaSO_4$-based mixtures have variable ignition performance. Although barium sulfate is insoluble in water and decidedly nontoxic, the reaction products produced by the $Si-BaSO_4$ compositions were found to release soluble barium ions when contacted with water [18]. Several alternative oxidants to be used in combination with silicon have been proposed, these include $CaSO_4$ [19], Sb_6O_{13} and Bi_2O_3 [20].

1.4 The Drive Towards "Green" Pyrotechnics

Many commercial pyrotechnic compositions still contain compounds associated with significant health and environmental concerns [21]. This includes perchlorates [22] and heavy metals such as lead, barium, and chromium as in chromate-based compounds [23]. These chemical entities are deemed to be environmentally unfriendly and may pose a potential health hazard especially when they leach into soil and water sources [22]. As a result, there are increasing health and safety legislative requirements designed to eliminate them from delay compositions [21]. This has led to concerted efforts to find 'green' replacements for traditional compositions. More 'environmentally friendly' oxidizers, e.g. potassium ferrate [24], and formulations have been proposed including B/Fe_2O_3 [25], Mn/MnO_2 [26], Ti/C-3Ni/Al [27], $B_4C/NaIO_4$/PTFE [4], $Si/CaSO_4$ [19], and W/MnO_2 [28].

2 Basic Thermodynamic Principles

2.1 Thermodynamics of Condensed Phase Reactions

Pyrotechnic compositions are usually made by mixing the fuel and oxidant as finely-divided powders (sometimes additives are included to promote particular properties) [29]. During combustion, some constituents remain in the solid state, while others melt, vaporize, or decompose to yield some gaseous products. Mechanisms encountered may thus cover the wide field of solid-solid, solid-liquid, solid-gas, and possibly even liquid-gas and liquid-liquid reactions.

Conventional gasless pyrotechnic time delays are based on oxidation-reduction reactions between an oxide and a metallic or non-metallic element. A unique characteristic of such reactions is the virtually complete dependence on a favorable enthalpy change ($\Delta H_R < 0$). The second law of thermodynamics demands, as condition for the spontaneity of a reaction conducted at constant temperature and pressure, that the Gibbs free energy change of the reaction, $\Delta G_R = \Delta H_R - T\Delta S_R$, be negative. The entropy change, ΔS_R, for reactions yielding crystalline solid products is usually very small. In addition, Kopp's rule states that the sum of the atomic specific heats remains unchanged. Thus, the only way in which ΔG_R can be large and negative is for ΔH_R to be negative, i.e. the reaction must be highly exothermic.

Ellingham diagrams [30] provide a first-cut approach to establish whether a proposed fuel/oxidant reaction is thermodynamically feasible. They show the variation with temperature of the standard Gibbs free energy of formation (ΔG°) of the oxides of metals and non-metals. The location of the plots on the Ellingham diagram indicate the relative tendencies of the elements to combine with oxygen. This permits rapid evaluation of the reducibility for a specific oxide or sulfide by a given elemental reducing agent. Figure 2 shows an Ellingham diagram for selected manganese oxides with oxygen taken as a gas at a partial pressure of 1 atm. In Figure 2 the formation of an oxide from its element is written in the following standard form:

$$(2x/y)\ \mathrm{M} + \mathrm{O_2} \rightarrow (2/y)\ \mathrm{M}_x\mathrm{O}_y$$

For example, consider the following oxidation reactions: $2Mn + O_2 \rightarrow 2MnO$ (I), and $Mn + O_2 \rightarrow MnO_2$ (II). The reduction of manganese dioxide by manganese metal is expressed by: $Mn + MnO_2 \rightarrow 2MnO$ (III). Note that this net reaction is obtained by adding the 'reverse of the second reaction (II), i.e. in the form of a reduction reaction, to the first reaction (I). Since O_2 then appears on both sides, it just cancels out and does not appear in the net reaction (III). Thus the difference at a given temperature, between the values of ΔG° on the diagram for these two reactions, represents the Gibbs free energy change or, in other words, the driving force for the reaction.

The lower down on the diagram the curve for a particular oxide lies, the greater is its stability and the lower is its

reducibility [30]. In Figure 2, for example, the curve for the formation of the oxide MnO lies lower than that of all the other manganese oxides. This implies a positive tendency for the net reaction to proceed and this insight led to the discovery of the 'green' Mn/MnO_2 pyrotechnic delay composition [26].

2.2 Adiabatic Reaction Temperature

The combustion events in the delay element must, per force, be associated with high-temperature reactions otherwise it will not be self-sustaining. An important parameter in this regard is the adiabatic temperature of combustion, T_{ad}. This thermodynamic parameter is the temperature to which the product is raised under adiabatic conditions as a consequence of the evolution of heat from the reaction itself [31]. Consider, as an example, an irreversible reaction: A(s) + B(s)→C(s). The adiabatic reaction temperature T_{ad} is the maximum temperature to which the product C, with melting point T_m, can be raised beyond an initial temperature (T_i) as a result of the exothermic heat of reaction. Assuming that melting is the only phase change that occurs, the adiabatic reaction temperature, for the reaction starting at T_i is calculated as follows:

$$\Delta H_R = \int_{T_i}^{T_m} Cp_s dT + \Delta H_m + \int_{T_m}^{T_{ad}} Cp_l dT \quad (1)$$

where ΔH_R and ΔH_m are the enthalpy changes associated with the reaction and the melting of the product; C_p is the heat capacity and the subscripts *s* and *l* refer to the solid and liquid forms of the reaction product. Clearly, preheating of the reactant mixture will result in a higher T_{ad}. When no phase transition occurs, and physical properties can be assumed constant and independent of conversion, the adiabatic reaction temperature is

$$T_{ad} = T_i + (-\Delta H_R)/C_p \quad (2)$$

In most cases phase changes will occur at some temperatures below the actual reaction temperature. Later on elementary models for ignition and the burning rate will be explored and it will be convenient to use equation (2) even when there are phase changes with associated latent heats. Usually the temperature gradients are extremely large in the vicinity of the combustion front. In such cases ignoring the phase change details is an admissible approximation provided the heat of reaction is adjusted for their effect. Therefore, equation (2) will be assumed valid except that the quantity $-\Delta H_R$ is replace by the 'heat of the reaction' *Q*. The latter is equivalent to the enthalpy of the reaction corrected for all phase changes occurring below the reaction temperature.

Numerous thermite and intermetallic energetic compositions can be considered for delay composition design. Fischer and Grubelich [32] provide comprehensive lists with energetic properties, including the adiabatic reaction temperature, that are useful for identifying promising candidate systems.

3 Condensed Phase Reactivity

The theoretical redox reaction normally postulated in inorganic chemistry takes place in a solvent. In contrast, the reactions of inorganic redox systems used for pyrotechnics take place as solid-solid, solid-liquid or solid-gaseous state reactions [33]. The reaction mechanism, of pyrotechnic delay compositions, is intimately linked to the fuel/oxidant phases at the temperature of the reaction [34]. Possibilities include: (a) molten fuel/solid oxidant, (b) solid fuel/molten oxidant, (c) solid fuel/solid oxidant, and (d) solid fuel/decomposed oxidant.

A 'true" solid-solid reaction is reportedly [35] presented by the tantalum/carbon reactive system. It features a very high energy of reaction and an adiabatic combustion temperature of 2743 K. This is still significantly below the melting points of both the reactants, as well as any intermediate phases and final products. Nevertheless, a combustion wave can propagate in nano-scale Ta/C mixtures owing solely to a solid-solid reaction [35].

It is possible to infer aspects of the reaction mechanism from differential scanning calorimetry (DSC) traces [34]. The temperature at which the oxidant undergoes physical or chemical changes, plays a significant role at the start of the main reaction. If either the fuel or the oxidant is in the molten form at the reaction temperature, a single exothermic peak is observed while with truly solid-solid reactions, the DSC traces have a double peak appearance [34].

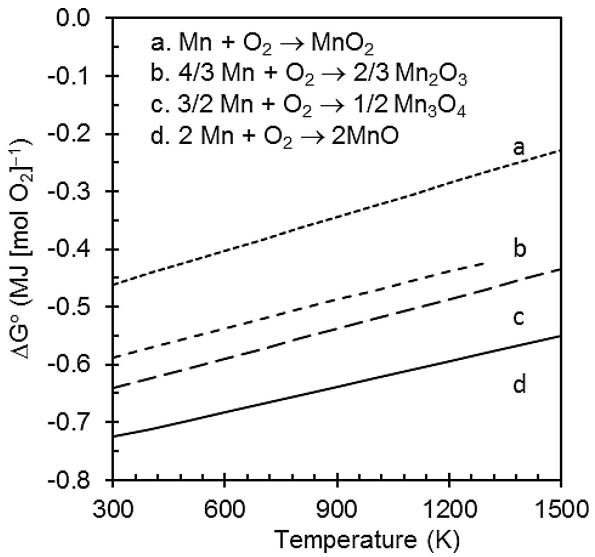

Figure 2. Ellingham diagram for manganese oxides at a system pressure of 0.1 MPa [26].

3.1 The Solid State

Most solids are crystalline in nature, i.e. they have a homogeneous structure in which the constituent atoms are arranged in a regularly repeated pattern. These repeated units are linked together in different ways: covalent bonds, ionic, metallic, or sometimes hydrogen and van der Waal's bonds. The physical properties of a solid depend largely on the bonding forces and the specific crystal structure. With pyrotechnics the crystal habit, i.e. morphology also plays an important role [36]. However, the reactivity of a solid is highly dependent on the presence of imperfections such as lattice defects in the bulk solid [37]. The lattice defects that play a major role in the reactivity of solids include (a) inherent defects, e.g. Frenkel and Schottky defects which are related to interstices and vacant sites in the lattice respectively; (b) non-stoichiometric defects due to the presence of some cation vacancies, e.g. $Fe_{1-x}O$, and (c) crystal dislocations. It has been observed that reactions of a liquid with a crystal often begin at defect locations where bonds have been weakened [37].

Solid-state reactions. In the course of a solid-solid reaction, different steps such as nucleation, growth, and transfer of matter across phase boundaries (by diffusion) occur. Besides defect thermodynamics, the diffusion theory forms the basis for the explanation of solid-solid reactions. Reaction between a metal and a non-metal proceeds by two possible mechanisms: either the non-metal migrates through the product layer to the metal interface, or the metal migrates in the reverse direction. Since the reactant can migrate through the ionic product layer only as ions, electrons must also accompany the ionic migration. It seems that reaction will not take place if the product layer is not capable of conducting electrons [37].

The role of defects in semi-conductors [37], is illustrated by the reaction $Ge + 2\ MoO_3 \rightarrow GeO_2 + 2\ MoO_2$. Ge doped with an n-type dopant (As or Sb) reacted with MoO_3 much faster than Ge doped with p-type dopants (Ga or In). The reactivity of Ge also depended on the concentration of the dopants. Increasing the concentration of the n-type dopants increased the rate of reaction, whereas increasing the concentration of p-type dopants decreased it. These observations are in agreement with the postulate that an oxidation-reduction reaction necessitates the transfer of electrons and can usefully be compared with semi-conductor activity. The reducing agent is the electron donor and the oxidizing agent is the electron acceptor. This is analogous to the activity at an n-p semi-conductor junction where the n-type crystal creates the space charge potential by donating electrons to the p-type crystal. Therefore, an n-type reducing agent (Si doped with As) should be more reactive than a p-type (Si doped with Al) [37].

Tribelhorn *et al.* [38] studied the burning behavior of Zn/$KMnO_4$ mixtures, compacted to pressure up to 150 MPa, in the composition range 30–75 wt-% Zn. Based on thermal analysis results, they suggested that the Zn diffuses into the solid residue formed during the first stage of $KMnO_4$ decomposition. An exothermic reaction starting at 520 °C was observed and attributed to the reaction of Zn with this '$KMnO_4$'-residue [11].

Drennan and Brown [39] studied the combustion of the Mn/BaO_2, Mo/BaO_2, Mn/SrO_2 and Mo/SrO_2 systems and Tribelhorn *et al.* [40] studied the Fe/BaO_2 and Fe/SrO_2 combinations. Considering the corresponding radii of the different metal atoms and ionic species involved in the combustion, the diffusion via cation vacancies in the oxidant structure should be favored in the BaO_2 lattice rather than in the SrO_2 lattice. However, for comparable oxidation states, the differences between the behavior of Mn and Mo based on geometry should be small.

Examination of the products from the combustion of Zn/peroxide systems showed that oxidation of the metals was generally incomplete, probably because of the presence of protective oxide layers [38].

The above observations lead one to the conclusion that diffusion effects will almost always affect the reaction rate in solids. Diffusion effects should therefore be taken into account when modelling the solid-state reactions of pyrotechnic compositions.

Solid-liquid reactions. Howlett and May [41] have shown that for the B-$K_2Cr_2O_7$ system, the ignition process is dependent on the transport of matter through a liquid phase. The combustion zone then propagates as a molten front. Hence, eutectic oxide compositions have been used to increase the velocity of the combustion wave front. They probably improve the reaction kinetics by increasing the interfacial contact area between the reactants. In these systems the surface tension of the liquid phase is relevant, because it determines the wettability of the granular reactants. Tribelhorn *et al.* [38] noted that the surface tension of Zn at its melting point is high compared to other low melting point metals, i.e. about twice that of Sb and Pb. Therefore, the movement of liquid Zn through pores and channels does not occur readily because the oxidant surfaces are not easily wetted.

Solid-gas reactions. There are stark differences in the burning behaviors of loose and consolidated (compressed or compacted) powders [11]. Consider a container filled with a loose pyrotechnic composition. An uncontrolled reaction ensues on initiation of the reaction because of the low bulk density of the filling, the convection of combustion products (gases, liquid and thermal radiation) and the hot air through the voids. This may eventually lead to an explosion because of the confinement imposed by the container. By contrast, in the compressed sample convective transport of the combustion products through the consolidated column is strongly impeded. Combustion is therefore confined to a relatively thin propagation zone known as the 'burning front'.

Pyrotechnic systems differ with respect to their sensitivity to compaction [38,40]. The burn rate in the Fe/BaO_2

system initially increases with increase in compaction pressure [40]. Increase in compaction pressure increases interparticle contact and this aids solid-solid reactions. At higher compaction pressures the rate decreases again. This suggests that gas transport ahead of the burning front is also important. In fact it was concluded that the combustion wave in this iron system is preceded by a flow of oxygen generated by the decomposition of the oxidant.

In other systems, e.g. Zn/$KMnO_4$, the burning rate is decreased by compaction [38]. This behavior suggests that in this case the reaction rate is determined by solid-gas reactions: Oxidants such as SrO_2 and $KMnO_4$ decompose without melting to produce oxygen gas and a solid residue. Increased compaction may decrease the surface accessible to the oxygen gas or may trap the gas in closed pores. In loose powders the oxygen gas flow is not impeded and burning is fast.

Burning in the Sb/$KMnO_4$ system also occurs via gaseous intermediates. In this case the gas (O_2) arose from the decomposition of the oxidant and possibly even from the volatile Sb_2O_3 reaction product [42]. The Zn/Pb_3O_4 system is even more complex. Here the gas phase contains Zn and Pb vapors as well as the O_2 generated by the decomposition of the oxidant.

3.2 Solid Reactivity

Chemical reactivity of solids is affected by the degree of lattice vibrations. As temperature rises, crystal atoms or ions vibrate with increasing amplitude about their average positions in the lattice. This can be thought of as the 'loosening' of the bonds holding the solid together. Diffusion is enhanced and the atoms may exchange positions. At a sufficiently high temperature this leads to melting. In addition, at a lower temperature this may induce a transition from one solid state to another, i.e. a phase change. Tamman used the ratio of the temperature of the solid to its melting point as a rough measure of lattice loosening [43]. Ionic surface mobility becomes effective at $T/T_m \approx 0{,}3$ and lattice diffusion at $T/T_m \approx 0{,}5$ [37]. Enhanced reactivity is also observed near other phase transition temperatures, due essentially, to a similar occurrence of lattice disturbances. This is called the 'Hedvall effect' [37].

Mclain [37] lists the following important factors that influence solid reactivity: Deviations from the normal crystallographic or amorphous structure of a substance; lattice defects in the form of hereditary structures; formation of imperfect structures, e.g. transition from one modification to another on thermal decomposition; presence of guest entities in the lattice; differences in the crystallographic formation of different surfaces; corrosion; adsorption and catalysis; irradiation by absorbable wavelengths, and changes in the magnetic state or the electric state of the material.

Hereditary structures. The history of the sample and the way in which the material was prepared or crystallized, its impurities and defect content, all influence its further behavior. For example, sulfate-derived oxide (Fe_2O_3) was more reactive than Fe_2O_3 derived from iron oxalate despite the fact that the former had a larger average particle size [37]. X-ray powder diffraction patterns revealed that the sulfate-derived Fe_2O_3 was less crystalline. Another example is provided by the large differences in the reactivity of fine iron powders obtained through different routes, i.e. atomization, iron carbonyl decomposition, electrolysis and reduction of an iron (II) compound [44]. In this case it was the nature of the iron oxide layers that formed on the surface of the particles during synthesis that affected the reactivity.

Mechanochemical activation. Milling, pulverizing, atomizing and grinding are considered to be interesting techniques for breaking down as many atomic bonds as possible before the materials are used in combination with another reactant. Fracturing macroscopic crystals creates new surfaces, edges and corners where the atoms are not bonded as strongly as internal atoms. This enhances the reactivity. Similarly milling may enhance reactivity more by introducing lattice defects and distortions rather than by reducing the particle size [37]. Mechanochemical preparation imparts unique ignition properties to- and affects combustion mechanisms of reactive materials [45].

Doping and co-crystallization. Doping $KClO_3$ with $Cu(ClO_3)_2$ made it supersensitive to the extent that its mixtures with sulfur were capable of a spontaneous high-order detonation [37]. Similarly, doping of NiO with LiO_2 and Cr_2O_3 had a positive effect on the reactivity of NiO. Doping achieved via co-crystallization of precursors also makes Fe_2O_3 more reactive [37]. The doping was accomplished by growing crystals of $CuSO_4{\cdot}FeSO_4.xH_2O$ or $NiSO_4{\cdot}FeSO_4.xH_2O$ in an acidic solution of the salts. The crystals were subsequently decomposed in O_2 at 200–250 °C to produce Fe_2O_3. This also improved the calorific value of a 50 : 50 Fe_2O_3-Ti mixture.

Passivating oxide surface layer. The outer surface of most metal- and also silicon particles are covered by a passivating oxide layer. The thickness of this layer, and especially the relative thickness in the case of nanoparticles, has a major effect on ignition behavior [46]. Suitable coatings applied to the fuel particles can protect them against oxidation [47]. However, this approach can be a double-edge sword, because some chemical coatings can react with the underlying metal, especially when the coating was applied on particles which did not already possess an adequate oxide layer with passivating properties. In the case of aluminum, surface coatings of perfluoropolyethers can promote surface activity [48].

Presence of water. The role of water vapor as catalyst and accelerator in pyrotechnic reactions is well known. The burning rate and color of firework star compositions depend markedly on minor changes in the moisture content. A very small amount of 0.1 % H_2O (moisture content) seems

to be most effective. Above this proportion, there is an inhibiting effect [37]. Moreover, it is well known that the presence of water vapor has a noticeable effect on sintering, structural rearrangement and crystal coarsening of oxides. These phenomena are ascribed to the chemisorption of water vapor on oxide surfaces and interfaces. This leads, among other things, to an increase in the surface and particle boundary mobility of ions.

Corrosion inhibition. Chemical treatment to protect powder against corrosion by atmospheric moisture or against contact with water is also a form of inhibition. This process does, therefore, lengthen the life of more reactive materials, including Al, Zn and Mg [37]. Chemical treatment has also been used to prevent hydrogen evolution form fuels during wet mixing of compositions [49].

4 Kinetics

4.1 Condensed Phase Reaction Kinetics

The expression to be used for describing the chemical reaction rate in solid pyrotechnic composition is a contentious issue. The reaction mechanisms in condensed phase processes are very complex as they occur in multiple steps with diffusion effects also playing a role. Some sort of simplification is essential in order to make mathematical analysis tractable. The single-step kinetics approximation employs the assumption that the reaction rate can be expressed as a product of two separable functions that are independent [50]. The first one, i.e. the reaction constant $k(T)$, depends solely on the temperature T and the other one, $f(x)$ depends solely on the conversion of the reactants:

$$r = \frac{dx}{dt} = k(T)f(x) \tag{3}$$

Equation (3) is named the general rate equation as it resembles a single step kinetics equation, even though it is a representation of the kinetics of a complex condensed-phase process [50]. While it is primarily a convenient approximation, its validity can be justified for processes that either involve just a single-step or that are dominated by a sole rate-limiting step [50].

Temperature dependence of the apparent kinetic constant. It is conventional to assume that the rate constant k follows simple Arrhenius kinetics:

$$k = k_o \exp(-E_a/RT) \tag{4}$$

where k_o is the pre-exponential factor and E_a is the activation energy.

While, in general, the single-step approximation cannot represent a 'true' kinetic model, it can be considered a valid approximation when it fits, simultaneously, all experimental thermal analysis data yielding an unique $f(T)$ function [51]. That means that validation of the hypothesized rate expression requires that the kinetic analysis must simultaneous fit all the experimental data representative of the solid-state reaction obtained under different temperature evolution conditions, i.e., isothermal, linear heating rate, modulated temperature, and sample controlled [51]. Every experimental *T-x-dx/dt* triplet should fit the general differential equation independently of the experimental conditions used for recording such a triplet. A valid kinetic model would fit all of the experimental data yielding a unique activation energy and pre-exponential factor.

Apparent activation energies determined from pyrotechnic temperature profile analyses yielded values about an order of magnitude less than results obtained by thermal analysis [52]. Such low activation energies for the pyrotechnic reaction likely imply control by a diffusion mechanism [53]. To correct for such diffusion effects, Laye [52] proposed the apparent rate constant should be viewed as a combination of a "true" Arrhenius reaction rate constant (k_{Ar}) and an activated diffusion:

$$\frac{1}{k} = \frac{1}{k_{Ar}} + \frac{1}{B\,T^n} \tag{5}$$

The second term on the right, in equation (5), represents the contribution by a diffusional effect. Equation (5) combines Arrhenius behavior dominating at low temperatures (which predicts a rapid rise with temperature) with diffusion-controlled behavior at high temperature, where the rate becomes less dependent on temperature.

Condensed phase kinetics. Many solid-state kinetic models have been developed over the years. Models currently used in solid-state kinetic studies can be classified according to their mechanistic basis as nucleation, geometrical contraction, diffusion, and reaction order [54]. The kinetics of solid-state pyrotechnic reactions are affected by particle size and shape and also the particle-size distribution [55]. At the particle level the reactions proceed by the advance of the reaction interfaces inward toward the center of the particles. In practice, the conversion values of the individual particles vary because of gradients in the temperature and variations in the partial pressure of evolved gas within the sample matrix caused by mass and the heat-transfer phenomena [55]. Khawam and Flanagan [56] summarized the commonly employed conversion models and present their mathematical development. These feature rather complex $f(x)$ expressions. Pérez-Maqueda *et al.* [51] found that most of the models extensively used in the literature and even their deviations produced by effects such as particle size distributions or heterogeneities in particle morphologies, are adequately approximated by the empirical equation

$$f(x) = x^m(1 - x)^n \tag{6}$$

where m and n are adjustable constants. The great advant-

age, of using this expression, is that it facilitates the combined kinetic analysis of data obtained under any experimental conditions without any previous assumption about the kinetic model followed by the reaction [51].

In pyrotechnic studies, models based on homogeneous kinetics (e.g., those applicable to chemical reactions in gas or solution phases), have been popular for kinetic studies. Assuming Arrhenius kinetics for the rate constant, the general expression for n^{th} order reaction kinetics is:

$$r_s = \frac{dx}{dt} = k_o \exp(-E_A/RT)(1 - x)^n \quad (7)$$

Where k_o and E_A are the pre-exponential and activation parameters for the Arrhenius expression detailing the effect of temperature, R is the gas constant and x is the degree of conversion.

4.2 Elementary Model for a Cylindrical Delay Element

Figure 3 shows a schematic of an elementary but valuable model for investigating the conditions necessary for ignition and sustained combustion in a cylindrical delay element [57]. The model and analysis are based on the following assumptions: The element takes the form of a symmetric cylindrical body; the solid phase is treated as one-dimensional homogeneous continuum in which heat transfer takes place by conduction only; the chemical reaction is the only source of the local heat generation and heat is lost to the environment at the surface of the body and occurs because of the differences in temperature between the surface and the external medium; phase changes such as melting and evaporation are neglected, and physical and transport properties are assumed constant, i.e. independent of temperature and conversion.

Figure 3 illustrates schematically the configuration as considered in cylindrical coordinates. The element center line forms the z-axis and the ignition surface corresponds to the position $z = 0$. The system is initially at an ambient temperature T_o. At the start the surface of the cylinder at $z = 0$ is maintained at the same temperature as the ignition temperature (T_*) throughout the reaction and the surface of the cylinder at the far end from the ignition surface is maintained at the initial temperature throughout the reaction. Once ignited, a self-propagating combustion wave may proceed in the positive z-direction. With these assumptions the energy equation for this setup is:

$$\rho C_p \frac{\partial T}{\partial t} = \lambda \frac{\partial^2 T}{\partial z^2} + \rho Q r_s - \frac{4h}{d}(T - T_o) - \frac{4\sigma\varepsilon}{d}(T^4 - T_o^4) \quad (8)$$

where T is the local temperature; T_o is the ambient temperature; z is the axial position; t is the time; ρ is the bulk density; C_p is the heat capacity; λ is the effective thermal conductivity; Q is the heat of the chemical reaction; r_s is the rate of the chemical reaction; h is the heat transfer coefficient; d is the diameter of the delay column; σ is the Stefan-Boltzmann constant, and ε is the emissivity of the outer surface. The first term on the right is the rate of local energy redistribution in the axial direction by heat conduction. The second term is the rate of energy generation by the exothermic reaction corrected for any phase changes. The third and fourth terms are the rates of surface heat loss by convection and radiation respectively. It is further assumed that the following initial and boundary conditions apply [57a]:

$$t = 0 \quad z > 0 \quad T = T_o$$
$$t > 0 \quad z = 0 \quad T = T_*$$
$$t > 0 \quad z \to \infty \quad T = T_o \quad (9)$$

This model captures the essential physics of the process and allows meaningful analysis of ignition criteria for gasless self-propagating reactions through an ignition temperature analysis.

The calculation and analysis using the differential equation (8), as well as other relevant energy and mass continuity equations, are simplified by converting them into dimensionless form. This automatically leads to characteristic dimensionless parameters that are included in the list of dimensionless groups or numbers enumerated in Table 1 [57a].

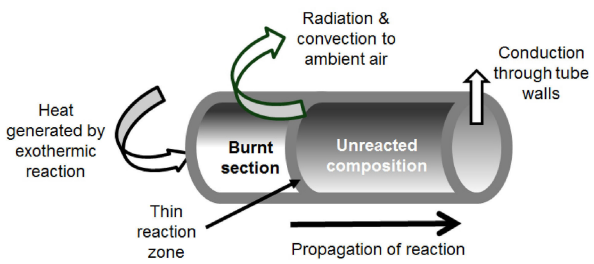

Figure 3. Schematic illustration of the simplified model of a delay element showing the heat flows affecting performance.

4.3 Ignition

The combustion of the delay composition starts with the initial process of ignition. Ignition can be defined as the initiation of the self-sustained burning of the pyrotechnic material, i.e. the visible appearance of a steady combustion. External factors influencing ignition include the heating rate, the ambient temperature and the size, geometry and nature of the surface of the sample.

Table 1. Dimensionless groups relevant to combustion processes in delay elements [13, 57a, 61].

Dimensionless number	Interpretation
$\gamma = E/RT_R$	Arrhenius number: A ratio of activation energy to thermal energy
$\omega = hd/\lambda$	Nusselt number: Ratio of convective to conductive heat transfer across (normal to) the surface boundary
$\delta = \sigma\varepsilon T_R^3 d/\lambda$	Ratio of radiative to conductive heat transfer across (normal to) the surface boundary
$\chi = \rho k_o Q d^2/\lambda T_R$	Rate of local heat generation to conductive heat transfer
$\xi = k_o \rho C_p d^2/\lambda = k_o d^2/\alpha$	Rate of reaction rate of local heat generation to conductive heat transfer
$\theta = E(T_f - T_o)/RT_f^2$	Zel'dovich number: A measure of the activation energy in combustion processes
$Se = \frac{\rho VQEk_o}{hART_o^2} e^{-E/RT_o}$	Damköhler number (or Semenov number [60]): Ratio of the heat generation rate by the reaction to the rate of convective heat transfer
$Fk = \frac{\rho QEd^2 k_o}{4\lambda RT_o^2} e^{-E/RT_o}$	Frank-Kamenetsky number [60]: Ratio of the heat generation rate by the reaction rate to the rate of conductive heat transfer

Ignition of a bulk sample. The critical ignition temperature, T_{ign}, is the minimum temperature to which a pyrotechnic charge of specified size, shape and boundary constraints must be heated in order to induce a thermal runaway [58]. Figure 4 shows a schematic plot of the heat generated versus heat loss as a function of temperature. Heat is generated by the chemical reaction occurring inside the sample. In the first instance, this can raise the temperature of the sample itself up to a maximum value corresponding to the adiabatic reaction temperature. The generation of heat by the reaction initially increases exponentially with temperature. This accords with the Arrhenius temperature dependence of the reaction rate constant. However, part of this heat is also lost to the environment from the surface due to heat transfer by conduction, convection and by radiation. The rate of conductive and convective heat loss is roughly proportional to the difference in temperature between the flame and the surroundings. Radiative heat loss is proportional to the difference in absolute temperature to the fourth power.

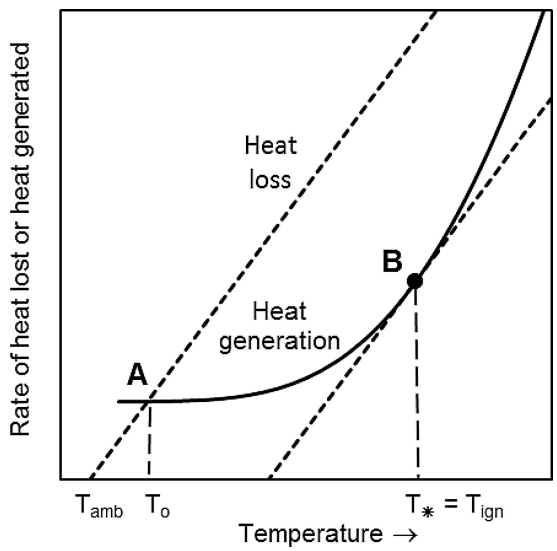

Figure 4. Semenov diagram of heat generation by the reaction (solid line) and heat lost to the environment (broken lines) versus sample temperature. Two different heat loss scenarios are indicated.

The ignition temperature is the critical temperature (T_{ign}) at which any specific size and shape of explosive can self-heat to a thermal run-away condition [59]. The essence of the physics of ignition phenomenon is best understood through analysis of the least sophisticated model, described in the previous paragraph, in conjunction with a Semenov diagram [60]. The model assumptions are that the heat-generating reaction follows zero order kinetics with an Arrhenius temperature dependence and that surface heat loss occurs by convection. The temperature inside the sample is assumed uniform and physical properties are temperature independent. Under these conditions the heat balance over the sample is described by the differential equation:

$$\rho C_p \frac{dT}{dt} = \rho Q k_o \exp(-E/RT) - h(A/V)(T - T_o) \qquad (10)$$

where T and T_o are the reactant and ambient temperatures respectively; t is the time; ρ and C_p are the density and heat capacity of the sample; Q is the reaction heat; k_o and E denote the Arrhenius pre-exponential and activation energy; R is the gas constant; A is the heat transfer surface and V the volume of the sample.

The left-hand side of equation (10) gives the rate of heat build-up in the sample. The first term on the right is the rate of heat generation and the second term represents convective heat loss to the environment. The dependences of the heat-generation and the heat-loss terms are compared on the Semenov diagram in Figure 4. The former shows an exponential-like increase with temperature whereas the heat loss term only varies linearly with temperature. Consequently there are two possibilities with respect to the location of the heat loss curve relative that for the heat-generation. If the two curves intersect at a low temperature, a stability analysis shows that the temperature will be maintained at the temperature corresponding to the lower point of intersection. However, if the curves do not

intersect, then the sample will rapidly self-heat to a very high temperature and a thermal run-away will occur. The critical condition for ignition is found when the heat-loss curve is a tangent to the heat-generation one. At the tangency temperature T_*, the slopes of the curves (with respect to the temperature) are equal in addition to their values, and these conditions yield:

$$\rho Q k_o \exp(-E/RT_*) = h(A/V)(\mathrm{T}_*-\mathrm{T}_o) \tag{11}$$

And

$$T_* - T_o = RT_*^2/E \approx RT_o^2/E \tag{12}$$

where the approximation is justified by the fact that it gives a conservative estimate and the realization that in practical situations $\beta = RT/E \ll 1$. Substitution and simplifying finally results in the condition for the critical temperature of ignition. It is conveniently stated in terms of the Semenov number defined as

$$Se = \frac{\rho VQEk_o}{hART_o^2}\exp(-E/RT_o) \tag{13}$$

The condition for ignition is given by the requirement that $Se > Se_{\mathrm{crit}}$ where, for the simplistic model described here $Se_{\mathrm{crit}} = 1/e$ (where e is the natural number).

This condition is general except that the expression for the critical Semenov number needs revision for more realistic conditions [60]. For example, it is not realistic to assume that there are no temperature gradients inside the sample nor is a zero order rate equation realistic. This means that the effects of conversion through the reaction kinetics must be accounted for. This has been done and finds expression in the Frank-Kamenetsky number that is used to define the critical condition

$$Fk = \frac{\rho QEd^2k_o}{4\lambda RT_o^2}\exp(-E/RT_o) \tag{14}$$

where d is a characteristic dimension of the sample (thickness of an infinite slab, or diameter of a sphere or an infinite cylinder). If the reaction follows n^{th} order kinetics, then

$$Fk_{crit} = a_{crit}(1+\beta)f(\gamma) \tag{15}$$

where $\beta = RT_i/E$; a_{crit} equals 0.88, 2.00 or 3.32 for a slab, cylinder or sphere respectively; $f(\gamma)$ is a correction factor that depends on $\gamma = C_pRT_o^2/QE$, with

$$f(\gamma) = 1 + 2.703(n\gamma)^{2/3} \tag{16}$$

Induction time for a bulk sample. The heat generation rate with temperature increasing does not grow indefinitely but tends to the limit ρQk_o. Consider the situation where the heat loss term is negligible compared to the heat generation term. This corresponds to a further shift of the heat loss line to the right so that there is no intersection with the heat-generation curve. Disregarding the second term on the right of equation (1) yields the differential heat balance describing the adiabatic heating of the sample

$$\rho C_p \frac{dT}{dt} = \rho Qk_o \exp(-E/RT) \tag{17}$$

Employing the initial conditions: $t = 0$: $T = T_i$ and conducting an approximate analysis yields the following expression for the adiabatic time, taken as the induction period [60]:

$$t_{ad} = (1+2\beta)\frac{C_pRT_i^2}{k_oQE}\exp(E/RT_i) \tag{18}$$

where, as before, $\beta = RT_i/E$. If the reaction follows n^{th} order reaction kinetics, the ignition time is given by

$$t_{ign} = (n\gamma)^{-1/3}t_{ad} \tag{19}$$

More precise analyses for more realistic situations have been done and were reviewed elsewhere [60, 62]

Ignition in a delay column. Elementary models for ignition in a delay column consider a semi-infinite reactant in one dimension [63]. This is equivalent to assuming that the tube wall in Figure 3 provides perfect insulation, thus allowing the reaction inside the composition to proceed adiabatically. Ignition is considered to arise on the flat outer surface. Bulk physical properties (thermal conductivity, density, thermal capacity, heat of reaction) as well as the activation energy and pre-exponential factor defining the chemical reaction are assumed constant, i.e. independent of conversion and temperature. Two heating conditions are considered throughout the process, i.e. either a constant incident heat flux or a constant surface temperature are applied suddenly, and the time to ignition is estimated.

The simplest model for ignition assumes that the ignition temperature, T_{ign}, is a constant for a given composition [58]. It is taken as that temperature to which composition must be heated for it to ignite and combust without further energy input from external source. The most rudimentary model ignores reagent conversion [58]. This simplifies the governing differential equation to transient heat conduction into a semi-infinite slab subjected to a constant heat flux entering at the ignition end of the column. The ignition time is estimated by calculating the time necessary for the outer surface to reach T_{ign}. This approach yielded the following expressions for the ignition time for a sample subjected to a constant incident heat flux [58]:

$$t_{ign} = \frac{\lambda\rho C_p}{\pi e}\left(T_{ign} - T_a\right)q^{-2} \tag{20}$$

The required energy input to achieve ignition is

$$Q_{ign} = \frac{\lambda \rho C_p k_o^2}{\pi e q} (T_{ign} - T_a)^2 \quad (21)$$

This analysis can be extended to include the effect of the heat contributed by the chemical reaction [63]. It is assumed that the ignition onset occurs at a low degree of substance conversion, with the kinetics described by a zeroth-order reaction. For this situation the governing equation for the elementary model is:

$$\frac{\partial T}{\partial t} = \alpha \frac{\partial^2 T}{\partial x^2} + \frac{Q}{\rho C_p} k_o \exp\left(-\frac{E}{RT}\right) \quad (22)$$

The two different types of boundary conditions can be considered:

(a) A constant heat flow through the outer surface that causes the surface temperature to increase: $q_o = -\lambda(\partial T/\partial x)|_s = \text{constant}$. Analysis leads to the following result for the ignition time:

$$t_{ign} = 0.46 \lambda \rho C_p (T_b - T_i)^2 \left[1 + \frac{12RT_b^2}{E(T_b - T_i)}\right] q_o^{-2} \quad (23)$$

(b) Application of a constant surface temperature in which case the heat flow at the surface drops with time: $T_s = T_o = \text{constant}$. Analysis lead to the following approximate expression

$$t_{ign} = \frac{(T_o - T_i)}{k_o} \exp\left(\frac{E}{RT_o}\right) \quad (24)$$

In reality the initiation of the pyrotechnic reaction can be accomplished by a variety of methods. This includes ignition by a combustion wave from a chemical reaction (or igniter) [64]. The ignition of the starter composition in the time delay train is initiated by a spit from the shock tube. This situation is probably more correctly described by a heat impulse condition which has been dealt with elsewhere [63]. A physical interpretation of the requirement necessary for achieving ignition for this situation is as follows. With an impulse supplying the energy, ignition can occur only in the case when, at the moment of cessation of the external heating, the heat removal from a reaction zone is less than a critical one defined by

$$q_{crit} = \sqrt{2\lambda Q k_o \left(RT_s^2/E\right) \exp(-E/RT_s)} \quad (25)$$

In other words, for the substance to be ignited, it is necessary to create at the outer surface a heated layer of sufficient depth. Ignition will not occur if the heating-up ceases before this layer has been formed.

Zhang and Stangle [57a] employed the model of Section 4.2 to investigate ignition in a delay element. They introduced dimensionless groups associated with the rate of local heat generation (β), activation energy (γ), the rate of surface heat loss by convection (ω), the rate of surface heat loss by radiation (δ), and the rate of reaction (λ). The reaction kinetics were assumed second order in conversion. The differential equation (8), in its dimensionless form, was solved numerically subject to the boundary conditions stated in equation (9). A parametric analysis was then performed to determine the ignition criteria for gasless self-propagating reactions through an ignition temperature analysis. The relative significance of each of these parameters on the ignition of the self-propagating combustion reaction was evaluated to be $\gamma > \beta > \delta > \omega$. The key result of this study was that only compositions with $\Delta H_R/C_p > 1500$ K are capable of self-propagating combustion reaction without external energy input. This value can be used as an approximate guide for the existence of self-sustaining combustion.

Scrutiny of the ignition expressions leads to the following conclusions. Overall, ignition is promoted by low thermal conductance, low heat capacity, small particle sizes, and high heat of reaction [65]. Excessive heat loss to the environment is the main reason for failure to propagate through the entire length of the column. This is more likely to occur in small diameter metal tubes and at low ambient temperatures.

Ignitability is also affected by stoichiometry as the data for both ignition temperatures and time to ignition measurements (measured at 800 °C) for the silicon/bismuth oxide showed [66]. Furthermore, the stability of the reactant oxides has important effects on the ignitability of the pyrotechnic mixtures [64]. Some oxides (e.g. TiO_2, NiO and Nb_2O_5), are so stable and inert that an external source of oxygen, e.g. air, is required for ignition. The appearance of a liquid oxide phase (e.g. B_2O_3 which melts at 450 °C) or the volatilization of the reactant oxides (e.g. MoO_3 or WO_3 which sublime) may increase the rate of the oxidation-reduction reaction and thus facilitate ignition. The ignition event can also result from the oxygen liberated by the decomposition of the oxidant (e.g. V_2O_3, CrO_3, and BaO_2).

4.4 Burning Rate in Delay Tubes

Spice and Staveley [67] were among the first to measure the linear rate of the self-propagating reaction in binary solid mixtures of an oxidizing and a reducing agent. The powders were compressed in the form of cylindrical rods. It was observed that, when ignited at one end, the rate of progression of the reaction zone along the axis is fairly uniform and reproducible for a given mixture. This type of behavior, generally referred to as 'layer- to-layer' burning, is observed only when the reaction is strongly exothermic, i.e. when a considerable amount of heat is evolved in the chemical change [68]. Booth [68] developed one of the first general theories for the variation of the rate of progression of the

reaction zone in terms of the physical properties of the powder, its chemical composition and the kinetics of the slow reaction between the constituents.

The burning process in actual pyrotechnic time delays is actually analogous to the self-propagating high temperature synthesis (SHS) method for ceramics [31]. In fact, SHS research has driven mathematical progress with respect to understanding the combustion process in pressed powder columns and how the burn rate is affected by the numerous variables [31]. Of these the state of subdivision of the powders and the exothermicity of the reaction [68], in addition to the natures of the fuel and oxidant and the mixture stoichiometry [67], appear to be the most important. However, slow-reacting compositions have to be highly exothermic in order to be sustainable [69]. Adjusting the reagent stoichiometry, or adding inert substances, affects the exothermicity, i.e. the reaction temperature, and hence the rate. The thermal diffusivity of the mixture is also important as wave propagation depends on repeated re-ignition of adjacent layers along the burning path. Good mixing and adequate inter-particle contact between reactants is required for stable and reproducible burning owing to the low values of the diffusion coefficients [40].

Numerous theoretical models for the self-propagating layer-to-layer reactions in the solid phase have been developed [68–70]. They link the rate of progression of the reaction zone, along a cylindrical column, with the chemical nature and physical properties, as well as the state of subdivision of the powders and the apparent reaction kinetics between the constituents [68]. It is implicitly assumed that the composition is well mixed. Two limiting kinetic cases can be discerned. Purely homogeneous chemical kinetics controlled or heterogeneous mass transport (i.e. diffusion) limited [70a]. Both types of processes may be analyzed in the realistic limit of large activation energies for either diffusion or reaction kinetics. The simplest chemical kinetic theory [69] assumes composition- and temperature-independent physical properties, absence of phase transitions, a thin reaction zone and postulates a gasless exothermic n^{th} order solid-state reaction and an Arrhenius-type temperature dependence for the rate constant. This yields the following expression for the linear burning rate under adiabatic reaction conditions:

$$u^2 = \frac{g(n)R\,T_c^2}{E_a(T_c - T_o)}(\alpha k_o)e^{-E_a/RT_c} \tag{26}$$

where u is the combustion wave velocity in $m\,s^{-1}$; $g(n)$ is a dimensionless function of the reaction order n that assumes values between 0.5 and 2; R is the gas constant ($8.314\ J\,mol^{-1}K^{-1}$); T_o is the initial temperature and T_c is the maximum temperature of the burning column in K; k_o is the Arrhenius pre-exponential factor of the reaction rate constant in s^{-1}; E_a is the apparent Arrhenius activation energy in $J\,mol^{-1}$; and α is the effective thermal diffusivity in $m^2\,s^{-1}$.

Alternatively, when the condensed phase reactions are mass and energy transport limited, the reaction rate is determined by the thermal and mass diffusivities together with the reagent particle sizes [71]. The latter determine the thickness of the diffusion barrier. Analysis of the diffusion controlled situation requires information on the geometric arrangement of the reacting particles including particle sizes. Quantitative correlations between the reaction rate and the number of contact points between particles are potentially useful for reaction-rate analysis of a wide range of powder systems in which particle sizes and the mixing ratio are varied independently [72].

Once again, only the simplest theoretical model is considered presently as it suffices to rationalize the available experimental observations. The reactant geometry is approximated by a structure of alternating layers of the components with the relative thicknesses determined by the reagent stoichiometry and their densities [70e, 71]. This yields the following expression for the velocity of propagation [70e].

$$u^2 = \frac{6\,RT_c^2}{E_D(T_c - T_o)}\left(\frac{\alpha\,D_o}{d^2}\right)e^{E_D/RT_c} \tag{27}$$

where D_o [$m^2\,s^{-1}$] and E_D [$J\,mol^{-1}$] are the effective pre-exponential and apparent activation energy for the diffusion coefficient and d is a measure of the particle size distribution of the reactants expressed in m. The interpretation of the other variables is similar to those in equation (26).

The two equations indicated above hold in the asymptotic limit where the ratio of typical spatial temperature differences to the Frank-Kamenetsky temperature is a very large parameter, i.e. it holds for large Zel'dovich numbers,

$$\theta = E(T_c - T_o)/RT_c^2 \gg 1 \tag{28}$$

Equation (27) predicts that the burning rate should vary linearly with the inverse of particle size. Numerous studies on the effect of the fuel particle size, especially on compositions containing Si as fuel, confirmed that the burning rate increases with decreasing particle size and increasing surface area [20, 73]. Wider particle size distributions lead to increased packing density which in turn also translates into faster burning rates [74].

Equations (26) and (27) both suggest that a slow burning rate requires a composition characterized by a reaction with a very large activation energy and a relatively low exothermicity. They also identify the combustion wave temperature, T_c, as a significant variable affecting burning rate. Adjusting stoichiometry and the addition of inert substances can control it. The temperature of the wave front is also affected by transverse heat losses and hence by the nature of material used for tube construction.

Equations (26) and (27) were derived under the assumption that no phase transition occurs. However, the effect of the latter on the steady reaction wave propagation rate

only expresses itself in terms of a reduction in the combustion temperature T_c. Thus it may easily be taken care of by considering an effective heat capacity for the mixture [75].

More sophisticated theoretical models, that deal with the ignition and combustion of beds of compacted reactive particles [13, 61a, 70d, 76] or with layered media (e.g. multilayer foils) [77], are available. Aspects such as variable physical properties (e.g. thermal conductivity, density, and heat capacity), the inclusion of non-reacting diluents and differences in the thermophysical and chemical properties of the reactants compared to the products [61a], interparticle diffusion effects [78] are among the issues addressed in these works.

The contact points (or alternatively the contact surface area) between the reacting particles is an important issue, especially so when the mechanism involves solid-solid reactions. Similarly, the contact area between reactants has a strong influence on reactions in powder mixtures even when one species may melt [79]. It has been found that the reactivity of the system can be expressed in terms of the number of contact points between the two components, together with the particle size ratio, in addition to the nature of the reacting system [80]. Brown *et al.* [81] tested this hypothesis for various pyrotechnic mixtures. However, they had to assume uniform spherical particles in their calculations. Despite this severe approximation, they found a qualitative connection between the calculated numbers of contact points and the measured burning rates. Since then much progress has been made with respect to calculating the contact area between reactants, even for ternary systems where the third "component" can represent pores [79]. The approach was to mesh the surface of the particles with small 'tiles', and to solve a combinatorial problem formulated to map all the tiles onto each other.

Following a different approach, Dalvi and Suresh [82] developed an improved contact-point model that showed the right asymptotic behavior for large numbers of contact points, i.e. the expression converges to continuum behavior. The validity of this model, with respect to the formation of tricalcium aluminate from its immediate precursors as a candidate reaction, was experimentally confirmed [83]. It would be interesting to see these types of models being applied to pyrotechnic systems.

The intrinsic granularity of compositions comprising compacted powders is also specifically addressed in the so-called "hot spot" models [84]. The 'hot spots' are taken to correspond to the locations of burning particles. Therefore, in these models the combustion wave propagation manifests itself as a process of sequential ignition and burning of particles. This means that the size of the particle and their distribution influences the burning rate. Hence, the "steady" combustion wave speed is related to particle ignition temperature, particle geometry and the ratio of heat diffusion to reaction times.

5 Factors Affecting the Burning Rate

Ultimately the intrinsic burning rate of a delay composition is determined by the chemical nature of the ingredients, their relative proportions and the thermo-physical properties of the system. However, apart from those intrinsic to the compositions themselves, a wide range of other factors can influence the burning rate. This includes aspects related to the device into which they are filled and combustion environment itself [11]. However, variation of the chemical constituents of a binary mixture generally has the greatest effect on burning rate, followed often by variation of the composition in a given combination [29].

5.1 Thermochemistry: The Heat of Reaction and Stoichiometry

Spice and Staveley [67] measured the linear rate of the self-propagating reaction, and of the heat of this reaction, in compressed binary solid mixtures of an oxidizing and a reducing agent. The thermochemical results allowed conclusions to be drawn about the chemistry of the reactions involved and the maximum temperatures reached during burning. They were first to discuss the dependence of the rate of reaction on the heat it evolves and to give an explanation for the fact that the rate usually reaches its maximum at a higher amount of reducing agent than that at which the heat of burning has its greatest value [67].

In practice it is found that $T_c > 2\ T_o$. Note that, in the absence of phase changes, external heat losses, and under the assumption of constant physical properties, $T_c = T_o + Q/C_p$. Taking cognizance of these relationships, differentiation of equation (26) gives

$$\frac{du}{dQ} = \frac{u}{2}\left[\frac{T_c - 2T_o}{T_c(T_c - T_o)} + \frac{E}{RT_c^2}\right] > 0 \qquad (29)$$

Equation (29) indicates that a fuel that produces more heat on oxidation, e.g. boron ($\Delta H_R = 58.96\ \mathrm{MJ\,kg^{-1}}$), should react faster than a less exothermic fuel such as silicon ($\Delta H_R = 32.40\ \mathrm{MJ\,kg^{-1}}$).

Stoichiometry can also influence the product spectrum as shown in Table 2 for the reaction of silicon with PbO_2 [37]. Such changes also influence the heat released. This is illustrated in Table 3 for the oxidation of manganese metal.

Heat is also removed from the system when a component undergoes a phase change at higher temperature during the combustion process. This has the effect of slowing down the progression of the burning front. Heat loss through the tube walls has a similar effect but is discussed in more detail in Section 9.4.

The effect that the fuel to oxidant ratio has on the pyrotechnic reaction in binary mixtures has been well-studied on an extensive range of delay compositions [20, 26, 39, 73a, c, 81, 85]. The results, in most cases, show an increase in

Table 2. Proposed reactions for the Si/PbO_2 system.

Si (wt-%)	Reactions	Products [37]	$-\Delta H_R$ (MJ kg^{-1})
2.85	$Si + 4PbO_2$	$Pb_4SiO_6 + O_2$	0.71
3.77	$Si + 3PbO_2$	$SiO_2 + 3PbO + {}^1/_2\ O_2$	1.00
5.55	$Si + 2PbO_2$	Pb_2SiO_4	1.64
7.26	$2Si + 3\ PbO_2$	$2PbSiO_3 + Pb$	1.89
10.5	$Si + PbO_2$	$SiO_2 + Pb$	2.38
15.0	$3Si + 2PbO_2$	$SiO_2 + 2SiO + 2Pb$	1.00
19.0	$2Si + PbO_2$	$SiO_2 + Pb + Si$	2.15
26.1	$3Si + PbO_2$	$Pb + Si + 2SiO$	-.23

Table 3. Effect of reagent stoichiometry on the heat of oxidation of manganese [11].

Stoichiometry	$-\Delta H_R$ (MJ kg^{-1})
$Mn_{(s)} + 0.5\ O_{2(g)} \rightarrow MnO_{(s)}$	5.43
$Mn_{(s)} + O_{2(g)} \rightarrow MnO_{2(s)}$	5.98
$2\ Mn_{(s)} + 1.5\ O_{2(g)} \rightarrow Mn_2O_{3(s)}$	6.07

burn rate from fuel-lean compositions until close to the stoichiometric amount of fuel. A maximum burn rate is often observed just above the stoichiometric amount of fuel. The burn rate once again decreases as the composition becomes more fuel-rich. Compositions containing pure metal fuels tend to show larger deviations from this concept due to the high thermal conductivity of the metals leading to more efficient energy transfer.

5.2 Particle Size, Particle Size Distribution and Particle Shape

The average particle size and particle size distribution of both the fuel and the oxidant has been shown to significantly influence the burn rate of pyrotechnic delay compositions. The particle-size of the fuel is another extremely important factor affecting burning rates [29]. The burning rate varies inversely with iron particle size in the system Fe/BaO_2 system irrespective of the stoichiometry of the mixture (i.e., Fe 25 or 36 wt-%) [67]. This accords with the predictions of equation (27). The effect of particle size on Si has also been extensively researched [20, 73]. In all cases the effect of the particle size was most significant in large (micron-sized) particles where particle size decreases of only a few microns lead to burn rate increases of over 200 %. As expected, the burning rate increased as the particle size decreases and the surface area available for reaction increases. A significant increase in the burning rate is found when the particle size changes from being in the micron-size range to nano-sized particles. For further reduction in particle size in the nano-sized range there is not a corresponding increase in burn rate. This is likely due to the increase in the relative content of the passivating oxide layers present on the surface of the nano-fuel particles that inhibits the reaction. The effect of this oxidation layer is however not fully understood as different studies have led to contradictory conclusions [46, 85–86]. One conclusive result is that the nano-sized particles ignite much easier and burn faster than large particles [46]. The effects of using nano-sized particles ($<$ 100 nm) and applying them to pyrotechnic delay elements is currently an active area of research [46, 87].

Unlike the case for micron-sized aluminum powders, thermite compositions based on nano-sized Al particles show a decreased flame speed with increase in compaction [88]. This unexpected behavior has been attributed to a melt-dispersion oxidation mechanism and a convective mode of flame propagation [89]. It appears that the volume change due to the melting of Al induces huge pressures that cause catastrophic spallation of the oxide shell covering the particles. The subsequent unloading wave creates high tensile pressures that cause rapid dispersion of liquid aluminum clusters. Consequently the oxidation reaction is not limited by diffusion and very fast burning rates are achievable with nanothermites.

Very little has been established on the effect of particle packing on the burning rate of pyrotechnic delay elements. Dugam *et al.* [74] investigated the effect of particle size distributions and found higher packing densities for wider distributions of oxidant particle sizes and lower packing densities when the fuel and oxidant particles have similar sizes. Montgomery *et al.* [90] investigated the effect of particle packing through variations in fuel to oxidant particle size ratios. The particle packing was found to be unaffected by the volumetric ratio of the fuel to oxidant particles. The effect of particle porosity was however found to play a significant role.

For the same nominal mesh size, flakes show a greater reactivity than spherical particles and they can be raised more quickly to their ignition temperature [37]. Similar behavior is found when comparing jagged particles with smooth ones.

5.3 Effect of Thermal Conductivity and Density on Wave Propagation Rate

The burning front in a compressed delay composition propagates in a layer-by-layer fashion along the burning path. This requires repeated re-ignition of adjacent layers. According to equation (26) the thermal conductivity and density are the primary physical properties that determine the rate of burning. With all other parameters and properties fixed, it predicts that $u^2 \propto \lambda/\rho$ so that it can be deduced that:

- Increasing the thermal conductivity enhances the burning rates, and
- The more loosely the powder is packed, the more rapid is the burning velocity [68].

The last deduction is counter-intuitive but borne out in practice! However, it should be remembered that the model used is based on apparent rate laws and physical constants

that are interrelated. In reality it is difficult to separate individual effects as the kinetics are strongly dependent on particle packing and hence density.

Adding inert material changes the thermal conductivity of the mixture. Adding low thermal conductivity fillers, e.g. kaolin, reduces the rate of heat transfer through the mix. Conversely, adding thermally conductive fine Cu and Ag powders to gasless delay compositions can significantly increase the rate of burning [37]. However, the thermal conductivity of the composition can be too high! Hardt and Holsinger [91] studied the reaction characteristics of several exothermic intermetallic reactions experimentally. Boron and carbon mixtures with titanium and zirconium were found to be self-propagating at room temperature. However, aluminide mixtures and other types of intermetallic reaction mixtures reacted only at elevated temperatures. However, self-sustaining reactions were initiated when additives, which reduced the thermal conductivity, were included in the formulations.

5.4 Effect of Gassing

Aldushin and Zeinenko [92] and Norgrove *et al.* [93] investigated the case of a steady combustion wave in a porous reacting mass. They considered the effect of gas formation on the combustion wave. Depending on the confinement conditions, the produced gas moved either forward or backward relative to the flame front [93]. For a sealed element, the ratio of gas flow forwards to gas flow backwards will depend on the confinement conditions and will change as the flame passes along the delay element. When the gas moves ahead of, rather than through, the flame, the reduction in the amount of mass heated leads to a relative increase in the flame temperature. According to Aldushin and Zeinenko [92] it may even exceed the adiabatic reaction temperature. Consequently the mixture burns noticeably faster [93]. When the gas moves with the combustion wave, it may assist the propagation of the front by means of a convective mechanism [92]. The travelling gas phase preheats the system, increases the adiabatic combustion temperature and accelerates the rate of burning.

5.5 Effect of Pressure

The burning rate of most pyrotechnic compositions is expected to increase with pressure according to Vieille's law:

$$u/u_o = (P/P_o)^n \quad (30)$$

The constant n is system specific and typically varies between 0.1 and 0.6. Its value depends on the amount of gas produced during the combustion.

In practice it is found that burning rate initially increases but that it stabilizes or even decreases above a certain threshold limit. Consider, for example, the slow burning B/Si/$K_2Cr_2O_7$ (4:5:91) gasless delay formulation used in accurate missile delay detonators. Its burning rate increases sharply with pressure between 0.1 and 0.4 MPa. Thereafter, the burning rate increase is slower. Above about 2 MPa the burning rate is unaffected by pressure [41]. Other examples include the Si/PbO, Si/Pb_3O_4 and Si/$KMnO_4$ systems. In all of these the velocity of propagation increased with pressure until a maximum value, depending on the composition, was reached [37]. With the silicon/red lead compositions the burn rate decreases beyond pressures of approximately 6.90 MPa. This effect was attributed to pressure stabilization of the PbO phase in the reaction mixture [37].

5.6 Environmental Factors

The temperature of the delay column, both prior to and during combustion, also influences the burning rate. For military and aerospace applications, delay elements must provide an accurate time interval, which is specified to within certain limits over a set environmental temperature range, often between -40 and $+60\,^{\circ}C$ [11]. Depending on the formulation, most gasless delay compositions burn about 25% slower/faster at the lower/higher temperature than they would at room temperature. Gassy delay compositions are less affected by temperature variations [11]. Boddington and Laye [94] conducted burning rate measurements on three gasless pyrotechnic mixtures over an extended range of ambient temperatures.

6 Formulating Delay Compositions

6.1 Pyrotechnic Delay Compositions

The delay composition should be non-hygroscopic, stable on storage and have good flow properties for the filling of elements [14]. Preferred delay compositions will burn in an essentially gasless fashion (volume of gas evolved less than 10 mL g^{-1} of mixture [95] and at a constant predetermined rate. The reaction must be exothermic, self-sustained and self-contained [15]. Mclain [37] has enumerated the factors that should be considered when designing a new pyrotechnic time delay compositions. Preferably the formulation should be non-hygroscopic; stable during handling and compaction; not affected by temperature; be readily ignitable and react without releasing gases to minimize the effects of pressure on the burn rate. A relatively low melting point or a polymorphic transition at a relatively low temperature tends to be beneficial [37].

6.2 Selecting the Fuel

Table 4 lists some of the fuels used in delay compositions. Silicon is probably the most commonly used fuel. Silicides such as ferrosilicide ($FeSi_x$) and calcium silicide ($CaSi_2$) [98] can also be used. The oxidation of transition-metal silicides occurs at a faster rate than the oxidation of pure silicon and refractory-metal silicides, possibly owing to higher electron mobility [99]. Metal fuels include Al, Al/Mg, Cr, Fe, Mg, Zr, W and Zn. Table 4 lists phase transition temperatures and adiabatic flame temperatures for the combustion of selected fuels. Organic fuels (e.g. sorbitol, hexamethylenetetramine, potassium benzoate, etc.) and some inorganic fuels (C, S, P) generally produce much gas during combustion. This causes pressure build-up that affects the reaction rate and thus the delay time. As a result, the main charge may be ignited prematurely [9].

Table 4. Adiabatic combustion temperature (T_{ad}); melting (T_m) and boiling points (T_b) for metal or metalloid fuels and their stable oxides at 298.15 K and 0.1 MPa [96,97]. Carbon is included for comparison purposes.

Fuel	T_m	T_b	Oxide	T_m	T_b	T_{ad}	Ref.[c]
B	2349	4200	B_2O_3	723	2130[a]	3300	1
C			CO_2			2670	1
Mg	923	1336	MgO	3105	3873	3432	2
Al	933	2791	Al_2O_3	2328	3253	4005	2
Si	1867	3538	SiO_2	1986	3220	3240	1
Ti	1939	3631	Ti_2O_3	2115	3300	3993	2
Fe	1809	3133	FeO	1650	3678[b]	3400	2
Zr	2125	4703	ZrO_2	2950	4548	4278	2
Mo	2896	4912	MoO_3	1068	1428	2660	1
W	3695	6203	WO_3	1746	1995	3100	1
Pb	874	2295	PbO	1161	1750	1830	1

[a]Sublimates at 1773 K; [b]Decomposition temperature (T_d); [c]References: 1 = [97], 2 = [96].

Usually it is found that the maximum burning rate occurs at a somewhat higher reductant content than does the maximum heat of reaction. This displacement is generally greater for metal reductants such as Fe, Sb and Mn and is smaller for non-metal reductants such as S and C or the metalloids B and Si [37]. This phenomenon is associated with the effect of heat transfer on columnar burning.

The slope of the burning rate curve is usually steeper below the maximum than above (reductant above stoichiometry). This is ascribed to the fact that the addition of a good heat conductor, while it causes departure from the stoichiometry, may increase the thermal conductivity sufficiently to cause a net increase in the burning rate. In effect, an excess of either oxidant or fuel represents an inert diluent. Excess oxidizer acts like a heat insulator and this retards the burning. In contrast, the excess of a conductive metal reductant accelerates the burning rate [37].

6.3 Selection of the Oxidizer

The following heavy metal oxides are suitable for use in delay compositions: Fe_2O_3, Sb_2O_3, Cu_2O, Bi_2O_3, Pb_3O_4, PbO_2, ZnO, and MnO_2. Complex oxides, e.g. $Cu_2O.Sb_2O_3$, $ZnO.Sb_2O_3$ or $BaO.MoO_3$ are also used [98]. Nitrate, chromate, chlorate and perchlorate salts are mainly used for other pyrotechnic effects (light emissions, signaling smokes, whistling sounds, etc.) [9]. Conkling [15] discusses factors affecting oxidizer selection. The most important factor is the relative affinity towards oxygen between the metals of the oxidizer and the fuel.

6.4 Binders for Pyrotechnic Compositions

It is common practice to add binders to pyrotechnic compositions in order to obtain granules, which are easier to process. Binders can be organic or inorganic in nature. Organic binders include synthetic polymers, biopolymers (dextrin and starch) and natural resins e.g. gum Arabic and gum acaroid. Inorganic binders include gypsum, water glass and bentonite. The type and amount of the binder used, tends to affect reaction parameters such as burn rate and energy output [33]. Polymeric binders play multiple roles in pyrotechnic compositions and, in general they contribute towards better mechanical strength and provide moisture-absorption resistance. This latter leads to improved shelf life. Binders are also used to maintain the homogeneity of the blended mixture. They also play a minor role as internal lubricants during the compacting phase [98].

Binders also contribute significantly to the performance of composition by lowering the activation energy (ignition temperature) and increasing the combustion temperature and burning rate [100]. Boiled linseed oil (~2%) was added to a 15 wt-% Sb (< 53 μm)/$KMnO_4$ composition, which does not normally burn. The composition with the binder did burn. Addition of 2 to 3% of acaroid resin to a mixture of Mg/BaO_2 lowered the ignition temperature by more than 200 °C [101].

Generally, the silicon and red lead system is slurried in an aqueous solution of a polymer, e.g. carboxymethyl cellulose, which aids dispersion and acts as a binder. The slurry is stirred thoroughly to ensure even distribution of the two species, and the water is evaporated by placing the slurried composition on a steam-heated copper tray. The binder prevents segregation of Si and Pb_3O_4 [73a]. It was also observed that the addition of the binder makes the composition more sensitive to impact and friction.

Han and Yan [102] studied the effects of binders (shellac and fluoro-elastomer) on storage stability of a silicon delay composition. Both improved temperature and humidity stability under storage conditions. However, the binders behaved like "heat sinks" reducing the burning rate and delay precision of the composition.

Spontaneous ignition ensues when potassium permanganate comes into contact with organic substances such as glycerol, ethylene glycol, acetaldehyde, etc. [103]. It is therefore not advisable to use organic binders when this oxidizer forms part of the pyrotechnic composition.

6.5 Additives

The burning rates of a binary system can be modified by conversion to a ternary system through incorporation of additives [26, 100, 104]. These additives can either be inert or chemically active. They can function as processing aids, fluxing agents, heat sinks, thermal insulators, sensitizers or catalysts within the main pyrotechnic composition. The presence of additives influences any of the activation energy, heat of reaction or efficiency of energy feedback in a given composition [105].

Additives are mixed to the main composition to effect the following: ensure intimate contact between the particles; protect against the environment; prevent premature reaction or to improve mechanical properties. Addition of a third component can alter the burning rate of a binary system. Such additives may be chemically inert substances; an additional fuel; an additional oxidant, or a source of some reactive intermediate. Additives include:

Formulation aids such as anti-caking agents (pyrogenic SiO_2, Al_2O_3, $CaCO_3$, $MgCO_3$) and lubricants (graphite, talc, wax, Teflon, silicone). For example, the addition of 1–5% of waxy lubricants (stearic acid or calcium stearate) was found to have a profound effect on the burning rate of the W/Sb_2O_3/KIO_4 delay composition [104b].

Catalysts, e.g. Fe_2O_3, $CuO.CrO_2$, V_2O_5 and MnO_2, are sometimes used in pyrotechnic compositions. These act by lowering the decomposition temperature of the oxidizer which in turn lowers the ignition temperature of the composition [17]. Sensitizers are sometimes added to compositions with a high ignition temperature. They act by reacting before the main reaction to provide the heat required to initiate the main reaction [106].

Burning rate modifiers. Since burning propagates by re-ignition from layer-to-layer along the burn path, the thermal diffusivity of the mixture plays a significant role in the burn rate [107]. The addition of inert materials may alter the thermal properties of the system, leading to a reduction in the rate of heat transfer through the mix, thus slowing the reaction. Mclain [37] noted that the addition of inert materials with low thermal conductivities, such as kaolin, reduce the burn rate, while thermally conductive fine Cu and Ag powders increase it. Addition of hollow spheres and fumed silica to a number of formulations significantly decreased the burn rates [26, 73c].

Inert material, e.g. kieselguhr, diatomaceous earth, fumed silica, may also act by reducing the contact between fuel and oxidant [100]. This alters the thermal properties of the system (e.g. additives of high heat capacity may lower the combustion temperature). Inert additives with a low melting point may act as fluxes. The effect of inert additives such as Al_2O_3 or SiO_2 on the systems studied has generally been the expected decrease in the burning rate [29], probably through physical blocking of reactant contact, combined with heat capacity effects. The presence in, or addition of small amounts of water to the systems had a similar effect. Increasing the proportion of additive (or water) eventually causes failure of burning. Table 5 illustrates the use of the inert additive SiO_2 for reducing the burning rate in the Sb/$KMnO_4$ system.

Table 5. Effect of SiO_2 on the burning rate of a 30:70 Sb:$KMnO_4$ composition [42].

SiO_2 content (wt-%)	Burning rate (mm s^{-1})
0	1.9
7	1.6
19	1.3

Fluxes. Fluxes are materials that reduce the effective melting temperature of a mixture. They introduce an amount of liquid phase that accelerates the solid-solid reactions. Fluxing agents are metals or metal compounds that melt at temperatures that are lower than the burning temperature of the base composition. The molten phase increases the contact surface area, resulting in faster burn rates and fewer failures upon ignition [17, 100].

Addition of aluminum particles. Addition of thermally conductive material (e.g. fine Cu and Al powders) may increase the burn rate of gasless delay mixtures [37]. Instead, addition of aluminum powder to $Si + Sb_2O_3$ and $Si + CuSb_2O_4$ decreased the burn rate [73c]. The burn rate of pyrotechnics is sensitive to the reaction temperature. This effect could therefore be due to a dilution effect and also to the latent heat of fusion being absorbed. Aluminum melts at 660 °C, i.e. well below the expected adiabatic reaction temperature.

Addition of fumed silica. Fumed silica is a flow-conditioner additive, especially the hydrophobic version [108]. It helps to overcome particle agglomeration, allowing powders to become free flowing. This facilitates mixing, prevents powder separation during storage of pyrotechnic devices and aids powder filling [108]. Equation (26) predicts that decreasing the heat of reaction, e.g. by adding inert thermal insulator particles, might reduce the burning rate. In accordance with this expectation, addition of 1% fumed silica reduced significantly the burn speed of compositions with silicon as fuel with $PbCrO_4$, Sb_2O_3 or $CuSb_2O_4$ as oxidants. At this addition level the oxidants became free flowing powders but the silicon remained "sticky".

Carbon nanotubes. It was found that adding carbon nanotubes improves the reliability of ignition but also increases the burning rate of Si/Pb_3O_4 [109]. The nanotubes

were incorporated during the milling of the silicon into a fine powder.

Nanodiamonds. Detonation nanodiamonds proved useful as coatings on submicron-sized bismuth oxide particles [110]. They feature antifriction properties and showed impressive desensitization of the Bi_2O_3/Al system at very low levels, making it safe to handle. In addition, the presence of the nanodiamonds at ca. 1 wt-% also halved the propagation velocity of the flame front.

6.6 Empirical Rules for the Design of New Mixtures

McLain [37] recommended that the following rules of thumb be observed when designing a new pyrotechnic mixture:

- Maximize the burning rate for a given mix by using slightly more than the stoichiometric proportion of the reducing agent.
- Decrease the heat of reaction to reduce the burning rate: use a fuel that produces less heat or reacts in several different ways depending on its proportion in the mix (e. g. Mn), or add an inert thermal insulator such as powdered glass, kieselguhr, fuller's earth or fumed silica.
- Use tubes with an inside diameter of 6 mm or larger for mixtures which burn slower than 25 mm s^{-1}.
- Do not use tubes made from good heat conductors like brass or copper.
- A mixture with the highest possible propagation index should be used to achieve the desired burn rate. The propagation index ($PI = \Delta H/T_c$) provides an indicator for the ability of a gasless delay composition to sustain combustion.

The following factors should be kept in mind. The particle size and size distribution of the constituent powders; the size and chemical nature of guest particles; adsorbed gases on the particle surfaces; the loading method and pressure; the mix homogeneity; temperature and type of ignition; the mix type (low gas or gassy) and the humidity during mixing and loading.

7 Selected Thermite Delay Compositions

Table 6 shows the minimum and maximum burning rates measured for selected delay systems together with the tube materials that were employed.

Table 6. Slowest-to-fastest burning rates (*u*) reported for selected delay compositions and thermites. The tube wall materials is also indicated.

Fuel/Oxidant	Tube	*u* (mm s^{-1})	Ref.
Si/Pb_3O_4	CM	2.2–3.8	[109]
$Si/Pb_3O_4 + CNT$[a]	CM	4.4–5.85	[109]
$Si/CaSO_4$	Al	6.9–12.5	[19]
Si/Sb_2O_3	Pb	7–14	[73c]
$Si/BaSO_4$	Al	8.4–16	[18]
$Si/Cu(SbO_2)\cdot xZn\ (SbO_2)_2$	Pb	6–20	[73c]
Si/Sb_6O_{13}	Pb	4.8–20.4	[20]
$Si/CaSO_4$	Al	12.7–31.8[b]	[104a]
$Si/PbCrO_4$	Pb	10–30	[73c]
Si/Bi_2O_3	Pb	15–155	[20]
Al/WO_3	–	0.08–4.1	[113]
Al/MoO_3	–	4–12	[46]
Al/Viton B	–	12.5–40	[8]
Al/MoO_3	Acrylic	600–1000	[86]
$Al + Si/CuO + Bi_2O_3$	MS	115–655	[106]
Mn/MnO_2	Al	2.4–7.3	[114]
$Mn/CuBi_2O_4$	Al	9.3	[26]
Mn/Sb_2O_3	Pb	4.2–9.4	[90]
Mn/Cu_2O	Al	5–10	[26]
Mn/V_2O_5	Al	7.5–10	[26]
Mn/MnO_2	Al	6–19	[26]
Mn/Bi_2O_3	Al	11–22	[26]
W/Sb_2O_3, KIO_4	–	1.38[c]–2.99	[104b]
W/MnO_2	Al, SS	1.62–4.7	[28]
MgSi/Viton B	—	22–82	[8]
$B_4C/NaIO_4 + PTFE$	Al	0.48–7.69	[3]
Ti/C + 3Ni/Al	Al	2.1–38.1	[27]

[a]CNT = carbon nano tubes; [b]With aluminum as additive; [c]Calcium stearate additive; Al = Aluminum; CM = Cast metal; Pb = lead; SS = stainless steel. MS = mild steel.

7.1 Silicon as Fuel

Koch and Clement [111] reviewed the use of silicon as a fuel in common pyrotechnic and explosive compositions. Silicon combustion takes place in the condensed phase owing to the high vaporization temperatures of both Si ($T_b = 3538$ K) and SiO_2 ($T_b = 3220$ K). Silicon is by far the most studied fuel for gasless pyrotechnic time delays.

Several workers have investigated the behavior of silicon as fuel [73a, 112]. The oxidation of silicon by gaseous oxygen occurs in the temperature range of 990 to 1200 °C. The rate of oxidation in wet oxygen atmospheres is faster than in dry oxygen atmospheres. The kinetics of oxidation in wet and dry atmospheres is a function of the partial pressures of H_2O and O_2 respectively [99]. The oxidation occurs at the Si/SiO_2 interface and O_2 has to diffuse through the oxide layer for the reaction to occur. The layer of SiO_2 that adheres to the silicon particle surface represents a diffusion barrier. If this coating layer is very compact, further oxidation could be inhibited. The rate of oxidation depends on the thickness of the oxide layer. In general a parabolic rate law describes the oxide growth:

$$AL^2 + BL = t + C \quad (31)$$

where *L* is the thickness of the oxide layer; *t* is the time and *A, B* and *C* are empirical constants.

7.1.1 Silicon/Metal Oxide Systems

Figure 5 illustrates the range of burning rates that are possible with different metal oxide oxidants. Table 7 lists the particle size and BET surface areas for the reagents for which burn rates are reported in Figure 5 to Figure 7. It also shows the stoichiometric ranges where sustained burning occurs. The burning rate varies over two orders of magnitude and increases in the sequence $Fe_2O_3 < Sb_2O_3 < SnO \approx Sb_6O_{13} < Bi_2O_3 < Pb_3O_4$.

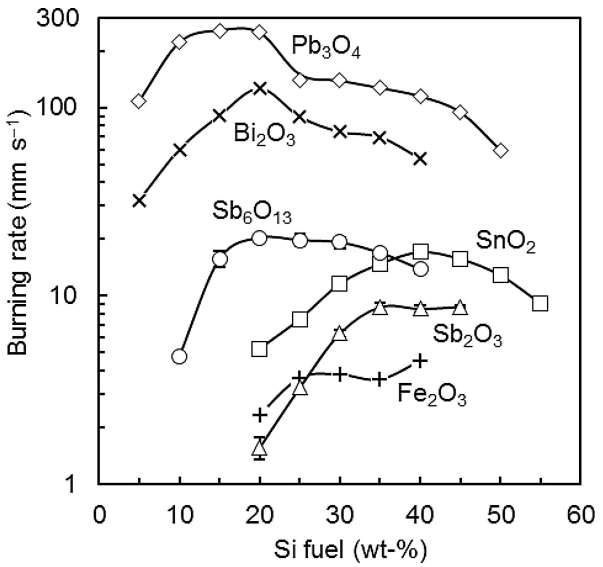

Figure 5. The effect of stoichiometry and the nature of the metal oxide oxidant on the burning rate of silicon fuel-based delay compositions. Details of the reagent properties are listed in Table 7.

Table 7. Properties of silicon fuel and metals of metal oxides reported in Figures 5 to 7. The material of construction of the delay element tubes are given too.

Tube	Oxidant/Fuel	d_{50} (μm)	BET ($m^2 g^{-1}$)	Ref.
Stainless steel channel	Si	3.4	10	[115]
	$FeSi_7$	6	3.2	
	$CaSi_2$	25.8	n.d.	
	Sb_2O_3	0.60	3.8	[116]
	Fe_2O_3	0.40	1.2	[104c]
	SnO_2	9.7	8.7	
Lead tubes	Si	0.91	10.1	[20]
	Sb_6O_{13}	n.d.[a]		
	Bi_2O_3	6.0[b]		
Cast metal tubes	Si	1.9	6.26	[73a]
	Pb_3O_4	5.0	0.422	

[a]Colloidal precursor Sb_2O_5; [b] Precursor bismuth subcarbonate

Figure 6 shows the effect of oxidant blends on the burning rate of silicon-fueled compositions containing 40 wt-% silicon. The burning rate trends are highly nonlinear with respect to oxidant composition. Fe_2O_3/Sb_2O_3 blends burn significantly faster than the parent oxide-based compositions. However, when the metal oxide oxidizer content is kept fixed, and the ratio between two fuels is varied instead, the burning rate varies approximately linearly as shown in Figure 7.

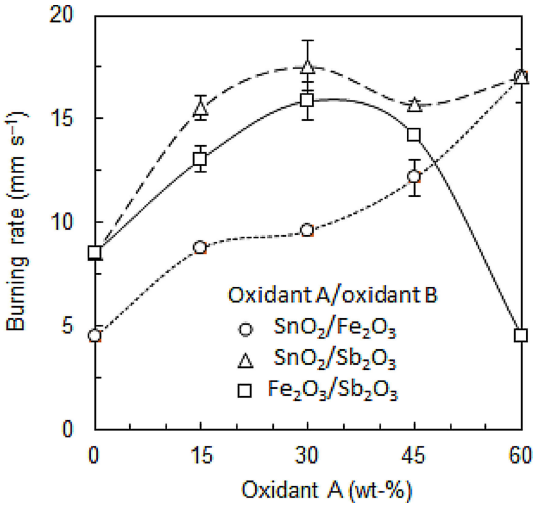

Figure 6. Ternary mixtures containing 40 wt-% silicon showing the effect of binary metal oxide on the burning rate.

Silicon/lead oxides. Silicon/lead oxide preparations have found widespread application as millisecond gasless time delay systems [73a].

Si/PbO system. The DTA response of a 30:70 Si/PbO powder mixture in air exhibits three exotherm peaks at 590, 665 and 710 °C respectively [73a]. The first reaction corresponds to the conversion of PbO to Pb_3O_4 (red lead) and commences at 350 °C [99]: $6\ PbO + O_2 \rightarrow 2\ Pb_3O_4$. The Pb_3O_4 reacts with silicon above 540 °C and regenerates PbO: $2\ Pb_3O_4 + Si \rightarrow 6\ PbO + SiO_2$.

At 665 °C more silicon is oxidized by the freshly formed PbO and O_2: $PbO + {}^1/_2\ O_2 + Si \rightarrow Pb + SiO_2$.

Si/PbO_2 system. DTA analysis of PbO_2 reveals several endotherms corresponding to its step-wise decomposition:

$$PbO_2 \xrightarrow{435^\circ} PbO_{1.56} \xrightarrow{465^\circ} PbO_{1.43} \xrightarrow{495^\circ} Pb_3O_4 \xrightarrow{573^\circ} PbO$$

The fifth endotherm observed at ~875 °C indicates the melting of PbO [37]. The observed and calculated heats of reaction ΔH_R show a maximum near 10.5 % Si [73a]. This suggests that this is the stoichiometric quantity of Si that is required to consume all the oxidizer and it is consistent with the reaction: $PbO_2 + Si \rightarrow Pb + SiO_2$. The maximum burning rate of Si/PbO_2 mixtures occurs at 35 % Si. This burning rate also decreases with increasing particle size [37].

Si/Pb_3O_4 system. Al-Kazraji and Rees [73a] investigated the fast pyrotechnic delay composition silicon/red lead. Their thermal analysis results revealed three main exother-

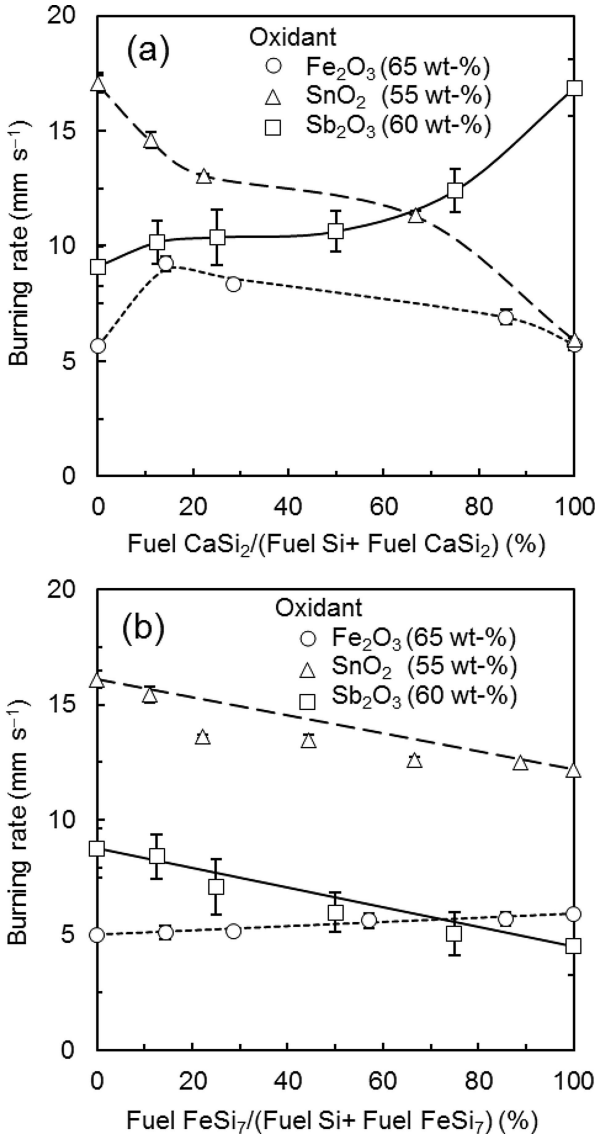

Figure 7. Ternary mixtures containing fixed amount (in wt-%) of a metal oxide oxidant showing the effect of binary fuel mixtures on the burning rate.

mic peaks: 590, 670, and 760 °C. Their observations can be explained in terms of the following sequence of events. The red lead (Pb_3O_4) decomposes above 540 °C to yield a solid residue of PbO that reacts readily with silicon. This occurs at the onset of the first exothermic peak (590 °C) obtained from DTA. The proposed reaction mechanism is:

$$Pb_3O_4(s) \rightarrow 3PbO(s) + {}^1\!/_2\ O_2(g)$$

$$2\ Pb_3O_4(s) + Si(s) \rightarrow SiO_2(s) + 6PbO(s)$$

$$PbO(s) + Si(s) + {}^1\!/_2 O_2(g) \rightarrow Pb(l) + SiO_2(s)$$

The reaction corresponding to the second exotherm (665 °C) releases more heat and is associated with the oxidation of molten lead from the previous reaction to lead oxide, which in turn reacts with excess silicon at the onset of 665 °C. That produces sufficient heat to raise the temperature for a further reaction to take place in bulk after diffusion through the layer of reaction products formed around the reactants. When the flow was nitrogen, the second reaction was less violent because of the absence of atmospheric oxygen. The third peak (760 °C), smaller than the second and very pronounced for silicon-rich compositions, is possibly due to the reaction between PbO and $PbSiO_2$ (lead silicate) at the melting point of the silicate.

Moghaddam and Rees [117] suggested that the mechanism for the reaction in the Si/Pb_3O_4 system is essentially the formation of a eutectic of PbO with SiO_2 around 720 °C. The PbO and SiO_2 melt at 886 °C and 1610 °C respectively. Thus, the delay time depends on the kinetics of the formation of the eutectic.

The maximum burning rate was observed at approximately 30 wt-% Si for coarse silicon ($d_{avg} \approx 5$ μm) and 15 wt-% Si for fine silicon ($d_{avg} \approx 1.9$ μm) [99]. In addition, the composition at which the maximum burning rate occurred did not correspond to the composition of maximum enthalpy (~10%). The maximum burning rate increased (from 16 to 300 mm s^{-1}) when the specific surface area of the silicon was increased from 0.08 to 5.36 $m^2 g^{-1}$ [73b].

Jakubko and Černošková [118] used differential thermal analysis, X-ray diffraction and infrared spectroscopy to examine the thermal behavior of the Si-Pb_3O_4 system and to characterize its combustion products. It was concluded that the Si-Pb_3O_4 system exhibits a rather complicated reaction mechanism including both gas-solid and solid-solid reactions (proceeding below oxidant decomposition temperature) whose relative importance depends on the fuel content of the mixture.

Jakubko [119] reported additional experimental and theoretical results pertaining to the silicon-red lead pyrotechnic system. Jakubko [16] investigated the effects of ambient pressure ranging from 101 up to 3040 kPa and temperature from 233 up to 353 K on burning rate of both high and low fuel content Si-Pb_3O_4 mixtures. Adding sodium and calcium fluorides diminished the pressure dependency of the burning rate for the low fuel content mixture, but left it almost unaffected for that containing a high amount of silicon. This difference in behavior of the mixtures was explained in terms of differences in the combustion mechanisms. The rate of burning increased linearly with ambient temperature.

Due to its weak oxidative power, ferric oxide has found application delay as an inhibitor in pyrotechnic formulations [112]. The inhibition effect is attributed to the formation of plumbates. See Table 8 for its effect in the system Si/Pb_3O_4.

Silicon/bismuth oxide. The use of the Si/Bi_2O_3 system in pyrotechnic delay systems has been patented [120]. The main reaction may be represented by: $3Si + 2Bi_2O_3 \rightarrow 3SiO_2 + 4Bi$. This corresponds to about 8.3 wt-% Si in the composi-

Table 8. Retarding effect of ferric oxide on the burning rate of the Si/Pb_3O_4 system.

Fe_2O_3 (wt-%)*	Burning rate (mm s^{-1})
0	125
10	78
20	45
30	25

Add-on to a Si/Pb_3O_4 composition containing 40 wt-% silicon.

tion. Little gas is produced during combustion and the maximum heat release occurs at about 20 wt-% Si [66]. Burning rate measurements have been reported [66]. The effect of fuel particle size and stoichiometry on the burning rate are illustrated in Figure 8 [20]. Addition of Zr as a co-fuel enhanced ignitability and increased the burning speed (See Table 9). Burn speeds up to 100 mm s^{-1} were obtained with Zr contents above 25 wt-% (expressed as part of the fuel).

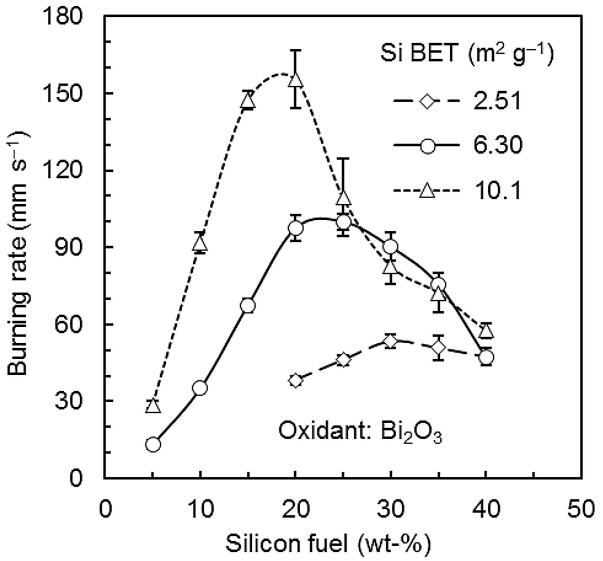

Figure 8. The effect of stoichiometry and fuel particle size on the burn rate (in lead tubes) for the Si-Bi_2O_3 system [20]. Surface average particle sizes: −△−0.91 μm; −○−2.35 μm; −◇−3.94 μm.

Table 9. Effect of zirconium, as partial replacement of silicon, on the burning rate of Si/Bi_2O_3 [120].

Composition[a] (wt-%)				Burning rate (mm s^{-1})
Si	Zr	Bi_2O_3	TiO_2	
28	5	67	–	76
30	20	50	–	100
3	10	60	27	9

[a]Particle sizes: Silicon: 3 μm; zirconium: 2 μm; titanium oxide: < 1 μm; and Bi_2O_3: 5 μm.

7.1.2 Silicon/Non-Oxide Oxidizers

Classic thermite-type composition comprise metal/metal oxide mixtures. However, some compositions contain oxy salts, e.g. chlorates, perchlorates, nitrates, chromates and sulfates [21, 37], of alkali, alkali earth or transition metals. These oxidizers may release oxygen to the reducing fuel via lattice destabilization, melting, sublimation and thermal decomposition [15, 37, 121]. A key characteristic of compositions with non-oxide oxidizers is the generation of significant amounts of gaseous products [122].

Silicon/barium sulfate. The slow burning $Si/BaSO_4$ has found use in long-period delays [17]. The system burns only in the Si-content composition range 34–50 wt-%; with a specific surface area between 0.45 and 2.36 $m^2 g^{-1}$ for the $BaSO_4$. The 42 wt-% Si composition gives a burning rate of ca. 4.3 mm s^{-1}.

Addition of V_2O_5 as an ingredient acting as a flux significantly improved the firing reliability of 45.5 wt-% $Si/BaSO_4$ delay compositions [17]. The burning rate (ca. 4.05 mm s^{-1}) was independent of the V_2O_5 content up to an add-on of 10 wt-%. This implies that the melting flux assisted in the initiation of the $Si/BaSO_4$ without affecting the main combustion reaction. Above 10 wt-% the dilution effect of the inert flux tended to quench the reaction [17]. Addition of potassium perchlorate or manganese dioxide to the $Si/BaSO_4$ system apparently improves reliability and reduces the temperature dependence of the burning rate [123].

Silicon/calcium sulfate. In view of environmental concerns, the inexpensive anhydrous calcium sulfate was investigated as an alternative "green" oxidant in place of $BaSO_4$ [19]. Combustion was only supported in the range of 30—70 wt-% Si. In this range the reaction rate and energy output decreased with increasing silicon content. The reaction product was a complex mixture that contained crystalline phases in addition to an amorphous calcium silicate phase.

Non-oxide based systems tend to proceed via complex reaction mechanisms and produce a variety of reaction products. This is exemplified by the $Si/BaSO_4$ and $Si/CaSO_4$ compositions [18–19]. For example, the proposed multistage reaction mechanism for the $Si/CaSO_4$ composition is:

$$CaSO_4 + 2Si \rightarrow CaS + 2SiO_2$$

$$CaSO_4 \rightarrow CaO + SO_2 + {}^1/_2\ O_2$$

$$Si + O_2 \rightarrow SiO_2$$

$$SiO_2 + CaO \rightarrow CaSiO_3$$

Figure 9 shows that the burning rates of the Si-$CaSO_4$ system are comparable to those for the slow-burning $Si/BaSO_4$ pyrotechnic delay composition [18]. Both formulations were insensitive to impact, friction, and electrostatic discharge stimuli. The reaction products were a com-

plex mixture that contained crystalline phases in addition to an amorphous phase. Although barium sulfate is insoluble in water and decidedly nontoxic, the reaction products produced by the Si/$BaSO_4$ compositions were found to release soluble barium ions when contacted with water.

The Si/$CaSO_4$ system was found to be sensitive to the presence of inert material, addition of as little as 1 wt-% fumed silica stifled combustion in the aluminum tubes [104a].

Si/lead chromate and Si/copper antimonite. Conventional mine detonators include a small starter increment that is easy to ignite and that acts as a sealing composition. It was found that, unlike most other slow- or medium-fast burning compositions, antimony trioxide, lead chromate, and copper antimonite time-delay compositions were all directly ignitable by shock tubing [73c]. Figure 10 shows measured burn rates for the latter two systems. Lead chromate mixtures burned fastest under comparable conditions. Addition of aluminum powder or fumed silica reduced the burning rates.

Co-precipitated copper antimonite-zinc antimonite. $CuSb_2O_4{\cdot}xZnSb_2O_4$ co-precipitates provided for faster burning than neat copper antimonite-silicon mixtures [73c]. The effect of zinc content on burning rate was determined using mixtures containing 40 wt-% Si. Co-precipitates with $x=1$ and $x=2$ burned at a rate of ca. 20 mm s^{-1}, i.e. almost twice as fast as neat copper antimonite.

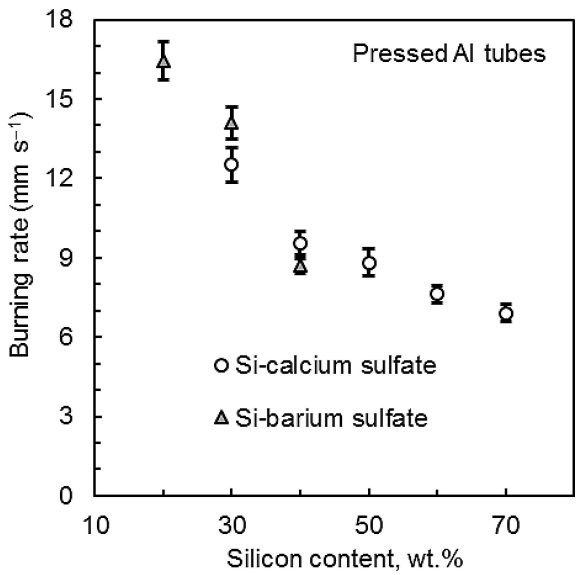

Figure 9. Effect of fuel content on the burning rate of Si/$BaSO_4$ and Si/$CaSO_4$ compositions measured in rigid aluminum elements. Median particle size (d_{50}) and BET surface areas of the reagents were as follows: barium sulfate: 4.31 μm & 0.82 $m^2 g^{-1}$; calcium sulfate: 4.05 μm & 3.78 $m^2 g^{-1}$ and silicon 1.85 μm & 11.0 $m^2 g^{-1}$.

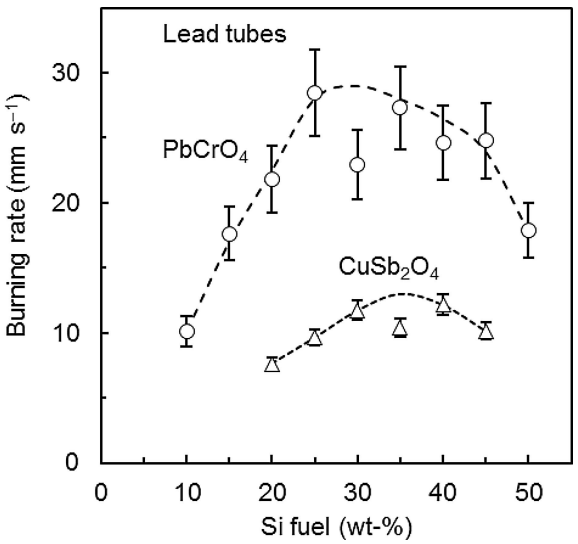

Figure 10. Effect of fuel content on the burning rate of Si/$BaCrO_4$ and Si/$CuSb_2O_4$ compositions measured in rolled lead tubes. Median particle size (d_{50}) of the silicon powder was 1.83 μm and BET surface area was 8.30 $m^2 g^{-1}$. The BET value for the $PbCrO_4$ and the $CuSb_2O_4$ was 16.7 $m^2 g^{-1}$.

7.2 Zinc as Fuel

Zinc/lead oxides. Zinc has a low melting point (420 °C) that is readily reached during combustion in Zn/oxidant pyrotechnic systems. Zinc burned in combination with any of the lead oxides (PbO_2, Pb_3O_4 and PbO) over a range of compositions (10–70 % Zn) [38]. The burning rates varied in the range 2.2 to 90 mm s^{-1} for compositions containing 20 to 50 wt-% Zn. However, as the compaction pressure was increased the range of compositions that burned decreased. For example, at a compaction pressure of 55 MPa, only Zn/PbO_2 sustained combustion and then only in the range 20–45 wt-% Zn. Mixtures of Zn/PbO only burned in loose powder form. It was observed that compositions with higher Zn contents were gassier and burned more rapidly and violently. It is likely that the gas was a mixture of O_2 and vapors of Zn and Pb. Only in the case of Zn/Pb_3O_4 was the oxidant fully reduced and converted to Pb. The maximum combustion temperatures reached of Zn/PbO_2 or Zn/Pb_3O_4 mixtures exceeded 1800 °C. The Zn/PbO_2 combustion residues had a spongy appearance that indicated gas evolution. This systems is not suitable for use as gasless pyrotechnic delays because of the gassy combustion [38].

7.3 Iron as Fuel

Iron/barium oxide. Spice and Staveley [67] investigated the slow reaction between iron and barium peroxide by compressing the mixture into pellets, heating uniformly to vari-

ous temperatures below the ignition temperature and following the amount of iron present by a magnetic method.

Tribelhorn *et al.* [40] investigated the effect of formulation variables, including the compaction pressure, on the behavior of iron-fueled binary pyrotechnic systems. Burning rates for the iron/barium oxide system ranged from 23 to 39 mm s^{-1} reaching a maximum around 30 wt-% Fe. The burning rates for compositions compacted at 55 MPa were higher than those for loose compositions. Increasing the compaction pressure beyond 55 MPa led to a decrease in burning rates. Compaction promotes inter-particle contact and hence the rate of solid-solid reactions. When solid-gas reactions are also involved, increased compaction slows the rate of burning as the fuel surface area accessible to the gas is decreased.

The effect of additives and environmental factors was studied using 20% Fe/BaO_2 as the base formulation. Addition of 5% barium hydroxide [$Ba(OH)_2$] inhibited combustion. Although mixtures containing >15% $BaCO_3$ supported combustion, its formation on the surfaces of BaO_2 decreased the reactivity of the system. The presence of even 1% water inhibited the ignition of the composition. This was attributed to the formation of a coating of $Ba(OH)_2$ on the BaO_2 particles. Such layers apparently inhibit combustion more than having a few separate particles of $Ba(OH)_2$ interspersed throughout the mixture. It was also observed that the endothermic decomposition of the hydroxide regenerated water vapor during the combustion and this also affected the combustion rate. Water may have a deleterious effect on the burning rate by corroding the surfaces of the iron particles to form oxides and hydroxides.

The main reactions likely to be involved in combustion of the Fe/BaO_2 system are:

$$2\ Fe(s) + 3BaO_2(s) \rightarrow Fe_2O_3(s) + 3BaO(s)$$

$$3\ Fe(s) + 4BaO_2(s) \rightarrow Fe_3O_4(s) + 4BaO(s)$$

$$Fe(s) + BaO_2(s) \rightarrow FeO(s) + BaO(s)$$

The reaction order varied with the Fe content of the mixture and ranged from 0.50 to 0.71. The corresponding activation energies varied erratically with the Fe content but ranged between 7 and 13 kJ mol^{-1}. These low apparent activation energies are indicative of diffusion-controlled processes.

7.4 Zirconium as Fuel

Zirconium/iron oxide. Cheng *et al.* [124] investigated the use of the Zr/Fe_2O_3 system as a pyrotechnic delay element. DSC showed a strong exotherm at 395 to 430 °C for mixtures containing from 10 to 80 wt-% Zr. Cheng *et al.* [124] also observed a pre-ignition of the reaction in the range of 310 to 330 °C. The overall reaction is: $3Zr(s) + 2Fe_2O_3(s) \rightarrow 4Fe(s) + 3ZrO_2(s)$

The nature of the combustion products, identified by XRD analysis, depended on the fuel content of the mixture. See Table 10. Interesting is the fact that at 70 wt-% Zr both a classic thermite oxidation-reduction reaction and an intermetallic reaction occur. The excess zircon reacts with the reduced iron to form $ZrFe_2$ as follows: $2Zr(s) + 2FeO(s) \rightarrow ZrO_{2(s)} + ZrFe_2(s)$

Table 10. The combustion products of the Zr/Fe_2O_3 system.

Zr (wt-%)	Products
30	ZrO_2, Fe, FeO
50	ZrO_2, Fe
70	ZrO_2, $ZrFe_2$

Burning rate and the heat of reaction showed similar trends with respect to the composition dependence. The burning rate did not vary significantly in the Zr content range 48 to 56 wt-%. The maximum heat of reaction was obtained with 50% Zr. The compaction pressure had only a slight effect on the burning rate.

7.5 Manganese as Fuel

Wang and Sundman [125] and Grundy *et al.* [126] presented thermodynamic parameters of the Mn–O system, including the phase diagrams. The metal itself can exist in several different crystalline phases. There are four known oxides, manganosite ($Mn_{1-x}O$) a nonstoichiometric compound with a deficit of Mn, hausmannite (Mn_3O_4), bixbyite (Mn_2O_3), and pyrolusite (MnO_2). The system exhibits a wide liquid miscibility gap on the Mn–$Mn_{1-x}O$ side and a eutectic point on the $Mn_{1-x}O$–Mn_3O_4 side.

Manganese/metal oxides. Manganese metal as fuel provides for medium to slow burning pyrotechnic compositions when combined with the following oxidizers: Bi_2O_3, $CuBi_2O_4$, MnO_2, Cu_2O, V_2O_5, Sb_6O_{13} and CuO [26]. Burning rates were measured for delay compositions press-filled in aluminum or compaction-rolled in lead tubes. See Figure 11. They varied between 5 and 22 mm s^{-1} but slower burning ternary and quaternary compositions were also found. For the mixtures pressed in aluminum tube, the reaction with Bi_2O_3 was the fastest at 22 mm s^{-1} and with Cu_2O it was the slowest at ca. 5 mm s^{-1}. It was possible to decrease the burning rate to below 5 mm s^{-1} by formulating suitable multicomponent mixtures. Adding ca. 5 wt % hollow glass spheres was particularly effective in this regard.

Mn/BaO_2 and Mn/SrO_2. Drennan and Brown [39] studied binary and ternary pyrotechnic systems with manganese fuel and BaO_2 and SrO_2 as the oxidants. The Mn/BaO_2, Mn/SrO_2 systems burned over a wide range of compositions with the burning rate ranging from 2 to 12 mm s^{-1}. Burning rates were increased by the use of smaller particle-sizes of

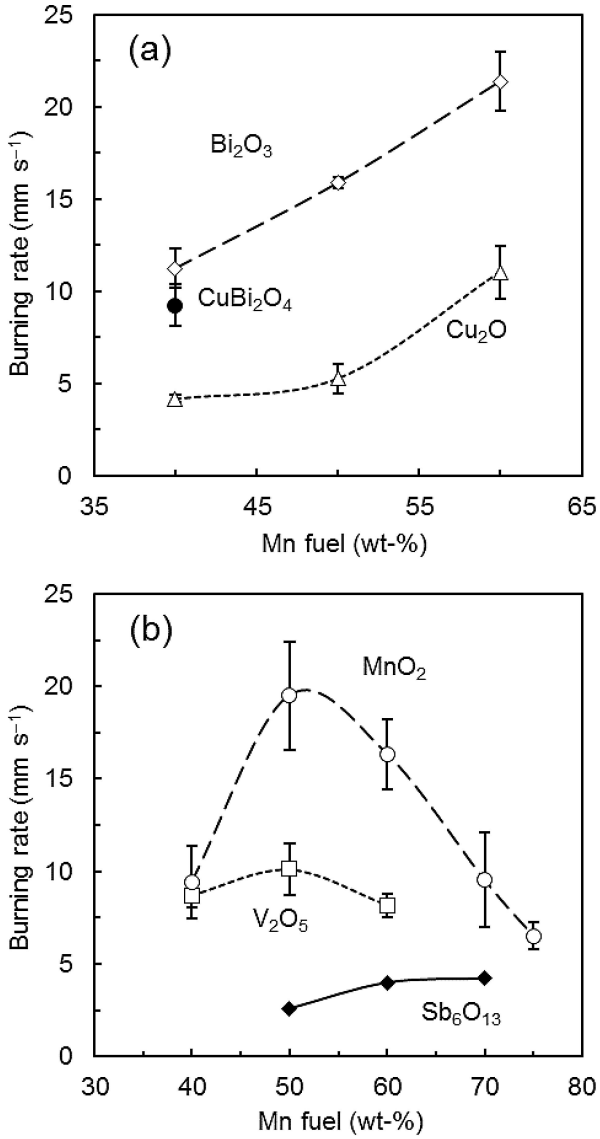

Figure 11. The effect of different oxidants on the burning rate for delay compositions with manganese as fuel. (a) The effect of the oxidants Bi_2O_3, Cu_2O and $CuBi_2O_4$ on burning rate in aluminum tubes. (b) MnO_2- and V_2O_5-based compositions were press-filled in aluminum tubes but the Sb_6O_{13} composition was compacted in rolled lead tubes. The d_{50} particle size of the Mn fuel was 6.0 μm and the BET surface area was 0.60 $m^2 g^{-1}$.

fuel and higher compaction pressures while inert additives generally decreased the burning rate. The mass burning rate increased with compaction for both systems and this suggests the possible occurrence of a genuine solid-solid reaction [37].

Manganese/antimony trioxide. EKVI thermodynamic modelling predicted two maxima in the adiabatic reaction temperature for the binary Mn/Sb_2O_3 pyrotechnic system [90].

The local maximum, at a manganese fuel content of ca. 36 wt-%, corresponds to a pure thermite-type redox reaction according to: $3Mn + Sb_2O_3 \rightarrow 3MnO + 2Sb$. The overall maximum in the adiabatic reaction temperature (ca. 1640 K), at the fuel-rich composition of 49 wt-% Mn, is consistent with a combination of the standard thermite reaction with an additional exothermic intermetallic reaction $5Mn + Sb_2O_3 \rightarrow 3MnO + 2MnSb$. XRD analysis of combustion residues confirmed the formation of MnSb and Mn_2Sb for fuel-rich compositions.

Burn rates were measured using delay elements assembled into commercial detonators. The d_{50} particle sizes were 23.4 and 0.92 μm for the Mn fuel and Sb_2O_3 oxidant powders, respectively. The delay elements comprised rolled lead tubes with a length of 44 mm and an outer diameter of 6.4 mm. The rolling action compacted the pyrotechnic compositions to 74 ± 2% theoretical maximum density. The burning rate (see Figure 12) increased approximately linearly from 4.2 to 9.4 $mm s^{-1}$ over the composition range 25–50 wt-% Mn.

Manganese/manganese dioxide. Mn/MnO_2 mixtures, a system where the fuel and the oxidant share a common metal, showed reliable burning over a wide stoichiometric range [26]. The reactants combine to form the more stable intermediate oxide (MnO) releasing considerable quantities of heat in the process. The effect of stoichiometry is shown in Figure 11. The addition of fumed silica to the Mn/MnO_2 system had little effect on the propagation rate.

The Mn/MnO_2 reactive system is not sensitive to ignition by friction or electrostatic stimuli [114]. Stoichiometries with measured combustion temperatures between 1358 and 2113 K were found to be self-sustaining with burning rates ranging from 2.4 to 7.3 $mm s^{-1}$. The X-ray diffraction-de-

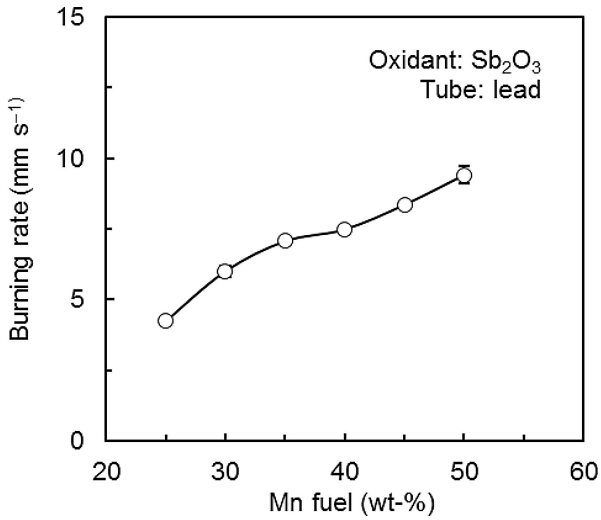

Figure 12. Experimental burning rates for the system Mn/Sb_2O_3 as a function of fuel content in rolled lead tubes [90]. The d_{50} values were 23.4 μm and 0.92 μm for the Mn fuel and the Sb_2O_3 oxidant respectively.

termined combustion products appeared to be benign based on current regulations. Miklaszewski *et al.* [114] concluded that Mn/MnO_2 appears to be a suitable low gas-producing, insensitive, less toxic delay composition with good longevity.

Kappagantula *et al.* [85] extended studies of the Mn/MnO_2 system to nano-energetics. Their results showed that heat conduction is the dominant energy-transfer mechanism for the reaction even in the loose powder configuration, regardless of the fuel particle size. Higher burning rates were achieved using nano-Mn as fuel despite the fact that the Mn_3O_4 passivating shell covering the fuel particles reduced the manganese content to only 86 wt-% Mn. This behavior was attributed to the manganese (II,III) oxide representing an oxygen-rich reactive covering. This contrast with nanometric aluminum (Al) particles where the inert alumina (Al_2O_3) passivation shell does not participate in the oxidation reaction and, instead, acts as a heat sink retarding energy propagation.

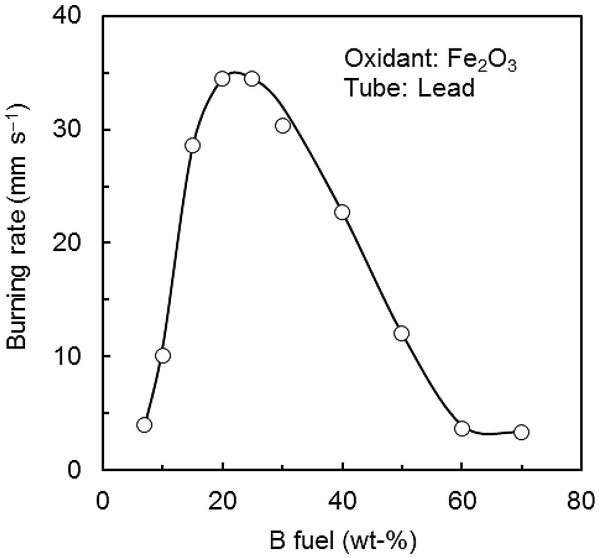

Figure 13. The effect of stoichiometry on the burning rate for B/Fe_2O_3 mixtures [25].

7.6 Boron as Fuel

Elischer *et al.* [25] considered the 'green' B/Fe_2O_3 composition. Boron has a low toxicity and iron oxide is regarded as being less hazardous to health than most other materials traditionally used in pyrotechnic delays. Delay lengths of 7 mm were pressed into lead tubes at pressures ranging from 160 to 400 MPa. There was no significant variation in the functioning time of the delay units with increased pressing load for the 25 wt-% B composition. The burning rate at this composition increased linearly with temperature at a rate of 2.2% in the temperature range −40 °C to 60 °C. The effect of stoichiometry on the burning rate is shown in Figure 13.

The burning rates of B/Pb_3O_4 delay compositions were also investigated [127]. The boron content was varied from 1 to 16% and the ambient temperature from −50 °C up to 70 °C. The measured burning rates increased as both parameters were increased and ranged from 12.8 to 31.2 mm s^{-1}. See Figure 14. For fixed compositions the burning rate increased linearly with temperature. The effect of composition was more pronounced than that of temperature. The effect of composition on burning rate showed a logarithmic dependence.

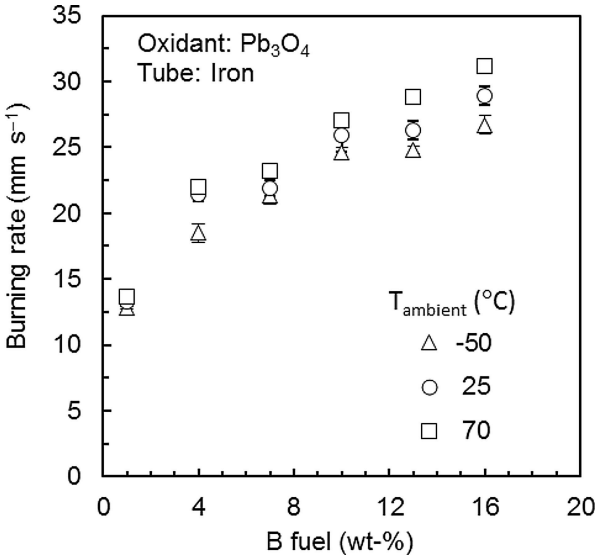

Figure 14. Effect of ambient temperature and stoichiometry on the burning rate for B/Pb_3O_4 mixtures [127].

Silicon/boron/potassium dichromate. In the B/Si/$K_2Cr_2O_7$ systems, ignition occurs immediately after fusion of the oxidant [41]. The boron acts as a trigger by burning with the molten oxidant prior to the combustion of the silicon. The silicon then reacts, as a follow-up reaction. Charsley and co-workers [10] showed that in the binary system B/$K_2Cr_2O_7$, the combustion reaction is self-propagating above a fuel content of 5%. For mixtures prepared from 4% B/$K_2Cr_2O_7$, the presence of a few percent of silicon is beneficial and indeed is responsible for propagating the combustion. The boron in the ternary mixture burns in a matrix of molten oxidant, which progresses through the burning compositions as a molten front. However, the rate-determining step of the kinetic mechanism involves the formation of a liquid phase [41]. The ignition temperature of the ternary mixtures is about 660 K. It was observed that the addition of silicon increased the maximum reaction temperature and the rising slope of the temperature profiles [10].

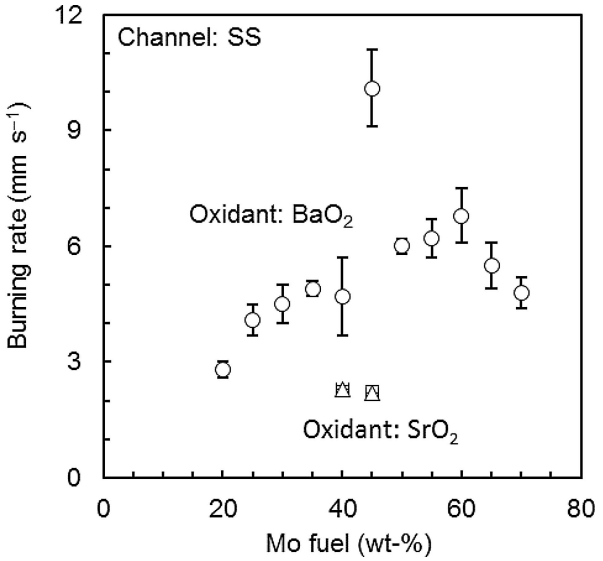

Figure 15. The effect of stoichiometry on the burning rate for Mo/BaO_2 and Mo/SrO_2 mixtures [39].

7.7 Molybdenum as Fuel

Drennan and Brown [39] studied binary and ternary pyrotechnic systems with molybdenum as fuel and BaO_2 and SrO_2 as oxidants. The Mo/BaO_2 system burned over a wide range of compositions, but the range of ignitable compositions for the Mo/SrO_2 system was very limited. The linear burning rates, for all these systems, range from 2 to 10 mm s^{-1} (see Figure 15) and burning rates were increased by the use of smaller particle-sizes of fuel and greater loading pressures. Inert additives generally decreased the burning rate. The mass burning rate increased with compaction for both systems and this suggests the occurrence of a genuine solid-solid reaction [37].

7.8 Tungsten as Fuel

Shachar and Gany [128] reported on a very slow burning W/$KClO_4$/$BaCrO_4$ time delay composition. Burning rates in the order of 1.6 mm s^{-1} were achieved. The presence of the potassium perchlorate in this systems was found to be vital for starting the solid state reaction. The postulated reactions are:

$$W + 3/8\ KClO_4 + BaCrO_4 \rightarrow WO_3 + 3/8KCl + 4/8Cr_2O_3 + BaO + 508\ kJ$$

$$BaO + WO_3 \rightarrow BaWO_4 + 307\ kJ$$

Tungsten/manganese dioxide. Koenig *et al.* [28] explored the W/MnO_2 composition as an environmentally benign time delay replacement. Measured maximum combustion temperatures ranged from 1466 to 1670 K as a function of mixture stoichiometry. The measured burning rates ranged from 1.62 to 4.61 mm s^{-1} and varied almost linearly with tungsten content in the range $40 \leq W \leq 60$ wt-%. The maximum measured gas production was 9.1 mL g^{-1}. The combustion products were characterized with powder X-ray diffraction and appear benign on the basis of known compound information. The primary reaction products were believed to be tungsten trioxide and MnO which then react to form manganese tungstate. The proposed reaction scheme is:

$$W + 3MnO_2 \rightarrow WO_3 + 3MnO$$

$$WO_3 + MnO \rightarrow MnWO_4$$

So that the overall result, as predicted by FactSage, is:

$$W + 3MnO_2 \rightarrow MnWO_4 + 2MnO$$

Analysis of the combustion products confirmed the formation of manganese tungstate ($MnWO_4$) but the residues also contained trimanganese tungstate (Mn_3WO_6), tungsten (W), and manganese (II,III) oxide (Mn_3O_4).

7.9 Intermetallic Systems

The possibility of intermetallic-based pyrotechnic devices was mooted as early as 1973 [71, 91]. Fischer and Grubelich [32] published a review listing numerous possible intermetallic reactions. Intermetallics have been a long-lasting research area in SHS and recently it has become a very intensely researched topic in nano-thermites through the development of multilayer intermetallics. The implication is that there simply must be possibilities to explore the use of intermetallics for delay applications. Promising hints can be found in the preparation of particle composites with intimate contact between the reactive metallic components achieved through the process of arrested milling [45] and by the development of novel manufacturing techniques for composite particles comprising multilayer intermetallics [129]. However, to date, only one study has dealt with intermetallic couples as reagents for a delay composition [27].

The Ti/C-3Ni/Al combination was shown to be a suitable delay composition with tunable burning rates ranging from 2.1–38.1 mm s^{-1} in aluminum microchannels with diameters ranging from 4.0–6.0 mm [27]. Increasing the Ti/C content resulted in faster burning rates while decreasing microchannel diameter had the opposite effect. It was found possible to overcome the heat losses associated with the small diameter microchannels by varying the relative amounts of Ti/C and 3Ni/Al. At 40 wt-% Ti/C content, the failure diameter was found to be between 3.0 and 4.0 mm, while at 30 wt- % Ti/C the failure diameter was between 4.8 and 6.0 mm. Measured combustion temperatures in metal mi-

crochannels were approximately 1700 K while those of unconfined pellets were around 100 K greater.

8 Processing Pyrotechnics Compositions

It is important in pyrotechnic technology to ensure the homogeneity of the mix as this will result in the regularity, reproducibility and uniformity of the combustion wave motion for a particular composition. Processing also has an effect on the ease of manufacture (e.g. press loading) and, in particular, safety.

8.1 Synthesis/Particle Fabrication

Co-precipitation. This approach is used to produce mixtures with intimate contact between the reductant and the oxidant. Examples include the co-precipitation of B-$BaCrO_4$ mixture and the co-precipitation of Mn-$BaCrO_4$-$PbCrO_4$ mixtures [37]; Si/$BaSO_4$/Pb_3O_4 mixtures [130], co-precipitation of the oxidant $CuSb_2O_4$.$x$$ZnSb_2O_4$ [73c].

Coacervation. Coacervation is a type of co-precipitation that depends on the ability of ethyl alcohol to pre-empt the solvent capacity of water. Soluble ionic compounds form stable solutions in water because of hydration i.e. the formation of a stable water hydration shell around the ions bonded by ion-dipole interactions. It is the enveloping water layers that prevent re-association and thus stabilize the solution. Ethyl alcohol molecules bond more strongly to the water molecules than do the cations. Consequently, the addition of the alcohol to a water solution of salt strips the ions of their protective coating and causes re-association and precipitation. This technique has been used in the preparation of Mg/$NaNO_3$ illuminating flare mixtures and Si/B/$K_2Cr_2O_7$ delay mixtures [37].

Composite particles. Intimate contact between the reacting components is achieved in multilayer intermetallics. Uniformly-shaped, micron-scale particles with nanoscale layers can be fabricated by depositing multilayer films onto mesh substrates with a square weave [129a]. Such films spontaneously break into individual particles at the weave intersections during removal. Compacts of such particles self-propagated up to 200 times slower than reactions in continuous multilayer foils with similar chemistries, layer thicknesses and ignition thresholds. It is also possible to create such reactive multilayer powders by milling previously cold-rolled stacks of alternating multilayer laminate sheets of the two components [129b].

8.2 Size Reduction/Comminution

A ball mill or micro pulverizer should not be used to mix a combustible pyrotechnic, nor should they be used interchangeably for oxidizers and reductants since small residues of the one can react with the other [37].

Grinding and milling. The milling of hygroscopic materials must be done under conditions of near-absolute dryness. As the particle size is reduced, the surface area increases and moisture absorption becomes extensive. When milled, the waxy materials must 'freeze' and become sufficiently brittle to fragment [108]. Micro pulverizers are used to reduce the particle size and to ensure that each batch is prepared in the same way. The standard operating procedure for all inorganic oxidizers is to dry, micro pulverize (no more than 2 days before use) and then dry again [37]. The addition of 1 to 2% of hydrophobic silica to pyrotechnic mixes proved to be efficient in the milling process [108]. In certain milling operations, synergism was observed when using a combination of molecular sieves and hydrophobic silica. The former dried the particles and the latter coats their surfaces once fragmented [108].

Ball milling. Ball mills also serve to reduce the particle size of relatively brittle substances, such as oxidizer salts. Milling increases the reactivity of reactants and this change may be the result of the reduction in particle size (increase of specific surface area), the distortion of the structure, the breaking up of agglomerates or, more likely, of stripping the metal particles from inhibiting surface layers [9]. The success of this technique is a function of material properties, such as fragility and hardness.

Magnetically assisted impaction mixing (MAIM) is an environmentally benign mechanical process, suitable even for processing nanoparticle mixtures [131]. With this process homogeneity of mixing levels approaches those achieved by rapid expansion of supercritical or high-pressure suspensions or sonication of a suspension of the nanoparticles in supercritical CO_2. The method has been used to prepare a time delay composition also known as T-10 which contains boron (B) and barium chromate ($BaCrO_4$) as powder components [132].

The preparation of energetic materials by mechanical milling is a challenge as they are easily initiated by impact or friction [45]. Nevertheless, arrested reactive milling has been exploited to prepare many inorganic reactive materials. The process yields fully dense composite particles with unique properties, combining high density with extremely high reactivity. The milling is done at cryogenic temperatures or a staged milling protocol is used to prepare such hybrid reactive materials with different components mixed on different scale.

8.3 Raw Material Preparation

A major problem in the processing of powdered formulations is agglomeration. This problem can be encountered when one or more of the powdered constituents are either hygroscopic, e.g. ammonium perchlorate or sodium nitrate; waxy or oily; or unusually shaped, such as flakes or

needle-shaped particles. The agglomeration increases as the particle size decreases and the moisture content increases. The latter leads to caking of the powder. This means that most fine particle powders have to be specially handled in all processing techniques, i.e. drying the powder at elevated temperature, screening to break up or remove agglomerates, and desiccating to prevent moisture uptake [108].

Drying. Molecular sieves are used to achieve near-absolute drying of powders. They are crystalline zeolites that have angstrom-sized pores that allow a selective adsorption of polar gases and liquids. Moisture is transferred from the powders to the molecular sieves. This is an equilibrium process. The efficiency of molecular sieves has been demonstrated in the milling of a water-ignitable pyrotechnic composition of B/AgF_2 [108]. Direct contact of molecular sieves with sensitive materials, such as explosives, must be avoided. The heat of adsorption might be sufficient to cause ignition of sensitive materials [108].

Heat treatment. Heat treatment enhances the uniformity of processed materials by desorption of moisture or other materials that have covered the surface of particulates. For example, $PbCrO_4$ and $BaCrO_4$ are preheated at 400 °C before use [37]. The heat treatment of a mixture delay composition requires precautions to avoid ignition. The temperature is therefore kept far below runaway conditions. For example, the fast burning Si/Pb_3O_4 mixture is dried below 70 °C.

Coating. In order to avoid possible surface deterioration of metal powders, protective coatings are applied. Coating materials such as paraffin, linseed oil, stearic acid and poly (vinyl chloride) (PVC) may be applied by dipping or spraying [37].

Powder conditioning. Flow-conditioner additives are extensively used to overcome agglomeration problems. These are usually very fine powders of sub-sieve particle size and include various types of silicates, stearates, phosphates, diatomaceous earth, starch, magnesium oxide, talc and fatty amines. These conditioners proceed in various ways to improve flowability and prevent agglomeration, e.g. they may form a solid barrier between the powder particles, reducing their attractive forces; lubricate the solid surfaces, reducing friction between the particles, or neutralize electrostatic charges [108].

Colloidal hydrophobic fumed silica, in powder form, is a powerful flow-conditioner additive at low dosages (<1 wt-%). Normal silica aerogel is hydrophilic. It can be converted to the hydrophobic state by replacing the surface hydroxyl groups with siloxane groups [108] by reaction with e.g. hexamethyldisilazane. The advantages of this flow conditioner are that it can be premixed before milling and will allow milling of waxy or oily materials; the treated powder becomes water repellent, even if initially hygroscopic; low dosages are required (less than one percent, on a mass basis, is often adequate); the resultant powder mix generally has a higher bulk density, and it is chemically inert, allowing it to be used with sensitive propellants, explosives and pyrotechnics.

The exceptionally high water repellence of powder conditioned with hydrophobic silica is attributed to air entrapment on the surface of the powder particles. Another advantage of this technology is associated with the increased bulk density. Because of the better flowability, the particles flow and slip past each other readily so that they compact better [108].

8.4 Mixing

Proper mixing eliminates non-uniformities and concentration gradients. This operation is essential to ensure homogeneity of the reaction mixture. Methods of processing highly hazardous mixes include wet and dry mechanical mixing. Different techniques are used for mechanical processing, e.g. rumbling, dough mixers and double-cone blenders. Bladed mixers and ribbon blenders can cause fires [37]. The MIGRAD mixer/granulator was specifically designed to mix, granulate and dry a pyrotechnic material (10–20 kg) within a single mixing chamber [133]. It provides a safer and more efficient method of mixing, granulating and drying, even highly energetic pyrotechnic compositions.

RAM mixing [134]. The recently developed RAM mixing technology possibly represents a breakthrough in mixing technology. It reportedly employs a resonant acoustic mixing mechanism. Material inside a mixing vessel is subjected to a low frequency acoustic field in the axial direction. The result is a phenomenon called acoustic streaming. It is a second order bulk motion of the fluid that results in a multitude of micro-mixing cells throughout the container. In effect the low frequency, high-intensity acoustic energy is used to create a uniform shear field throughout the entire mixing vessel. The result is rapid fluidization (as in a fluidized bed) and dispersion of material. The characteristic mixing lengths for the RAM technology, operating at 60 Hz, is nominally 50 μm.

Polymer precipitation. This process involves dissolving the polymer in a solvent, adding the dry ingredients and stirring vigorously, then adding a non-solvent to the system to cause precipitation of the mix. The end product is a homogeneously dispersed mix of ingredients uniformly coated with the precipitated polymer. The product does not require screening, which is of special benefit with compositions that are hazardous to screen because of friction sensitivity [37].

Brush screening. Powder mixing is accomplished on a set of brush screeners, similar to flour sifters that are assembled on top of each other. The rotating brushes are usually pulley-driven from a drive shaft connected to a motor [37]. They are remotely operated to avoid exposing personnel to the hazards of fire and toxic dust.

Vibrating screens. This is a classic method in which powder compositions are mixed by rolling conductive rubber balls passing the powders through sets of mesh screens. However, there are ignition problems associated with this approach.

Mixing as water slurries followed by spray drying. Spray drying of slurries is an appropriate method for obtaining free-flowing granules as it creates almost perfectly spherical particle agglomerates [135]. In addition to the acceptable flow properties, this process also yields well-mixed compositions from dispersions containing different powders and provides control over the agglomerate particle size distribution [134a, 136]. The spray-drying process requires that the fuel, oxidizer and other constituents first be slurried in water [135, 137]. This creates a potential hazard situation as water reacts dissociatively with most pyrotechnic fuels creating hydrogen gas [138]. It is therefore important to find strategies that can be applied to mitigate hydrogen formation. [49a], Tichapondwa *et al.* [139] investigated the effect of pH, adding organic corrosion inhibitors, controlled air oxidation of the silicon powder before slurrying and the introduction of competing cathodic reactions as means of eliminating hydrogen formation when silicon powder was slurried in water. Hydrophobization of the silicon particle surface by organic silane coatings was found to be the best strategy resulting of up to a 97% reduction in hydrogen production [49a].

9 Manufacture of Pyrotechnic Delay Elements

9.1 Design and Manufacturing Factors

Design and manufacturing factors that can affect the delay interval produced by a delay element include [11]:

- Design of the delay element, e.g. length and diameter of the column
- Density of the column packing
- Type of ignition source used
- Ignition transfer and mechanical strength of the column
- Thermal conductivity of the tube housing the column

9.2 Manufacturing Elements

Rolling lead tubes. The traditional method of manufacturing pyrotechnic delay elements consisted of filling large bore lead tube with the pyrotechnic composition and then extruding the lead tube through a rolling action. This method delivered very consistent results as the rolling action consolidated the particles to deliver a very consistent packing density throughout the tube. The tube is then cut into shorter sections of delay elements. Delay elements for longer time intervals have been made utilizing long, straight lead tubes made by the extrusion technique and pressing them into a flat 'C' section or by preparing spirally wound units. In this way time delays of several minutes were obtained [11]. These methods are being phased out as they employ lead, a contentious heavy metal.

Powder pressing. The method currently employed is incremental pressing of powders into a rigid delay tube (usually aluminum or brass). Pressing the powders incrementally does have some problems with obtaining consistent results. Since the powders are pressed in several increments, each increment has to be filled separately. The consistency of this filling technique is largely dependent on the flow properties of the delay composition and, if used, the binder. Each increment also has to be pressed at a constant pressure to ensure that the consolidation density remains constant. The consolidation pressure (pressing load) used during manufacturing is also very important as it determines the level of confinement of the composition. Usually, the higher the consolidation pressure, the higher the rate of heat propagation through the element and a correspondingly higher burning rate is achieved.

9.3 Porosity and Compaction Pressure

The degree of preheating of the reactants in a given system is affected by the forward intrusion of hot combustion products. This, in turn, is partly determined by the porosity of the compacted material. Consolidated compositions exhibit microscopic voids between the ingredients even when compressed at very high loads. Even at densities approaching the theoretical maximum (TMD), the voids may constitute upward of 2% of the total volume. The reason is that, beyond a critical density, further displacement of the particles is precluded. The loading pressure for a delay charge is usually around 200–275 MPa [124].

The level of confinement within the element is also a significant factor. When loosely packed powders burn, much of the heat generated is lost to the surrounding air, which slows the burning reaction. On the other hand when the delay element is well-confined, all the energy is retained within the delay element and it is used to propagate the reaction. Proper confinement can also increase the pressure inside the delay element due to small amounts of gasses formed which could further increase the burning rate.

The void volume of a composition depends on the formulation, the physical characteristics of the ingredients such as the size and the shape of the particles; and the presence of substances such as waxes or resins that can deform or flow under pressure [11].

The effect of compaction pressure on the burning rate should be considered when designing a delay element. With the incremental method of filling the delay elements, there will be periodic variations in the degree of compaction. It is believed that the interfaces between the individual increments may cause a momentary slowing of the burning front [11].

Dead pressing. Excessive loading pressure can, on the other hand, also lead to dead pressing. This occurs when the composition is consolidated to such a high density that the composition does not ignite or propagate. This is likely due to the limited space available for gas molecules to migrate and for mass transfer to take place. The activation energy is therefore much higher than usual and leads to propagation failures.

Extrusion. Interest in twin screw extrusion of energetic materials is growing due to the continuous nature of the process and the cost-effective production it potentially can provide compared to the more traditional batch processing methods [140]. It is actively applied to the production of flares, thermobaric devices, propellants and explosives [140]. A melt processable pyrotechnic composition, based on PVDF polymer (as the oxidizer) filled with aluminum powder as the fuel, was used to produce a filament for fused deposition modelling (FDM) purposes [141]. It was shown that the extrusion and printing process of the pyrotechnic composition did not negatively impact the energetic performance of the system. This opens up the possibility for the production of time delay fuses in a more continuous manner. Application of this technology would however require further development as at low fuel loadings, as in the abovementioned example, significant amounts of gaseous combustion products are expected [8]. Pyrotechnic time delays used for mining, civil and military purposes are generally preferred to be virtually gasless since they are implemented in enclosed systems [28, 104a, 114]. The generation of gaseous products can be decreased by increasing the fuel loading [8]. This, in turn, can lead to processing difficulties. However if applied as an unconfined fuse it may offer potential economic benefits.

9.4 Thermal Conductivity of the Tube Wall

Heat loss through the container walls is essentially dealt with by the tubular geometry. Radial heat flow decreases as the thickness of the tube increases and an increase in the diameter increases the heat loss for a constant wall thickness. Axial conduction along the tube wall affects the speed of a deflagration wave as it travels down the delay element [142]. Radial ignition is a possibility and leads to faster burning. The temperature of the metal wall at the charge end of the delay element is critical as this could cause premature initiation of a detonation wave. Therefore, an undesirable effect of high heat conductivity along the column wall may be a premature initiation of whatever terminal charge follows the delay column [9].

The effect of axial heat conduction in the metal wall of a delay element also affects the constancy of the burning rate. The flame speed is reduced below its one-dimensional adiabatic value at early times due to heat loss into the cold wall, but exceeds the adiabatic value at later times because the unreacted pyrotechnic ahead of the flame is preheated by radial conduction [143].

Table 11 compares the physical properties of potential tube materials with those of selected pyrotechnic ingredients. The heat loss will be greater from a tube with high thermal conductivity when placed inside a thermally conductive container. The internal tube diameter will have to be kept larger to sustain combustion in a tube of high thermal conductivity, e.g. one made from aluminum.

Table 11. Thermal conductivity (λ); density (ρ); heat capacity (C_p), and thermal diffusivity (α) of potential tube materials.

Material	λ $W\,m^{-1}K^{-1}$	$\rho \times 10^{-3}$ $kg\,m^{-3}$	C_p $J\,kg^{-1}K^{-1}$	$\alpha \times 10^{6}$ $m^2\,s^{-1}$
Al	220	2.7	960	85
Pb	35.3	11.34	160	19.45
SS	15	8.0	500	3.8
$CaSi_2$	0.42	2.5	960	2.04
Si	0.35	2.33	720	3.42
Al_2O_3	0.22	3.97	780	1.54
Nylon 6	0.24	1.12	1590	0.13
PC	0.20	1.2	1260	0.13
Teflon	0.30	2.20	1050	0.13
PMMA	0.2	1.2	1500	0.11

Table 12 shows the effect of wall thermal conductivity on the burning rate of a specific composition of the Sb-$KMnO_4$ system. The dramatic decrease in the burning rate in acrylic, i.e. poly (methyl methacrylate) tubes in an open system is attributed to severe melting and degradation. However, in a closed system the degradation products caused the development of high pressures. This increased the burning rate to approximately 8.2 $mm\,s^{-1}$ and caused a high proportion of tubes to burst.

Table 12. Effect of container material on the burning rate (u) of 30% Sb/$KMnO_4$ in open systems [100].

Container material	Burning rate ($mm\,s^{-1}$)
Column supported in air	1.9
Aluminum	2.2
Polyether imide	2.5
Acrylic	1.3
Packed in SiO_2	2.4
Packed in $CaCO_3$	2.2

The use of heat-resistant polymers (e.g. polycarbonate, PTFE, Kevlar and high-temperature 40% glass-filled polyether imide) did not reduce the quantity of gaseous degradation products sufficiently to prevent bursting of the detonator tubes. This suggests that polymers are not suitable tube materials for pyrotechnic delays.

Some work has been done on the use of ceramic containers [9]. The selection of ceramic bodies rather than met-

allic ones could have a favorable influence on marginal situations, especially where multiple columns occur in close proximity [9].

10 Characterizing Time Delay Compositions

10.1 Chemical and Phase Composition

The physical properties of solids, such as melting, decomposition temperatures and conductivity, depend greatly on the nature of the crystal bonding forces. The properties of crystals also depend on the specific crystal structure since the same atoms may link together in several different configurations. Crystal structures are characterized by the geometric symmetries of the unit cell repeated throughout the lattice and by the closeness of their packing. X-ray diffraction analysis is the primary characterization technique used to identify and quantify the different crystalline phases present in a composition or a mixture.

X-ray fluorescence is used as a complementary characterization technique to reveal the elemental composition of the reactants. This knowledge is important as pyrotechnic combustion characteristics are dependent on the chemical composition of the constituent components [122]. In addition to the main components, additives included, or contaminants present in the composition alter mechanical and energetic performance [104a,122]. Furthermore, crystal form and crystal defects in crystalline pyrotechnic materials influence the combustion properties of a composition [18]. For this reason analysis is performed to obtain information regarding the chemical purity of the constituents. While X-ray diffraction (XRD) analysis is performed in order to gauge the phase purity of component [90,104a,144], XRD analysis of combustion products also aids elucidation of the reaction pathway. This is done by analyzing recovered combustion residue and identifying the crystalline compounds present [8,18,28]. It is even possible to use XRD to estimate the quantity of amorphous phase present [19]. X-ray fluorescence (XRF) is used in order to determine the elemental composition of mixtures, be it a mixture of fuels or combustion products [8]. Identifying ratios in which elements were initially present and present in the solid residue following combustion provides further information as to the burning process and reaction scheme that was followed especially when combined with results from XRD analysis [8,18,28].

Most of the fuels used for pyrotechnics have a propensity to form protective oxide films on the surface which retard and in some cases prevent oxidation altogether. This oxide layer tends to influence the burn characteristics of the pyrotechnic composition. This occurs through reduced fuel-oxidizer contact as well as a reduced amount of available fuel per unit mass for reaction. This is particularly prominent in nano-sized materials where the oxide layer may account for a significant portion of the particle volume. Focused ion beam-scanning electron microscopy (FIB-SEM) has been shown to be an effective method of quantifying the extent of oxide formation on silicon powder [139]. In this method, an ion beam derived from a gallium source is used to mill the silicon particles into half, the particle cross-section can then be viewed and the thickness of the oxide layer determined.

Thermal analysis. Thermal analysis techniques have been used extensively to study energetic materials [10,29,52,121,145]. Recent reviews of the topic, including general principles of solid state reactions, are available [54,145a,146]. The thermal analysis methods employed include differential thermal analysis (DTA) [112]; differential scanning calorimetry (DSC); thermogravimetric analysis (TGA) [122,28,147,148]; bomb calorimetry and temperature profile analysis (TPA) [10,29,149]. Advanced thermal analysis techniques, recently reviewed [145a], include electrothermal explosion (ETE), electrothermography (ET), combustion velocity/temperature analyses, and other advanced in-situ diagnostics, including time-resolved X-ray diffraction (TRXRD).

Thermal analysis techniques are useful for studying pre-ignition phenomenon such as phase changes of individual components, their decomposition kinetics as well as ignition temperatures of the compositions. Special care should be taken when attempting to obtain kinetic data of thermal processes, including melting and crystallization; thermal decomposition; reactions of solids and hazardous processes [51,54]. The extraction of kinetic information from thermal analysis experiments for useful and reliable ignition and burning rate modelling purposes is on the wish list of all pyrotechnicians. The software packages developed by the Swiss society AKTS (Advanced Kinetics and Technology Solutions) can assist in this regard [150]. One of the most common DSC (or DTA) procedures is to estimate values for the activation energy, E, of the reaction rate with the Kissinger equation [151]. It posits a simple relationship between the kinetic parameters, E and k_o, and the temperature, T_m, at which the transformation rate is at its maximum namely,

$$E/RT_m^2 = (k_o/\beta)\exp(-E/RT_m) \quad (32)$$

Mukasyan and Shuck [145a] reviewed the chemical kinetics for self-propagating high-temperature non-catalytic reactions with a major focus on listing the activation energies for numerous systems, including the factors that influence them. However, the proper interpretation of activation energies for delay compositions remains an unresolved issue. Boddington and Laye [94] conducted burning rate measurements on three gasless pyrotechnic mixtures over an extended range of ambient temperatures. They used these results to estimate activation energy values for the combustion process. The obtained values (typically less than 50 kJ mol^{-1}) were low compared with those obtained by thermal analysis techniques under non-ignition conditions. Values obtained by analyzing measured temperature profiles along burning columns returned even lower numbers, in the range 10–30 kJ mol^{-1} [29]. At issue is

whether kinetic parameters obtained using the Arrhenius relationship predict too great a reaction rate for pyrotechnic compositions at low temperatures. Perhaps the reaction controlling steps depend on the temperature or maybe the control of combustion is by diffusion or heat transfer processes? This question needs further investigation.

Assessing the quality of mixing. The degree of mixing obtained between the fuel and oxidant particles is very important for obtaining consistent delay times from the pyrotechnic delay element. The degree of mixing is influenced by several factors including particle size, particle size distribution, mixing techniques and binders used during the manufacturing process [74]. Generally a wider particle size distribution of the oxidant leads to better mixing characteristics. There is however, currently no direct method for measuring the quality of mixing. The quality of mixing is typically evaluated though burning rate measurements and ignition characteristics. These indirect measurements are, however, also influenced by other parameter variations. Montgomery, *et al.* [90] used scanning electron microscopy to qualitatively probe the degree mixing. However, this only provides a two-dimensional representation of the mixing. Due to the significant impact of the degree of mixing on the consistency of the burning rate, it is a research area worthy of more attention.

Ignition sensitivity. Pyrotechnic time delay compositions, can be ignited by various external stimuli. Examples include static electricity, electromagnetic fields, friction, heat impact [8, 122]. When designing pyrotechnic mixtures the susceptibility to unwanted initiation should be kept in mind as the process of mixing, assembling, transporting and implementing the pyrotechnic device can potentially expose the composition to various such stimuli [8, 122]. A balance however needs to be maintained between insensitivity and the ignitibility for the proposed application. A time delay composition in a mine detonator should be able to be ignited by the shock tube or by a starter composition that transfers the impulse from the shock tube to the delay element [20, 73c]. The shock tube initiates the time delay composition via heat provided by means of convection and conduction due to hot combustion gasses and particulate material leaving the end of the shock tube [13]. For this reason it is important to characterize the thermal stability of the components. Pre-ignition phenomenon such as phase changes of individual components and decomposition kinetics as well as ignition temperatures of the compositions are investigated utilizing the thermal analysis techniques mentioned earlier. Combining these methods allows for development of systems that are safe to handle.

Lasers are widely used to ignite energetic materials for research purposes. Laser provides another method for determining ignition sensitivity and, more specifically, the time to ignition [46]. The ignitibility of a composition by means of a laser is influenced by various factors which include the confinement, optical and thermal properties of the composition as well those of the laser [152]. Various types of lasers are used in these tests such as Ar-ion ($\lambda = 500$ nm), diode lasers ($\lambda = 784$ nm) [152b, c] and CO_2 lasers ($\lambda = 10.6$ μm) [8, 46, 153]. Determining the time to ignition at a constant power flux provides useful information regarding the sensitivity of samples. An example of this is comparing the effect that particle size and stoichiometry has on the ignition sensitivity of compacted compositions [46, 153].

Youichi *et al.* [145b] studied the thermal reactivity and sensitivity of Bi_2O_3 as oxidant with aluminum (Al), magnalium (MgAl), boron (B), ferrosilicon (FeSi), and silicon (Si) as fuels. Thermal analysis, ignition temperature test, and burning test were carried out to examine the thermal reactivity of these mixed systems. The thermal reactivity was not affected by the mixing ratio but ignition energy and the minimum ignition temperature correlated positively with the thermal conductivity of the fuels.

Sensitivity testing (friction, impact & ESD). A key aspect in pyrotechnics composition design, is the sensitivity of the material to accidental external stimuli. The stimuli can be classified as mechanical stimuli (impact and friction) or electrostatic discharge (ESD) [105]. Other authors include thermal sensitivity among the stimuli [15]. Knowledge of the sensitivity of pyrotechnic compositions to these stimuli is important when processing, handling and transporting the compositions. A range of specialized characterization equipment has been developed and these are used following standardized procedures. Tichapondwa *et al.* [18] evaluated the sensitivity of Si/$BaSO_4$ and Si/$CaSO_4$ formulations, both were classified as insensitive towards impact, friction and ESD stimuli. In the case of ESD stimuli, the insensitivity is based on the approximate maximum ESD energy developed by the average person at 200 pF and 25 kV which is approximately 60 mJ [154]. It should be noted that humans are capable of acting as conduits passing higher ESD energy from other objects.

Czajka *et al.* [44] studied the ignition sensitivity of a Zr-$BaCrO_4$ mixture and Fe-$KClO_4$ mixtures. In the latter case the performance of iron powders obtained by different synthesis routes (atomization, iron carbonyl decomposition, electrolysis and reduction of an iron(II) compound) were compared. Major differences were observed in electrostatic discharge sensitivity tests. The required spark energy ranged from 0.08 to 14.2 J for the iron-based composition while it was 0.82 for the zirconium as fuel. The differences were attributed to differences in the nature of the oxides present on the surfaces of the iron particles.

Impact, friction, and electrostatic discharge tests have shown that the $B_4C/NaIO_4$/PTFE [4] and the Mn/MnO_2 [114] delay systems are insensitive to unintended ignition.

Burning rate measurement approaches. Several techniques have been developed to measure the burning rates of pyrotechnic delay elements. The first technique that employed a complete detonator was developed by Hedger [73b] in which a trigger started the timer as the detonator is initiated via an electric firing device. The timer was then stopped by the signal from a photoelectric cell when the

reaction reached the end of the detonator. This method is still employed in commercial application with the only change being the start of the timer via shock tube ignition. Tichapondwa *et al.* [19] provided a detailed description of this method. This method being simple to set up and relatively inexpensive, it is also used widely in laboratories for testing delay elements on their own [42, 73a, 155]. In another variation of this method, the timer is started via a sound sensor which is activated by the explosive noise emitted by the shock tube [20, 26]. Further variations of this method includes replacing the optical sensor with a thermocouple or using two optical sensors for the starting and ending condition [20, 127]. The use of optical sensors, however requires the delay element to be open-ended, which reduces the level of confinement in the delay element. The effect of open-ended burning has not been quantified adequately and could lead to some inconsistencies. The use of a high-speed cameras to measure the burning rates of luminescent pyrotechnic delay compositions have also been used [85]. This method is, however, limited to compositions pressed inside high-temperature resistant and transparent holders, e.g. a quartz tube. Another method extensively applied in laboratories is the use of two thermocouples to measure the temperature rise inside the delay element [73c, 149, 156]. The instant rise in temperature measured is then used to discern the position of the combustion wave at a specific instance in time. The temperature profiles recorded in this way can also be used to some extent to fit kinetic profile data [156a, 157]. The results are, however, significantly influenced by the size and type of thermocouples that are used. If the thermocouples are too large or the response is time too slow, the burning rates obtained are significantly slower than those measured using other methods [147]. Infrared cameras can also be used to measure the temperature profile development on the outside of the delay elements in real time [142b, 147]. This method is limited to application on delay elements constructed from tube materials with high thermal conductivities, as the heat has to transfer through the tube wall before it is detected by the infrared camera. Each measurement technique has its own limitations and problems. The need for an inexpensive, accurate and safe measurement technique, that can be used to gather continuous burning rate information, remains.

11 Computer Modelling

11.1 Modelling Thermochemistry

A new pyrotechnic system must be able to produce a specified effect for a given time within defined spatial constraints. Ensuring that these objectives are met is often difficult, time-consuming and costly, especially when the constraints are new and untried [101]. It is therefore important to be able to 'design' a pyrotechnic composition with the minimum amount of experimentation. To aid the designer, the application of computer programs is becoming more popular. These programs are capable of calculating the reaction products and their compositions, together with the thermodynamic properties of pyrotechnic formulations [15, 158]. The use of simulations also aids interpretation of other analysis techniques when investigating the reaction mechanism for a given composition.

Thermodynamic codes generally work on the principle of finding the chemical equilibrium composition, from the given reactants, by minimization of the Gibbs free energy. A number of pyrotechnics thermodynamics codes have been developed. However, the reliability of the results remains an issue [158]. Some of the more common include the ICT code, the EKVI code, NASA CEA, Cheetah, HSC, PROPEP and Factsage [158–159]. Most of these thermodynamic models are not well suited for pyrotechnic compositions that produce a relatively high proportion of solid species upon combustion as they tend to fail to converge to the true equilibrium solutions [158]. The EKVI code is less prone to this but it has a smaller database. However, Factsage has become more popular for delay modelling applications [159b].

11.2 Numerical Modelling of Burning Rates

One of the first transient models, corresponding to a one-dimensional energy balance over a delay element, was proposed by Beck *et al.* [14]. The model is based on the assumption that the reaction propagates in the lateral direction only and that there is a single source of heat generation with a planar waveform propagating forward. The model did not include any mass transfer effects. Various researchers have developed numerical models similar to this, with some changes in the simplifying assumptions [53, 71, 142a, 149, 155–156, 157, 160]. One of the main problems experienced, when applying numerical models in pyrotechnics, is the highly non-linear rate at which the exothermic reaction heat is generated. Consequently, the governing differential equations are very stiff in both time and length [160j]. This causes difficulties with respect to convergence to the correct solutions and it also requires significant computational power to solve. An interesting simplifying approach, designed to deal with these problems, involves linearization of the governing equations [53, 149, 156a, 157].

The numerical initiation of the pyrotechnic reaction presents another obstacle that needs to be overcome. One solution is to simulate pressing a hot plate against the ignition side of the delay element [160e, f]. However, the thermal resistance between the plate and the element leads to slight delays in ignition. Another approach, which has been implemented with great success, is to apply a heat pulse to the end of the delay composition [160d].

The chief problem is that the models are dependent upon the assumed, but unknown, reaction kinetics. Satisfactory solid state pyrotechnic reaction kinetics are not yet available as the required detail understanding is lacking. Apparent kinetics expression must therefore be informed from experimental data. The reaction temperatures are most commonly measured using thermocouples and recently also by infrared camera [53, 142b, 147]. Nevertheless, successful implementation of reliable numerical simulation of pyrotechnic delay element behavior will in the end provide important advantages. It will reduce the development time and cost as well as the risk associated with performing extensive experimental evaluations. Simulations allow facile control of variables to predict outcomes, something that is often difficult to do during real experimental evaluations. It is expected that over the next decade there will be a significant increase in the application of numerical models in this field as computing power keeps on increasing exponentially and understanding grows.

12 Concluding Remarks

Significant progress has been made toward the development of 'green' delay compositions. Mining and military applications may differ with respect to the need for gasless compositions. 'Green' gassy compositions, suitable for military pyrotechnic-based munitions, were successfully developed [4, 104b] Mining detonator delay systems are required to provide time delays ranging from milliseconds to several seconds. This need can be satisfied by an appropriate set of fast-, medium- and slow-burning compositions. Much progress has been made in the development of slow 'green' gasless compositions, e.g. B/Fe_2O_3 [25], W/MnO_2 [28], and Si/$CaSO_4$ [19]. Mn/MnO_2 [26, 114] and Si/Bi_2O_3 [20] offer 'green' medium-slow and medium-fast burning options respectively. Missing is a 'green' delay composition that can compete with the burning rates offered by the Si/Pb_3O_4 system. Nanothermites are a possibility as they can achieve extremely fast burning rates [45, 161] but the high temperatures generated may pose containment problems in detonator assemblies.

While nanothermites typically release much heat when they react, the fastest combustion velocities are obtained with loose powders. They burn far slower when they are compressed. It might be possible to find a compromise with the loose nanothermite powder just pressed sufficiently to form a cohesive material. If this corresponds to a low fraction of its TMD it means that the metallic tube will only be partially filled with the highly energetic material. In this way excessive heating of the delay composition can be avoided and the nanothermite could be the ideal delay compositions for very short times (in the range from μs to ms). In this regard it should be mentioned that there are indeed nanothermites compositions that show high combustion rates but that generate little to no gas, e.g. the Al/NiO system [162].

Fast burning rates are also possible even with micron-sized thermites. For example, fast burning rates, reaching 655 mm s^{-1}, were achieved in micron-sized Al/CuO thermite activated by a small amount of Si/Bi_2O_3 [106]. However, the high temperatures generated made it necessary to use steel tubes in place of the conventional aluminum tubing.

In the authors' opinion, future advances can be expected with the implementation of intermetallics. So far only one system (Ti/C-3Ni/Al), utilizing reagents that react to form an intermetallic compound, has demonstrated potential as a delay composition [27]. Particularly promising research avenues are suggested by the advances that have been made in the production of intermetallic particles, in which the reactive components are in intimate contact. This includes fully dense particle preparation mechanochemically via arrested milling [45] or by creating reactive multilayer powder particles by milling previously cold-rolled stacks of alternating multilayer laminate sheets [129b]. A problem, apparently experienced with attempts to implement intermetallic-based systems in actual detonator trains, are difficulties experienced with reliable transfer of the pyrotechnic impulse to the primary explosive. However, it is anticipated that this problem might be overcome by suitable combinations of intermetallics with thermites. This could simultaneously solve the problem of the excessive temperatures developed by thermite-based systems. A hint that this may indeed be possible, is offered by the fact that sustained combustion wave propagation was achieved by adding the thermite couple composed of 2Al/WO_3 to the W–Si reaction system [163].

With respect to modeling, progress will depend on the development of improved models for the temperature and conversion dependence of the chemical reaction in compacted particle beds.

As far as processing is concerned, manufacturing safety and efficiency was much improved by changing from powder mixing to water-based slurry mixing followed by spray drying. This yields spherical particles with good flow properties that facilitated press-filling of the powder. It is anticipated that in future it will be possible to mass produce delay fuse, whether gassy or not, by polymer extrusion technology. In this regard, suitable compositions based on fluoropolymers need to be developed.

Acknowledgements

This work is based on the research supported in part by AEL Mining Services (AEL/UP-4400021845) and by the National Research Foundation (NRF) of South Africa (Grant 83874). The opinions, findings, and conclusions or recommendations expressed in this publication are those of the authors, and neither AEL Mining Services nor the NRF accept any liability whatsoever in this regard.

References

[1] J. C. Poret, A. P. Shaw, L. J. Groven, G. Chen, K. D. Oyler, In *Environmentally Benign Pyrotechnic Delays*, 38th International Pyrotechnics Seminar, Denver, Colorado, USA, 10–15 June **2012**, pp 494–500.

[2] J. Silva, L. Li, J. M. Gernand. Reliability Analysis for Mine Blast Performance Based on Delay Type and Firing Time, *Int. J. Min. Sci. Technol.* **2017**, *28*, 195–204. doi.org/10.1016/j.ijmst.2017.07.004

[3] J. C. Poret, A. P. Shaw, C. M. Csernica, K. D. Oyler, J. A. Vanatta, G. Chen. Versatile boron carbide-based energetic time delay compositions, *ACS Sustainable Chem. Eng.* **2013**, *1*, 1333–1338. DOI: 10.1021/sc400187h

[4] A. P. Shaw, J. C. Poret, H. A. Grau Jr., R. A. Gilbert Jr. Demonstration of the $B_4C/NaIO_4$/PTFE Delay in the U. S. Army Hand-Held Signal. *ACS Sustainable Chem. Eng.* **2015**, *3*, 1558–1563.

[5] J. C. Poret, A. P. Shaw, E. J. Miklaszewski, L. J. Groven, C. M. Csernica, G. Chena, In *Environmentally Benign Energetic Time Delay Compositions: Alternatives for the U. S. Army Hand-Held Signal*, 40th International Pyrotechnics Seminar, Colorado Springs, Colorado, USA, 13–18 July **2014**, pp 305–314.

[6] a) M. Comet, B. Siegert, F. Schnell, V. Pichot, F. Ciszek, D. Spitzer. Phosphorus-Based Nanothermites: A New Generation of Pyrotechnics Illustrated by the Example of n-CuO/Red P Mixtures, *Propellants Explos. Pyrotech.* **2010**, *35*, 220–225; b) M. Comet, V. Pichot, B. Siegert, F. Schnell, F. Ciszek, D. Spitzer, Phosphorus-based nanothermites: A New Generation of Energetic Materials. *J. Phys. Chem. Solids* **2010**, *71*, 64–68.

[7] C. J. N. Kelly, W. C. Morrow, A. Zappalorti. *Fuse and its method of manufacture*, US Patent 3,908,509 A, Ensign-Bickford Co, USA, **1975**.

[8] G. Potgieter, W. W. Focke, O. Del Fabbro, G. D. Labuschagné, C. Kelly. Fluoroelastomer pyrotechnic time delay compositions, *J. Therm. Anal. Calorim.* **2016**, *126*, 1363–1370.

[9] H. Ellern. *Military and Civilian Pyrotechnics*, Chemical Publishing Company: New York, NY, **1968**.

[10] E. L. Charsley, C.-H. Chen, T. Boddington, P. G. Laye, J. R. G. Pude, Differential thermal analysis and temperature profile analysis of pyrotechnic delay systems: ternary mixtures of silicon, boron and potassium dichromate. *Thermochim. Acta* **1980**, *35*, 141–152.

[11] M. A. Wilson, R. J. Hancox, Pyrotechnic Delays and Thermal Sources, *J. Pyrotech.* **2001**, 13, 9–30.

[12] V. V. Andreev. Development of Nonelectric Explosion System SINV, Production Mastering and its Introduction into the Mining Industry, *Fiz. Goreniya Vzryva* **2001**, *37*, 137.

[13] D. K. L. Tsang. The initiation process inside a detonation delay element, *Int. J. Appl. Math. Mech.* **2005**, *2*, 12–39.

[14] M. W. Beck, M. E. Brown, D. Cawthorne. Pyrotechnic Delay Compositions, *ChemSA* **1984**, *10*, 398–399, 401.

[15] J. A. Conkling. Chapter 6: Heat and Delay Compositions, *Chemistry of Pyrotechnics: Basic Principles and Theory.* New York, New York, Marcel Dekker, Inc: **1985**.

[16] J. Jakubko. Pressure and Temperature Effects on Burning Rate of the Silicon – Red Lead System, *J. Energ. Mater.* **1997**, *15*, 151–161.

[17] M. W. Beck, J. Flanagan. *Delay Composition and Device*, US Pat 5,147,476 A, Orica Explosives Technology, Australia, **1992**.

[18] S. M. Tichapondwa, W. W. Focke, O. Del Fabbro, J. Gisby, C. Kelly. A Comparative Study of Si-$BaSO_4$ and Si-$CaSO_4$ Pyrotechnic Time-Delay Compositions, *J. Energ. Mater.* **2016**, *34*, 342–356.

[19] S. M. Tichapondwa, W. W. Focke, O. Del Fabbro, C. Kelly. Calcium Sulfate as a Possible Oxidant in "Green" Silicon-Based Pyrotechnic Time Delay Compositions, *Propellants Explos. Pyrotech.* **2015**, *40*, 518–525.

[20] L. Kalombo, O. Del Fabbro, C. Conradie, W. W. Focke. Sb_6O_{13} and Bi_2O_3 as Oxidants for Si in Pyrotechnic Time Delay Compositions, *Propellants Explos. Pyrotech.* **2007**, *32*, 454–460.

[21] G. Steinhauser, T. M. Klapötke. "Green" Pyrotechnics: A Chemists' Challenge, *Angew. Chem. Int. Ed.* **2008**, *47*, 3330–3347.

[22] M. R. Sijimol, M. Mohan. Environmental Impacts of Perchlorate with Special Reference to Fireworks-A Review, *Environ. Monit. Assess.* **2014**, *186*, 7203–7210.

[23] J. J. Sabatini. Advances Toward the Development of "Green" Pyrotechnics, In *Green Energetic Materials*, **2014**, pp 63–102.

[24] C. K. Wilharm, A. Chin, S. K. Pliskin. Thermochemical Calculations for Potassium Ferrate (VI), K_2FeO_4, as a Green Oxidizer in Pyrotechnic Formulations, *Propellants Explos. Pyrotech.* **2014**, *39*, 173–179.

[25] P. P. Elischer, G. Cleal, M. Wilson, *The Development of a Boron and Iron Oxide Delay System*. Report – Materials Research Laboratories (Australia) **1986**.

[26] D. Swanepoel, O. Del Fabbro, W. W. Focke, C. Conradie. Manganese as Fuel in Slow-Burning Pyrotechnic Time Delay Compositions, *Propellants Explos. Pyrotech.* **2010**, *35*, 105–113.

[27] E. J. Miklaszewski, J. C. Poret, A. P. Shaw, S. F. Son, L. J. Groven. Ti/C-3Ni/Al as a Replacement Time Delay Composition, *Propellants Explos. Pyrotech.* **2014**, *39*, 138–147.

[28] J. T. Koenig, A. P. Shaw, J. C. Poret, W. S. Eck, L. J. Groven. Performance of W/MnO_2 as an Environmentally Friendly Energetic Time Delay Composition, *ACS Sustainable Chem. Eng.* **2017**, *5*, 9477–9484.

[29] M. E. Brown. Some Thermal Studies on Pyrotechnic Compositions, *J. Therm. Anal. Calorim.* **2001**, *65*, 323–334.

[30] H. J. T. Ellingham. Transactions and Communications, *J. Soc. Chem. Ind. London* **1944**, *63*, 125–160.

[31] Z. A. Munir, U. Anselmi-Tamburini. Self-propagating Exothermic Reactions: The Synthesis of High-Temperature Materials By Combustion, *Mater. Sci. Rep.* **1989**, *3*, 277–365.

[32] S. H. Fischer, M. C. Grubelich. In *A Survey of Combustible Metals, Thermites, and Intermetallics for Pyrotechnic Applications*, 32nd Joint Propulsion Conference and Exhibition, **1996**; Lake Buena Vista; FL, pp 1–13.

[33] B. Berger. Parameters Influencing the Pyrotechnic Reaction, *Propellants Explos. Pyrotech.* **2005**, *30*, 27–35.

[34] A. Z. Moghaddam, G. J. Rees. Thermoanalytical Studies on Pyrotechnic Reactions, *Sci. Iran.* **2003**, *10*, 267–272.

[35] C. E. Shuck, K. V. Manukyan, S. Rouvimov, A. S. Rogachev, A. S. Mukasyan. Solid-flame: Experimental Validation, *Combust. Flame* **2016**, *163* (Supplement C), 487–493.

[36] K. L. Kosanke, B. J. Kosanke, R. C. Dujay. Pyrotechnic Particle Morphology – Low Melting Point Oxidizers, *J. Pyrotech.* **2000**, *12*, 5–15.

[37] J. H. Mclain. *Pyrotechnics from the Viewpoint of Solid State Chemistry*, Franklin Institute Press: Philadelphia, Pennsylvania, USA, **1980**.

[38] M. J. Tribelhorn, D. S. Venables, M. E. Brown. Combustion of some zinc-fuelled binary pyrotechnic systems, *Thermochim. Acta* **1995**, *256*, 309–324.

[39] R. L. Drennan, M. E. Brown. Binary and Ternary Pyrotechnic Systems of Mn and/or Mo and BaO_2 and/or SrO_2. Part 2, Combustion studies, *Thermochim. Acta* **1992**, *208*, 223–246.

[40] M. J. Tribelhorn, M. G. Blenkinsop, M. E. Brown. Combustion of Some Iron-Fuelled Binary Pyrotechnic Systems, *Thermochim. Acta* **1995**, *256*, 291–307.

[41] S. L. Howlett, F. G. J. May. Ignition and reaction of boron fueled pyrotechnic delay compositions: Part 1. Boron-Potassium Dichromate and Boron-Silicon-Potassium Dichromate Systems, *Thermochim. Acta* **1974**, *9*, 213–216.
[42] M. W. Beck, M. E. Brown. Burning of Antimony/Potassium Permanganate Pyrotechnic Compositions in Closed Systems, *Combust. Flame* **1986**, *65*, 263–271.
[43] K. L. Kosanke, B. J. Kosanke, Pyrotechnic Ignition and Propagation: A review. *J. Pyrotech.* **1997**, *6*, 17–29.
[44] B. Czajka, S. Styczyński, S. Tabat, D. Szal, L. Wachowski. Determination of Ignition Sensitivity of Selected Heat Powders, *Cent. Eur. J. Energ. Mater.* **2011**, *8*, 3–13.
[45] E. L. Dreizin, M. Schoenitz. Mechanochemically Prepared Reactive and Energetic Materials: A Review, *J. Mater. Sci.* **2017**, *52*, 11789–11809.
[46] J. J. Granier, M. L. Pantoya. Laser Ignition of Nanocomposite Thermites, *Combust. Flame* **2004**, *138*, 373–383.
[47] Y. S. Kwon, A. A. Gromov, J. I. Strokova. Passivation of the Surface Of Aluminum Nanopowders by Protective Coatings of the Different Chemical Origin, *Appl. Surf. Sci.* **2007**, *253*, 5558–5564.
[48] J. Mccollum, M. L. Pantoya, S. T. Iacono. Activating Aluminum Reactivity with Fluoropolymer Coatings for Improved Energetic Composite Combustion, *ACS Appl. Mater. Interfaces* **2015**, *7*, 18742–18749.
[49] a) S. Tichapondwa, W. Focke, O. D. Fabbro, R. Sandenbergh, E. Muller. Suppressing Hydrogen Evolution by Aqueous Silicon Powder Dispersions Through the Introduction of an Additional Cathodic Reaction, *Chem. Eng. Commun.* **2014**, *201*, 501–515; b) S. M. Tichapondwa, W. W. Focke, O. Del Fabbro, S. Mkhize, E. Muller. Suppressing H_2 Evolution by Silicon Powder Dispersions, *J. Energ. Mater.* **2011**, *29*, 326–343.
[50] P. Šimon. Considerations on the Single-Step Kinetics Approximation, *J. Therm. Anal. Calorim.* **2005**, *82*, 651–657.
[51] L. A. Pérez-Maqueda, J. M. Criado, P. E. Sánchez-Jiménez. Combined Kinetic Analysis of Solid-State Reactions: A Powerful Tool for the Simultaneous Determination of Kinetic Parameters and the Kinetic Model Without Previous Assumptions on the Reaction Mechanism, *J. Phys. Chem. A* **2006**, *110*, 12456–12462.
[52] P. G. Laye. Tying up loose ends, *Thermochim. Acta* **1997**, *300*, 237–245.
[53] T. Boddington, A. Cottrell, P. G. Laye. Combustion Transfer in Gasless Pyrotechnics, *Combust. Flame* **1990**, *79*, 234–241.
[54] S. Vyazovkin, K. Chrissafis, M. L. Di Lorenzo, N. Koga, M. Pijolat, B. Roduit, N. Sbirrazzuoli, J. J. Suñol. ICTAC Kinetics Committee Recommendations for Collecting Experimental Thermal Analysis Data for Kinetic Computations, *Thermochim. Acta* **2014**, *590*, 1–23.
[55] N. Koga, J. M. Criado. Kinetic Analyses of Solid-State Reactions with a Particle-Size Distribution, *J. Am. Ceram. Soc.* **1998**, *81*, 2901–2909.
[56] A. Khawam, D. R. Flanagan. Solid-State Kinetic Models: Basics and Mathematical Fundamentals, *J. Phys. Chem. B* **2006**, *110*, 17315–17328.
[57] a) Y. Zhang, G. C. Stangle. Ignition Criteria For Self-Propagating Combustion Synthesis, *J. Mater. Res.* **1993**, *8*, 1703–1711; b) P. G. Laye, C. P. Constantinou, F. Volk. Experimental Studies of the Propagation of Combustion in Solids [and Discussion], *Philos. Trans. Phys. Sci. Eng.* **1992**, *339*, 387–394.
[58] D. M. Johnson. *RDTR Report No. 56: Ignition theory: Application to the design of new ignition systems*; US Naval ammunition depot: Crane, Indiana, 1965.
[59] R. N. Rogers, Thermochemistry of Explosives, *Thermochim. Acta* **1975**, *11*, 131–139.
[60] A. G. Merzhanov, V. G. Abramov. Thermal Explosion of Explosives and Propellants. A Review, *Propellants Explos. Pyrotech.* **1981**, *6*, 130–148.
[61] a) M. Lakshmikantha, J. A. Sekhar. Analytical Modeling of the Propagation of a Thermal Reaction Front in Condensed Systems, *J. Am. Ceram. Soc.* **1994**, *77*, 202–210; b) A. Makino, Effect of Various Parameters on Flame Propagation in Combustion Synthesis, *Trans. Japan Soc. Mech. Eng. Ser. B* **1992**, *58*, 1931–1936.
[62] a) D. Sánchez-Rodriguez, J. Farjas, P. Roura, The Critical Conditions For Thermal Explosion in a System Heated at a Constant Rate, *Combust. Flame* **2017**, *186*, 211–219; b) A. G. Merzhanov, V. V. Barzykin, V. G. Abramov, The Theory of Thermal Explosion: From N. N.Semenov to Present Day. *Chem. Phys. Rep.* **1996**, *15*, 793–837.
[63] A. G. Merzhanov, A. E. Averson, The Present State of the Thermal Ignition Theory: An Invited Review, *Combust. Flame* **1971**, *16*, 89–124.
[64] L. L. Wang, Z. A. Munir, Y. M. Maximov, Thermite Reactions: Their Utilization in the Synthesis and Processing of Materials, *J. Mater. Sci.* **1993**, *28*, 3693–3708.
[65] P. V. Phung, A. P. Hardt, Ignition Characteristics of Gasless Reactions, *Combust. Flame* **1974**, *22*, 323–335.
[66] A. J. Brammer, E. L. Charsley, T. T. Griffiths, J. J. Rooney, S. B. Warrington. Paper 41: A Study of the Pyrotechnic Performance of the Silicon – Bismuth Oxide System, In *22nd International Pyrotechnics Seminar*, Fort Collins, Colorado, USA, **1996**.
[67] J. E. Spice, L. A. K. Staveley, The Propagation of Exothermic Reactions in Solid Systems, Part II. Heats of Reaction and Rates of Burning, *J. Soc. Chem. Ind. London* **1949**, *68*, 348–355.
[68] F. Booth, The Theory of Self-Propagating Exothermic Reactions in Solid Systems, *Trans. Faraday Soc.* **1953**, *49*, 272–281.
[69] B. I. Khaikin, A. G. Merzhanov, Theory of Thermal Propagation of a Chemical Reaction Front, *Combust. Explos. Shock Waves (Engl. Transl.)* **1966**, *2*, 22–27.
[70] a) S. B. Margolis. A Model For Condensed Combustion Synthesis of Nonstoichiometric Homogeneous Solids. *Combust. Flame* **1993**, *93*, 1–18; b) S. B. Margolis. Asymptotic Theory of Heterogeneous Condensed Combustion, *Combust. Sci. Technol.* **1985**, *43*, 197–215; c) S. B. Margolis. Asymptotic Theory of Condensed Two-Phase Flame Propagation, *SIAM J. Appl. Math.* **1983**, *43*, 351–369; d) S. B. Margolis, F. A. Williams. Flame propagation in Solids and High-Density Fluids with Arrhenius Reactant Diffusion, *Combust. Flame* **1991**, *83*, 390–398; e) A. P. Aldushin, B. I. Khaikin. Combustion of Mixtures Forming Condensed Reaction Products, *Combust. Explos. Shock Waves (Engl. Transl.)* **1974**, *10*, 273–280; f) J. Puszynski, J. Degreve, V. Hlavacek. Modeling of Exothermic Solid-Solid Noncatalytic Reactions, *Ind. Eng. Chem. Res.* **1987**, *26*, 1424–1434; g) A. G. Merzhanov. The Theory of Stable Homogeneous Combustion of Condensed Substances, *Combust. Flame* **1969**, *13*, 143–156.
[71] A. P. Hardt, P. V. Phung. Propagation of gasless reactions in solids-I. Analytical study of exothermic intermetallic reaction rates, *Combust. Flame* **1973**, *21*, 77–89.
[72] a) A. Shimizu. Suitability of the kinetic model for estimation of powder reaction rate. *Powder Technol.* **1998**, *100*, 24–31; b) A. Shimizu, Y. J. Hao. Influence of Particle Contact on the Estimation of Powder Reaction Kinetics of Binary Mixtures, *J. Am. Ceram. Soc.* **1997**, *80*, 557–568.

[73] a) S. S. Al-Kazraji, G. J. Rees. The Fast Pyrotechnic Reaction of Silicon and Red Lead: Heats of Reaction and Rates of Burning, *Fuel* **1979**, *58*, 139–143; b) J. T. Hedger. Factors Influencing the Pyrotechnic Reaction of Silicon and Red Lead, *Propellants Explos. Pyrotech.* **1983**, *8*, 95–98; c) I. M. M. Ricco, W. W. Focke, C. Conradie. Alternative Oxidants for Silicon Fuel in Time-Delay Compositions, *Combust. Sci. Technol.* **2004**, *176*, 1565–1575.

[74] A. G. Dugam, A. Muttalib, H. J. Gandhi, P. A. Phawade, A. John, R. R. Khare. Effect of Fuel Content and Particle Size Distribution of Oxidiser on Ignition of Metal-Based Pyrotechnic Compositions, *Def. Sci. J.* **1999**, *49*, 263–268.

[75] A. P. Aldushin, V. A. Vol'pert, V. P. Filipenko. Effect of reagent melting on combustion stability for gasless systems, *Combust. Explos. Shock Waves (Engl. Transl.)* **1988**, *23*, 408–420.

[76] a) A. Makino. Fundamental Aspects of the Heterogeneous Flame in the Self-Propagating High-Temperature Synthesis (SHS) Process, *Prog. Energy Combust. Sci.* **2001**, *27*, 1–74; b) A. G. Merzhanov, E. N. Rumanov. Physics of reaction waves, *Rev. Mod. Phys.* **1999**, *71*, 1173–1211; c) A. Ambekar, J. J. Yoh. A reduced order model for prediction of the burning rates of multicomponent pyrotechnic propellants, *Appl. Therm. Eng.* **2018**, *130*, 492–500.

[77] a) R. Armstrong. Models for Gasless Combustion in Layered Materials and Random Media, *Combust. Sci. Technol.* **1990**, *71*, 155–174; b) R. Armstrong, Theoretical Models for the Combustion of Alloyable Materials. *Metall. Trans. A* **1992**, *23*, 2339–2347; c) A. Makino. Heterogeneous Flame Propagation in the Self-Propagating, High-Temperature, Synthesis (SHS) Process in Multi-Layer Foils: Theory and Experimental Comparisons, *Combust. Flame* **2003**, *134*, 273–288; d) A. Makino. Effects of Layer Thickness on the Burning Velocity and the Range of Flammability in the SHS Process with Multi-Layer Foils, *Nihon Kikai Gakkai Ronbunshu, B Hen/Trans. Japan Soc. Mech Eng., Part B* **2006**, *72*, 2307–2314; e) C. He, C. Blanchetiere, G. C. Stangle, A Micromechanistic Model Of The Combustion Synthesis Process: Influence of Intrinsic Kinetics, *J. Mater. Res.* **1998**, *13*, 2269–2280.

[78] a) A. A. M. Oliveira, M. Kaviany. Role of Inter- and Intraparticle Diffusion in Nonuniform Particle Size Gasless Compacted-Powder Combustion Synthesis-I: Formulation, *Int. J. Heat Mass Transfer* **1999**, *42*, 1059–1073; b) A. A. M. Oliveira, M. Kaviany. Role of inter- and intraparticle diffusion in nonuniform particle size gasless compacted powder combustion synthesis-II: Results and comparison with experiment, *Int. J. Heat Mass Transfer* **1999**, *42*, 1075–1095.

[79] J. Kostogorova, H. J. Viljoen, A. Shteinberg. Role of particle geometry and surface contacts in solid-phase reactions, *AIChE J.* **2002**, *48*, 1794–1803.

[80] Y. J. Hao, T. Tanaka. Role of the contact points between particles on the reactivity of solids, *Can. J. Chem. Eng.* **1988**, *66*, 761–766.

[81] M. E. Brown, S. J. Taylor, M. J. Tribelhorn. Fuel-Oxidant Particle Contact in Binary Pyrotechnic Reactions, *Propellants Explos. Pyrotech.* **1998**, *23*, 320–327.

[82] V. V. Dalvi, A. K. Suresh. A Contact-Point Based Approach for the Analysis of Reactions Among Solid Particles, *AIChE J.* **2011**, *57*, 1329–1338.

[83] R. Amaresh, M. Pathak, A. K. Suresh. Kinetics of Solid-Solid Reactions: Influence of the Number of Contact Points, *Ind. Eng. Chem. Res.* **2014**, *53*, 11659–11667.

[84] a) J. M. Beck, V. A. Volpert. Nonlinear dynamics in a simple model of solid flame microstructure, *Phys. D (Amsterdam, Neth.)* **2003**, *182*, 86–102; b) J. M. Beck, V. A. Volpert. A Simple Model of Two-Dimensional Solid Flame Microstructure, *Combust. Theory Modell.* **2003**, *7*, 795–812; c) S. Knapp, V. Weiser, S. Kelzenberg, N. Eisenreich. Modeling Ignition And Thermal Wave Progression in Binary Granular Pyrotechnic Compositions, *Propellants Explos. Pyrotech.* **2014**, *39*, 423–433.

[85] K. S. Kappagantula, B. Clark, M. L. Pantoya. Flame Propagation Experiments of Non-Gas-Generating Nanocomposite Reactive Materials, *Energy Fuels* **2011**, *25*, 640–646.

[86] B. S. Bockmon, M. L. Pantoya, S. F. Son, B. W. Asay, J. T. Mang. Combustion velocities and propagation mechanisms of metastable interstitial composites, *J. Appl. Phys.* **2005**, 98, Art. no. 064903.

[87] a) S. M. Danali, R. S. Palaiah, K. C. Raha. Developments in Pyrotechnics, *Def. Sci. J.* **2010**, *60*, 152–158; b) R. G. Sarawadekar, J. P. Agrawal. Nanomaterials in Pyrotechnics, *Def. Sci. J.* **2008**, *58*, 486–495; c) D. A. Yagodnikov, A. V. Ignatov, E. I. Gusachenko. Ignition and Combustion of Pyrotechnic Compositions Based on Microsized and Ultra-Nanosized Aluminum Particles in a Moist Medium in a Two-Zone Gas Generator, *Combust. Explos. Shock Waves (Engl. Transl.)* **2017**, *53*, 15–23.

[88] M. L. Pantoya, V. I. Levitas, J. J. Granier, J. B. Henderson. Effect of Bulk Density on Reaction Propagation in Nanothermites and Micron Thermites, *J. Propul. Power* **2009**, *25*, 465–470.

[89] V. I. Levitas, B. W. Asay, S. F. Son, M. Pantoya. Melt Dispersion Mechanism for Fast Reaction of Nanothermites, *Appl. Phys. Lett.* **2006**, *89*.

[90] Y. C. Montgomery, W. W. Focke, M. Atanasova, O. Del Fabbro, C. Kelly. $Mn + Sb_2O_3$ Thermite/Intermetallic Delay Compositions, *Propellants Explos. Pyrotech.* **2016**, *41*, 919–925.

[91] A. P. Hardt, R. W. Holsinger. Propagation of Gasless Reactions in Solids-II. Experimental Study of Exothermic Intermetallic Reaction Rates, *Combust. Flame* **1973**, *21*, 91–97.

[92] A. P. Aldushin, K. I. Zeinenko. Combustion of Pyrotechnic Mixtures with Heat Transfer from Gaseous Reaction Products, *Combust. Explos. Shock Waves (Engl. Transl.)* **1991**, *27*, 700–703.

[93] A. H. C. Norgrove, A. F. Jones, J. A. King-Hele. Effects of solid to gas conversion in detonator delay elements, *Combust. Sci. Technol.* **1991**, *76*, 133–157.

[94] T. Boddington, P. O. Laye. Temperature dependence of the burning velocity of gasless pyrotechnics, *Thermochim. Acta* **1987**, *120*, 203–206.

[95] E. L. Charsley, P. G. Laye, M. E. Brown. Chapter 14, *Pyrotechnics*, In *Handbook of Thermal Analysis and Calorimetry*, **2003**, Vol. 2, pp 777–815.

[96] T. A. Steinberg, D. B. Wilson, F. Benz. The Combustion Phase of Burning Metals, *Combust. Flame* **1992**, *91*, 200–208.

[97] K. L. Cashdollar, I. A. Zlochower. Explosion temperatures and Pressures of Metals and Other Elemental Dust Clouds, *J. Loss Prev. Process Ind.* **2007**, *20*, 337–348.

[98] U. Krone, R. Lancaster, *Pyrotechnics*. In: W. B. Gerhartz, Ed. *Ullmann's Encyclopedia of Industrial Chemistry*, 5 ed.; VCH Publishers: Weinheim, **1992**, pp 437–452.

[99] R. A. Rugunanan, M. E. Brown. Reactions of Powdered Silicon with Some Pyrotechnic Oxidants, *J. Therm. Anal.* **1991**, *37*, 1193–1211.

[100] M. W. Beck, M. E. Brown. Modification of the Burning Rate of Antimony/Potassium Permanganate Pyrotechnic Delay Compositions, *Combust. Flame* **1986**, *66*, 67–75.

[101] T. Barton, T. Griffiths, E. Charsley, J. Rumsey, In *The Role of Organic Binders in Pyrotechnic Reactions*, 8th International Pyrotechnics Seminar, Colorado, USA, **1982**, pp 83–98.

[102] T. F. Han, S. L. Yan. Effects of the Binders on the Storage Stability of the Silicon Delay Composition, *Adv. Mater. Res.* **2014**, *977*, 135–140.

[103] J. C. Oxley. Non-traditional explosives: Potential detection problems, *Terror. Political Violence* **1993**, *5*, 30–47.
[104] a) S. M. Tichapondwa, W. W. Focke, O. Del Fabbro, G. Labuschagne. The Effect of Additives on the Burning Rate of Silicon-Calcium Sulfate Pyrotechnic Delay Compositions, *Propellants Explos. Pyrotech.* **2016**, *41*, 732–739; b) J. C. Poret, A. P. Shaw, *et al*. Development and Performance of the $W/Sb_2O_3/KIO_4$/lubricant Pyrotechnic Delay in the US Army Hand-Held Signal, *Propellants Explos. Pyrotech.* **2013**, *38*, 35–40; c) R. A. Rugunanan, M. E. Brown. Combustion of Binary and Ternary Silicon/Oxidant Pyrotechnic Systems, Part I: Binary Systems with Fe_2O_3 and SnO_2 as Oxidants. *Combust. Sci. Technol.* **1993**, *95*, 61–83.
[105] K. Kosanke, B. Kosanke, I. Von Maltitz, B. Sturman, T. Shimizu, M. Wilson, N. Kubota, C. Jennings-White, D. Chapman. Pyrotechnic Chemistry, Pyrotechnic Reference Series, No. 4. *J. Pyrotech., Inc., Whitewater,* CO, USA **2004**.
[106] K. Ilunga, O. Del Fabbro, L. Yapi, W. W. Focke, The Effect of Si-Bi_2O_3 on the Ignition of the Al-CuO Thermite. *Powder Technol.* **2011**, *205*, 97–102.
[107] a) R. Hill, L. Sutton, R. Temple, A. White. Slow Self-Propagating Reaction in solids. *Research* **1950**, *3*, 569–576; b) B. Khaikin, A. Merzhanov, Theory of thermal Propagation of a Chemical Reaction Front. *Combust. Explos. Shock Waves (Engl. Transl.)* **1966**, *2*, 22–27.
[108] A. J. Tulis, Flowability Techniques In The Processing Of Powdered Explosives, Propellants, And Pyrotechnics. *J. Hazard. Mater.* **1980**, *4*, 3–10.
[109] H. Ren, Q. Jiao, S. Chen, Mixing Si and Carbon Nanotubes by a Method of Ball-Milling and its Application to Pyrotechnic Delay Composition. *J. Phys. Chem. Solids* **2010**, *71*, 145–148.
[110] V. Pichot, M. Comet, J. Miesch, D. Spitzer, Nanodiamond for Tuning the Properties of Energetic Composites. *J. Hazard. Mater.* **2015**, *300*, 194–201.
[111] E. Koch, D. Clement, Special materials in pyrotechnics: VI. Silicon – An old fuel with new perspectives. *Propellants Explos. Pyrotech.* **2007**, *32*, 205–212.
[112] S. R. Yoganarasimhan, O. S. Josyulu, Reactivity of the Ternary Pyrotechnic System Red Lead – Silicon – Ferric Oxide. *Def. Sci. J.* **1987**, *37*, 73–83.
[113] P. Gibot, M. Comet, L. Vidal, F. Moitrier, F. Lacroix, Y. Suma, F. Schnell, D. Spitzer, Synthesis of WO_3 Nanoparticles for Superthermites by the Template Method From Silica Spheres. *Solid State Sci.* **2011**, *13*, 908–914.
[114] E. J. Miklaszewski, A. P. Shaw, J. C. Poret, S. F. Son, L. J. Groven, Performance and Aging of Mn/MnO_2 as an Environmentally Friendly Energetic Time Delay Composition. *ACS Sustainable Chem. Eng.* **2014**, *2*, 1312–1317.
[115] R. A. Rugunanan. Intersolid Pyrotechnic Reactions of Silicon. Rhodes University, Rhodes, **1992**.
[116] R. A. Rugunanan, M. E. Brown, Combustion of Binary and Ternary Silicon/Oxidant Pyrotechnic Systems, Part II: Binary Systems With Sb_2O_3 and KNO_3 as Oxidants. *Combust. Sci. Technol.* **1993**, *95*, 85–99.
[117] A. Z. Moghaddam, G. J. Rees, The Fast Pyrotechnic Reaction of Silicon with Lead Oxides: Differential Scanning Calorimetry and Hot-Stage Microscopy Studies. *Fuel* **1981**, *60*, 629–632.
[118] J. Jakubko, E. Černošková. Differential Thermal Analysis of the Mixtures of Silicon and Red Lead, *J. Therm. Anal.* **1997**, *50*, 511–515.
[119] J. Jakubko. Combustion of the Silicon-Red Lead System. Temperature of Burning, Kinetic Analysis and Mathematical Model, *Combust. Sci. Technol.* **1999**, *146*, 37–55.
[120] T. Boberg, S. Carlsson, B. Ekman, B. Karlsson, *Delay Charge and Element and Detonator Containing such a Charge.* US Pat 5,654,520, Nitro Nobel AB, **1997**.
[121] P. Laye, E. Charsley. Thermal Analysis of Pyrotechnics, *Thermochim. Acta* **1987**, *120*, 325–349.
[122] S. G. Hosseini, S. M. Pourmortazavi, S. S. Hajimirsadeghi. Thermal Decomposition of Pyrotechnic Mixtures Containing Sucrose with Either Potassium Chlorate or Potassium Perchlorate, *Combust. Flame* **2005**, *141*, 322–326.
[123] H. Zöllner, D. Funke, Pyrotechnischer Verzögerungssatz Militärischer Verzögerungselemente, EP3090232 A1, DynITEC GmbH, 2015.
[124] C.-K. Cheng, C.-R. Huang, Y. Y. Wu, In *Studies on the Delay Mix of Zr/Fe_2O_3*, 12th Symposium on Explosives and Pyrotechnics, San-Diego, California, USA, March 13–15, **1984**, pp 33–38.
[125] M. Wang, B. Sundman, Thermodynamic Assessment of the Mn–O system. *Metall. Trans. B* **1992**, *23*, 821–831.
[126] A. N. Grundy, B. Hallstedt, L. J. Gauckler, Assessment of the Mn–O System. *J. Phase Equilib.* **2003**, *24*, 21–39.
[127] Y. Li, Y. Cheng, Y. Hui, S. Yan, The Effect Of Ambient Temperature And Boron Content On The Burning Rate of the B/Pb_3O_4 Delay Compositions, *J. Energ. Mater.* **2010**, *28*, 77–84.
[128] E. Shachar, A. Gany. Investigation of Slow-Propagation Tungsten Delay Mixtures, *Propellants Explos. Pyrotech.* **1997**, *22*, 207–211.
[129] a) G. M. Fritz, H. Joress, T. P. Weihs. Enabling and Controlling Slow Reaction Velocities in Low-Density Compacts of Multilayer Reactive Particles, *Combust. Flame* **2011**, *158*, 1084–1088; b) A. K. Stover, N. M. Krywopusk, J. D. Gibbins, T. P. Weihs. Mechanical Fabrication Of Reactive Metal Laminate Powders, *J. Mater. Sci.* **2014**, *49*, 5821–5830.
[130] Q. G. Ren, X. J. Qiao, W. C. Li, C. G. Peng, Co-precipitation Preparation of Silicon Delay Composition and its Properties, *Hanneng Cailiao/Chinese J. Energ. Mater.* **2012**, *20*, 409–413.
[131] J. Scicolone, A. Mujumdar, S. Sundaresan, R. N. Davé, Environmentally Benign Dry Mechanical Mixing of Nano-Particles Using Magnetically Assisted Impaction Mixing Process, *Powder Technol.* **2011**, *209*, 138–146.
[132] R. Barrow, Y. Jun, R. Dave, R. Pfeffer, Dry-mixing of Sub-micron B and $BaCrO_4$ Particles for use in a Time Delay Composition, *SAFE J.* **2007**, *35*, 7–13.
[133] L. M. Aikman, T. E. Shook, R. M. Lehr, E. Robinson, F. Mcintyre, Improved Mixing, Granulation and Drying of Highly Energetic Pyromixtures, *Propellants Explos. Pyrotech.* **1987**, *12*, 17–25.
[134] a) J. G. Osorio, F. J. Muzzio, Evaluation of Resonant Acoustic Mixing Performance, *Powder Technol.***2015**, *278*, 46–56; b) J. G. Osorio, E. Hernández, R. J. Romañach, F. J. Muzzio, Characterization of Resonant Acoustic Mixing Using Near-Infrared Chemical Imaging, *Powder Technol.* **2016**, *297*, 349–356.
[135] S. K. Chan, N. Y. W. Hsu, R. Oliver, *Process for the Preparation of Gas-Generating Compositions*, EPatent Application 0735013 A1, Imperial Chemical Industries, London, GB **1998**.
[136] S. M. Umbrajkar, M. Schoenitz, E. L. Dreizin, Control of Structural Refinement and Composition in $Al-MoO_3$ Nanocomposites Prepared by Arrested Reactive Milling, *Propellants Explos. Pyrotech.* **2006**, *31*, 382–389.
[137] C. G. Morgan, C. Rimmington, Manufacture of Pyrotechnic Time Delay Compositions, WO2008035288 A3, AEL Mining Services, South Africa, **2012**.
[138] E. Boonekamp, J. Kelly, J. Van De Ven, A. Sondag, The Chemical Oxidation of Hydrogen-Terminated Silicon (111) Surfaces in Water Studied in Situ with Fourier Transform Infrared Spectroscopy, *J. Appl. Phys.* **1994**, *75*, 8121–8127.

[139] S. M. Tichapondwa, W. W. Focke, O. Del Fabbro, E. Muller, Suppressing Hydrogen Evolution by Aqueous Silicon Powder Dispersions by Controlled Silicon Surface Oxidation, *Propellants Explos. Pyrotech.* **2013**, *38*, 48–55.

[140] D. Dombe, Mehilal, C. Bhongale, P. P. Singh, B. Bhattacharya, Application of Twin Screw Extrusion for Continuous Processing of Energetic Materials, *Cent. Eur. J. Energ. Mater.* **2015**, *12*, 507–522.

[141] T. J. Fleck, A. K. Murray, I. E. Gunduz, S. F. Son, G. T.-C. Chiu, J. F. Rhoads, Additive Manufacturing of Multifunctional Reactive Materials, *Addit. Manuf.* **2017**, 17, 176–182.

[142] a) L. Clements, J. A. King-Hele, A. F. Jones, R. M. Thomas, Some Effects of Axial Temperature Gradients in the Wall of a Detonator Delay Element, *Combust. Sci. Technol.* **1995**, *107*, 205–221. b) Y. C. Montgomery, W. W. Focke, C. Kelly, Measurement and Modelling of Pyrotechnic Time Delay Burning Rates: Application and Prediction of a Fast Burning Delay Composition, *Propellants Explos. Pyrotech.* **2017**, *42*, 1289–1295.

[143] A. H. C. Norgrove, A. F. Jones, J. A. King-Hele, Effects of Axial Heat Conduction in the Metal Wall of a Detonator Delay Element, *Combust. Sci. Technol.* **1994**, *97*, 449–468.

[144] K. W. Watson, M. L. Pantoya, V. I. Levitas, Fast Reactions with Nano- and Micrometer Aluminum: A Study on Oxidation Versus Fluorination, *Combust. Flame* **2008**, *155*, 619–634.

[145] a) A. S. Mukasyan, C. E. Shuck, Kinetics of SHS Reactions: A Review, *Int. J. Self-Propag. High-Temp. Synth.* **2017**, *26*, 145–165; b) S. Youichi, N. Toshiyuki, F. Hisa-Aki. Thermal Reaction or Sensitivity of Bi_2O_3 and Metal Powder, *Sci. Technol. Energ. Mater.* **2013**, *74*, 93–99.

[146] E. L. Dreizin, M. Schoenitz, Correlating Ignition Mechanisms of Aluminum-Based Reactive Materials with Thermoanalytical Measurements, *Prog. Energy Combust. Sci.* **2015**, *50*, 81–105.

[147] Y. C. Montgomery, W. W. Focke, C. Kelly, Measurement and Modelling of Pyrotechnic Time Delay Burning Rates: Method and Model Development, *Propellants Explos. Pyrotech.* **2017**, *42*, 1161–1167.

[148] A. Hahma, A. Gany, K. Palovuori, Combustion of Activated Aluminum, *Combust. Flame* **2006**, *145*, 464–480.

[149] T. Boddington, P. G. Laye, J. R. G. Pude, J. Tipping, Temperature Profile Analysis of Pyrotechnic Systems, *Combust. Flame* **1982**, *47*, 235–254.

[150] AKTS Ag, *AKTS-Thermokinetics Software*, 2015.

[151] H. E. Kissinger, Reaction Kinetics in Differential Thermal Analysis, *Anal. Chem.* **1957**, *29*, 1702–1706.

[152] a) X. Fang, S. R. Ahmad, Laser Ignition of an Optically Sensitised Secondary Explosive by Diode Laser, *Cent. Eur. J. Energ. Mater.* **2016**, *13*, 103–115; b) S. R. Ahmad, D. A. Russel, Laser Ignition of Pyrotechnics - Effects of Wavelength, Composition and Confinement, *Propellants Explos. Pyrotech.* **2005**, *30*, 131–139; c) S. R. Ahmad, D. A. Russel, Studies into Laser Ignition of Confined Pyrotechnics, *Propellants Explos. Pyrotech.* **2008**, *33*, 396–402.

[153] M. L. Pantoya, J. J. Granier, Combustion Behavior of Highly Energetic Thermites: Nano Versus Micron Composites, *Propellants Explos. Pyrotech.* **2005**, *30*, 53–62.

[154] K. L. Kosanke, B. T. Sturman, R. M. Winokur, B J. Kosanke. *Encyclopedic dictionary of pyrotechnics:(and related subjects). J. Pyrotech.* **2012**.

[155] M. W. Beck, M. E. Brown, D. Cawthorne, Pyrotechnic Delay Compositions, *ChemSA* **1984**, *June 1984*, 398–399, 401.

[156] a) T. Boddington, P. G. Laye, J. Tipping, D. Whalley, Kinetic Analysis of Temperature Profiles of Pyrotechnic Systems, *Combust. Flame* **1986**, *63*, 359–368; b) E. L. Charsley, M. C. Ford, D. E. Tolhurst, S. Baird-Parker, T. Boddington, P. G. Laye, Differential Thermal Analysis and Temperature Profile Analysis of Pyrotechnic Delay Systems: Mixtures of Tungsten and Potassium Dichromate, *Thermochim. Acta* **1978**, *25*, 131–141.

[157] T. Boddington, A. Cottrell, P. G. Laye, A Numerical Model of Combustion in Gasless Pyrotechnic Systems, *Combust. Flame* **1989**, *76*, 63–69.

[158] R. Webb. Using thermodynamic codes to simulate pyrotechnic reactons, In *1st Workshop on Pyrotechnic Combustion Mechanisms*, 10 July 2004, Fort Collins, Colorado, USA, **2004**.

[159] a) J. C. Poret, J. J. Sabatini, Comparison of Barium and Amorphous Boron Pyrotechnics for Green Light Emission, *J. Energ. Mater.* **2013**, *31*, 27–34; b) A. P. Shaw, J. S. Brusnahan, J. C. Poret, L. A. Morris, Thermodynamic Modeling of Pyrotechnic Smoke Compositions, *ACS Sustainable Chem. Eng.* **2016**, *4*, 2309–2315.

[160] a) T. Basebi, R. M. Thomas, A Study of Moving Mesh Methods Applied to Thin Flame Propagating in a Detonator Delay Element, *Appl. Math. Comput.* **2003**, *45*, 131–163; b) A. G. Strunina, A. N. Firsov, S. V. Kostin. Transition Modes in the Combustion of Heterogeneous Systems with Solid-Phase Products. *Fiz. Goreniya Vzryva* **1981**, *17*, 24–30; c) A. G. Strunina, T. M. Martem'yanova, V. V. Barzykin, V. I. Ermakov, Ignition of Gasless Systems by a Combustion Wave, *Fiz. Goreniya Vzryva* **1974**, *10*, 518–526; d) T. P. Ivleva, P. M. Krishenik, K. G. Shkadinskii, Nonidentity of Steady Conditions of Combustion of Gas-Free Mixed Compositions, *Fiz. Goreniya Vzryva* **1983**, *19*, 87–90; e) K. G. Shkadinskii, B. I. Khaikin, A. G. Merzhanov, Propagation of a Pulsating Exothermic Reaction Front in the Condensed Phase, *Combust. Explos. Shock Waves (Engl. Transl.)* **1971**, *7*, 15–22; f) K. G. Shkadinskii, Transition to Steady-State Combustion of Gasless Compositions Ignited by a Hot Surface, *Fiz. Goreniya Vzryva* **1971**, *7*, 332–336; g) S. D. Dunmead, D. W. Readey, C. E. Semier, J. B. Holt, Kinetics of Combustion Synthesis in the Ti–C and Ti-C–Ni Systems, *J. Am. Ceram. Soc.* **1989**, *72*, 2318–2324; h) J. A. King-Hele, J. Williams, On Gas Flow Circulation in Detonator Delay Elements, *Combust. Sci. Technol.* **2000**, *161*, 323–349; i) H. S. Lee, C. Bulian, S. Claxton. In *Numerical Investigation of Reaction Front Propagation in Pressed-Column Pyrotechnic Time-Delay Device*, 47th AIAA/ASME/SAE/ASEE Joint Propulsion Conference and Exhibit, 31 July – 3 August 2011; j) T. S. Kang, C. H. Park, S. H. Kim, Characteristics of Exothermic Reaction Fronts in the Gasless Combustion System, *Ceram. Int.* **2011**, *37*, 825–833.

[161] E. Lafontaine, M. Comet, *Nanothermites*, Wiley-ISTE: London, **2016**.

[162] S. W. Dean, M. L. Pantoya, A. E. Gash, S. C. Stacy, L. J. Hope-Weeks, Enhanced Convective Heat Transfer in Nongas Generating Nanoparticle Thermites, *J. Heat Trans.* **2010**, *132*, 111201.

[163] C. L. Yeh, J. A. Peng, Fabrication of WSi_2-Al_2O_3 and W_5Si_3–Al_2O_3 Composites by Combustion Synthesis Involving Thermite Reduction, *Ceram. Int.* **2016**, *42*, 14006–14010.

Manuscript received: December 27, 2017
Version of record online: May 30, 2018

